UNIVERSITY OF CALIFORNIA SAN DIEGO

Developing peptides of MMP9 to activate Schwann cells through LRP1 signaling

A dissertation submitted in partial satisfaction of the requirements for the degree Doctor in Philosophy

in

Chemistry

by

John Hyun Joon Kim

Committee in charge:

Professor Jerry Yang, Chair
Professor Wendy Campana
Professor Thomas Hermann
Professor Akif Tezcan
Professor Emmanuel Theodorakis

2020

This Dissertation of John Hyun Joon Kim is approved, and it is acceptable in quality and form for publication on microfilm and electronically:

_____

_____

_____

_____

_____
Chair

University of California San Diego

2020

DEDICATION

This dissertation is dedicated to my grandparents who immigrated from South Korea to California to start a new chapter in our families lives, and to my parents who have sacrificed so much to raise me and my sister to have the lives we have now.

EPIGRAPH

“I was taught that the way of progress was neither swift nor easy.”

Marie Curie

“So do not fear, for I am with you;
do not be dismayed, for I am your God.
I will strengthen you and help you;
I will uphold you with my righteous right hand.”

Isaiah 41:10, NIV

TABLE OF CONTENTS

LIST OF FIGURES

LIST OF TABLES

LIST OF GRAPHS

LIST OF ABBREVIATIONS

AIDS	Acquired immunodeficiency syndrome
AKT	RAC-alpha serine/threonine-protein kinase. Protein Kinase B
Amp-100	Ampicillin (100 µg/mL)
Arg	Arginine
ATF3	Activating transcription factor 3
BCA	Bicinchoninic Acid
BSA	Bovine serum albumin
CCR	Clusters of Compliment like Repeats
CD	Circular dichroism
CD	Clusters of Differentiation
CHO	Chinese Hamster Ovary
CNS	Central Nervous System
DAB	3,3’-Diaminobenzidine
DAPI	4’,6-diamidino-2-phenylindole
DMEM	Dulbecco’s Modified Eagle Medium
DMSO	Dimethyl sulfoxide
DTT	Dithiothreitol
EDTA	Ethylenediaminetetraacetic acid
ELISA	Enzyme-linked immunosorbent assay
ELM	Eukaryotic Linear Motif
ERK	Extracellular signal regulated kinase

FBS	Fetal Bovine Serum
Fc	Fragment crystallizable of antibodies
GST	Glutathione *S*-transferase
H and E	Haemotoxylin and Eosin
HBSS	Hank's buffered Salt Solution
Hepes	4-(2-hydroxyethyl)-1-piperazineethanesulfonic acid
hSC	Human Schwann Cell
HIV	Human Immunodeficiency Virus
HPLC	High performance liquid chromatography
IPTG	Isopropyl ß-D-1-thiogalactopyranoside
IUCUC	Institutional Animal Care and Use Committee
kb	Kilobases
kDa	Kilodalton
LB	Lysogeny Broth
LDL	Low density lipoprotein
LRP	LDL Receptor-Related Protein
Lys	Lysine
MAPK	Mitogen-activated protein kinase
MMP	Matrix metalloproteinases
NHS	N-hydroxysuccinimide
NSAID	Non-steroidal anti-inflammatory drug
PBS	Phosphate buffered saline

PBST	Phosphate buffered saline with Tween 20
PDB	Protein Database
PDL	Poly-d-lysine
PEG	Poly(ethylene glycol)
Pex	Fusion protein of MMP-9 hemopexin domain with GST
PFA	Para formaldehyde
PMSF	Phenylmethylsulfonyl fluoride
PNL	Partial nerve ligation
PNS	Peripheral Nervous System
RAP	Receptor associated protein
RPM	Rotations per minute
rSC	Rat Schwann Cell
SC	Schwann Cell
SDS	Sodium dodecyl sulfate
TBS	Tris buffered saline
TBST	Tris buffered saline with Tween 20
TIMP	Tissue Inhibitor of metalloproteinases
Tris	Tris(hydroxymethyl)aminomethane

ACKNOWLEDGEMENTS

I am so thankful for the wonderful people I got to meet and work with during my stay at UCSD. I would like to first thank Professor Jerry Yang and Wendy Campana for trusting me, and giving the independence to work on this project during my stay here. Both of you have always been so supportive of my research and teaching interests, and I cannot thank you enough for your mentorship and support. I would also like to thank my other committee members: Professor Thomas Hermann, Professor Akif Tezcan, and Professor Emmanuel Theodorakis for their feedback and guidance from the classes I took in my first year, the departmental and candidacy exam and my defense.

I am so thankful for many of the Yang lab members who have been such a big support to me during my graduate career. I would like to first thank Takaoki Koyanagi who was one of my first friends in graduate school and always continued to check in with me on my progress. Yuchen Cao and Young Hun Kim took on the role of big sisters to me and always kept my moral high. Jamie for all of her youthful energy, who kept me on my toes and have deep conversations about life. Geoffray Leriche and Dan Sheik for helping me check out new and great restaurants for me to try. Jessica Cifelli and Kevin Cao who helped me so much with develop my methods and keeping me smiling. Richie Niederecker for keeping me on my toes and trusting me to train him in my project. And lastly, but most importantly, Kevin Sibucao who was my close

confidant, teaching mentor, and someone I can always rely on for watching over Ami.

I am also so thankful for so many Campana lab members for taking me into the lab and allowing me to become one of the members in the lab. Kenneth Henry was the first to help train me in almost every biochemical assay and trusted me to be independent in the lab. To all of the visiting scholars: Masataka Shibaya, Go Kubota, Yasuhiro Shiga, and Naoya Hirosawa for being so understanding and helpful in so many of my surgical methods. More recently I am so thankful for Kate, Halylie and Alicia for being understanding and accepting this jaded graduate student. Lastly, and most importantly, Andi Flütsch who was such an important part of my development as a scientist and kept me laughing with all of his jokes, while making fun of my gullible personality.

Many members of the Gonias lab have played a huge role in my development and growth as a scientist. I have so much respect and love for Elisabetta Mantuano who has always been willing to give up time to help me troubleshoot and guide me on anything that has to do with Schwann cells. Coralie Brifault for always having a warm smile to welcome me and always be willing to help me in any aspect of my project. Andrew Gilder who was a walking book in bacterial cloning and always willing to provide plasmids. Lipsa Das who was so willing to provide help with bacterial cloning and talking science. And lastly, and most importantly, Pardis Azmoon and Michael Banki

who were always willing to help and provide a warm smile when I needed the comfort.

Outside of my project, there were so many other members in various labs that have provided so much support in and help in all of my projects. In the Lin lab, Heike Kroeger and Priscilla Chan were such delightful people to always work with and talk to when working on the eye project. An even greater thank you to Heike for always being so honest with me and being such a role model in my life. Patricia Gaffney and Jessica Lawrence in the Sigurdson lab were also so warm to welcome me to their lab space and allow me to use their lab resources. They were always so happy to help as much as they could.

Lastly, to all of my friends in the Chemistry department who helped me settle into this university and became an important part of my support system. Tak, Megan Stone, Paul Koo, Davy Ho, Angie Kim, and Jimmy Han were some of my first friends in the chemistry department, and I miss them so dearly everyday, especially for the fun parties we had. Eunice, Wonho and JooHee, thank you for always knowing when to take me out to get Korean food and keep me grounded in my roots. The pokemon crew (Jim, Karen, Zaw, Geline, Wilson, Dion, Lauren, Hieu, Ben, Jaeson, Kevin and April) that have been so supportive and such a great, positive family to have around. J.O. thank you for being such a positive support as I dissertated!

To all of my family members, thank you. All of my grandparents worked so hard to bring this family to this country, and you have all been such an

inspiration to me about how to find happiness. Thank you to my parents for keeping me grounded in my religion and helping me grow into the man I am now. Ami, I love you!

And to all those who have made a huge impact in my life by being so open and supportive in my sciences and my personal life. I was able to make it this far because of you and your love.

Chapter 2 and 3 is currently being prepared for submission for publication as a communication in the development of peptides that can cause signaling in Schwann cell. John Kim, Jerry Yang, and Wendy Campana. This dissertation author is the primary researcher and author of this material.

Chapter 4 and 5 contains unpublished material co-authored with Jerry Yang and Wendy Campana. This dissertation author is the primary researcher and author of this material.

VITA

2010 Bachelors of Science in Biology, concentration in Microbiology, San Jose State University
Bachelors of Arts in Chemistry, San Jose State University

2010 – 2013 Lecturer, San Jose State University

2017 Master of Science in Chemistry, University of California San Diego

2020 Doctor of Philosophy in Chemistry, University of California San Diego

PUBLICATIONS

ABSTRACT OF THE DISSERATION

Developing peptides of MMP9 to activate Schwann cells through LRP1 signaling

by

John Hyun Joon Kim

Doctor of Philosophy in Chemistry

University of California San Diego, 2020

Professor Jerry Yang, Chair

Schwann cells play a vital role in maintaining homeostasis of the nerve and in recovery when an injury occurs in the peripheral nervous system. An improperly healed nerve or impaired Schwann cells can lead to the development of neuropathic pain. Most treatments for neuropathic pain treat the symptom but not the underlying cause. By developing drugs that can activate Schwann cells to become a recovery phenotype can be a method of treating neuropathic pain. The binding of the hemopexin domain of MMP9 to the LRP1 receptor of Schwann cells was previously found to cause the same signaling pathways that can activate these cells to differentiate into a recovery phenotype. Thus, developing small peptides of MMP9 to bind to LRP1 and

cause the same signaling response, would be a viable option for developing a treatment for neuropathic pain.

Using the crystal structure of MMP9 hemopexin domain as a template, 4 peptides were designed from the hydrophilic regions of the protein. These peptides were subjected to *in vitro* cell signaling studies, *in situ* pull downs assays and *in vivo* nerve crush assays to assess their biological similarity and relevance compared to the parent MMP9 hemopexin domain. Of the 4 peptides, peptide 2 with the sequence “SGRGKMLLFSGRRLWRFDVKAQ,” was seen to have similar activity to the parent MMP9 hemopexin domain.

To observe if the peptide would be capable of alleviating neuropathic pain, a drug delivery system needed to be developed to locally delivery the peptide to a PNL rat model. Alginate hydrogels were first used with a PNL injury model and seen to have no behavioral changes. However, due to high levels of inflammation seen in the immunohistochemistry and immunoblots, a PEG derived system was used to locally deliver the peptide to the nerve. Using the PEG system, peptide 2 was seen to alleviate pain 10 days post PNL operation compared to the controls. Although there are still many questions that need to be answered about the mechanism of action of peptide 2 and how it can alleviate neuropathic pain, this dissertation served as a starting point to this project.

Chapter 1

Schwann Cell's Role in Preventing Neuropathic Pain

1.1 Neuropathic Pain: An Overview

Neuropathic pain is abnormal pain that can be acute or chronic and stems from neuronal injury or hereditary abnormalities in the nervous system.[1] Neuropathic pain is an overarching term for many types of pain disorders that all have the common standpoint of continuous or spontaneous pain or hypersensitivity.[1–4] The pain symptom itself can affect different parts of the body and affect the patient's quality of life.[1–3] It is estimated that about 17.9% of Americans suffer from some form of neuropathy, but many neuropathies do not end up getting diagnosed.[2] Some examples of neuropathic pain are diabetic neuropathies, HIV/AIDS related neuropathy, trigeminal neuralgia, phantom limb pain, and trauma induced neuropathies.[1,3]

The mechanism to how neuropathies develop is currently not fully understood, since it can arise from physical nerve injury or complications from another disease.[1,4,5] Some neuropathies can develop to have similar symptoms, but can be caused by different mechanisms. Some symptoms include: temperature or touch sensitivities, spontaneous pain episodes that can feel like burning, tingling, or a combination of various pain or sensitivity symptoms.[1,5] Due to the various symptoms, causes, and severities of symptoms, treatment is usually handled on a patient to patient basis.[1,4,6] Most treatments attempt to block the pain itself and not treat the cause of pain, thus the patient is on the medication throughout their lifetime or until the pain episodes stop.[5,6] Although used as a treatment strategy, NSAIDs and opioids

are often ineffective for neuropathic pain. Moreover opioids are not a viable long term treatment, due to side effects of the medication.[1,6] There are currently only a few drugs that can alleviate neuropathic pain, which includes gabapentin and pregabin; yet, these drugs do not work for all neuropathies or patients. Some of these drugs act on the ion channels in the nerve do not treat the cause of the pain itself, or the mechanism of how they treat neuropathic pain is not fully understood.[4] Due to the high prevalence of neuropathic pain and the limited amount of treatments for the ailment, there is a need for more research into neuropathic pain and methods for treating the underlying causes.[4–6]

1.2 The Schwann Cell (SC) and Neuropathic pain

Neurons are responsible for sending signals to and from the brain to be interpreted as pain, thus neurons are an important cell to observe when studying pain. However, the neuron itself is not the only cell in the peripheral nervous system that is important for proper communication and interpretation of pain. In studies where SCs were altered, animals developed neuropathies. Genetic changes to the SCs that ranged from removing a membrane receptor that was important in axonal interactions or in the ability of SCs to differentiate, developed neuropathic pain after nerve injury.[7–9] Charcot-Marie-Tooth diseases and Guillain-Barre syndrome are examples of genetic disorders that affect SCs and cause neuropathies.[3,10,11] Thus, properly functioning SCs are just as important in preventing neuropathies.

The Schwann cell is a glial cell found only in the peripheral nervous system (PNS) and is an important cell in maintaining the nerve.[7,8,12] Starting from the development of the nervous system, the SC derives from the neural crest along with the nerves. As the nerves develop, they start to associate themselves with SC precursor cells[7,8,12]. SC precursors are known to develop into many different cell types including neurons[7,8]. As the nerve develops into the early postnatal stage, the SC precursors along the peripheral nerve develops into immature SCs. SC precursors found on the neuromuscular junction or near the cell bodies derive into specialized cells. For this dissertation, we will be focusing on the SCs that are found on the axons of the nerve.

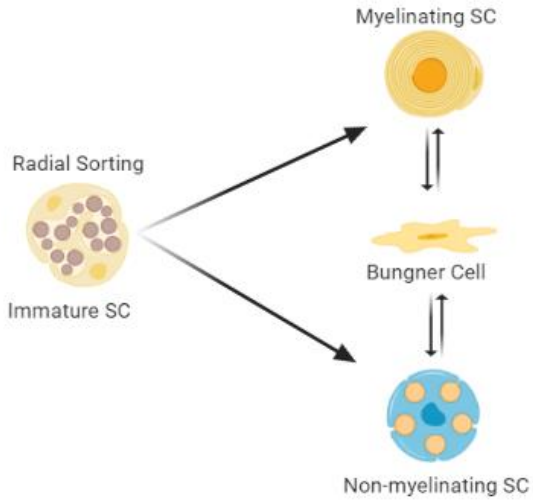

Figure 1.1 – Development of Schwann Cells (SCs) in the peripheral nerve. Immature SCs can differentiate into myelinating SCs or non-myelinating SCs depending on signals and interactions with nerves. These differentiated cells can dedifferentiate into Bungner, or recovery cells after nerve injury. (Created with Bio Render)

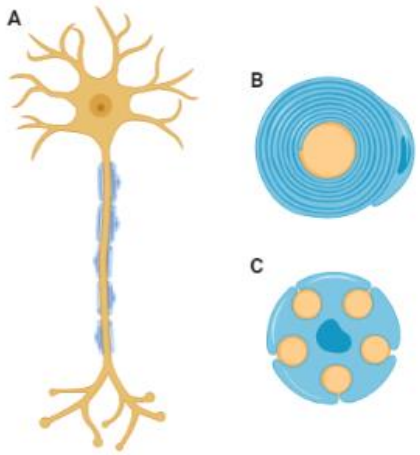

Figure 1.2 – Representation of the types of Schwann Cells found on the Axon. A. In yellow is the nerve and the blue cells are the SCs that span the whole length of the axon as myelinating SCs (B) or non-myelinating SCs (C). B. Myelinating SCs create myelin sheaths around a single neuron, supporting signal transduction. C. Non-myelinating SCs form Remak bundles with multiple smaller diameter neurons. (Created with Bio Render)

Immature SC along the axon undergo a process called radial sorting in which they can become a myelinating SC or a non-myelinating SC (Figure 1.1).[7,8] Myelinating SC wrap their cell bodies around large diameter axons creating myelin and allowing action potential to be conducted along the axon. Although SCs are most famously known for their myelin forming capabilities, the more abundant SC type in the peripheral nerve is the non-myelinating SC which form structures called Remak bundles and surround many small diameter neurons (Figure 1.2).[7,8] Small diameter neurons are usually sensory neurons and play a large role in pain signaling pathway.[7,8] Schwann cells have the ability to help clear or produce neurotransmitters, secrete growth factors and support the extracellular matrix of the nerve.[7,8] This close relationship between SC and nerves is important in maintaining homeostasis. The SCs not

only act as support cells during homeostasis, but are the main cells to deconstruct and re-organize the nerve after nerve injury.[7,8]

Most neuropathies occur after nerve injury, but not all nerve injuries lead to neuropathic pain.[4] Many events need to occur from the moment of neural injury to recovery, in which SCs play a major role. From the moment of injury, nerve tissue from the injury site to the distal end away from the spinal cord, need to be cleared away so that new nerves can reinnervate. All SCs from the injury site to distal ends change phenotypes into a specialized Bungner cell, or repair SCs.[7] These repair SCs specialize in organizing and clearing out old Myelin and nerve material.[13] At the same time, as the new nerve starts to grow, the SCs act as guides to navigate the regenerating nerve and differentiate back into specialized myelinating or non-myelinating SC phenotype.[14]

The SC plays a pivotal role in the health of the nerve and the potential to prevent neuropathies. Without properly functioning SCs, homeostasis cannot be maintained in the nerve and can results in misinterpretation of nerves signals, resulting in neuropathic pain.[8,13] In nerves that get injured, proper reinnervation and SC interactions are crucial to preventing neuropathic pain. SCs play a vital role in regeneration, thus being able to control or mediate the repair phenotype may help in proper nerve regeneration and preventing or treating neuropathic pain. Even when the nerve reinnervates properly, SCs need to properly remyelinate and interact with nerves to return to

homoeostasis. An important signaling receptor that plays a role in SCs becoming activated as repair SCs is the LRP1 receptor.[15,16]

1.3 The Schwann Cell and the Low density lipoprotein Receptor-Related protein 1 receptor

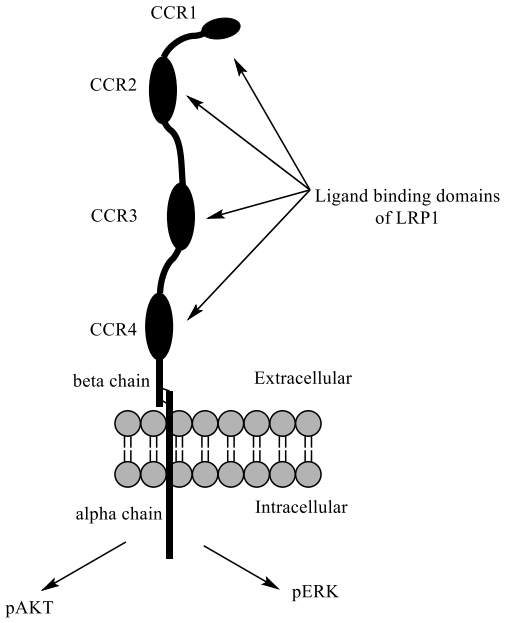

Figure 1.3 – Schematic representation of LRP1. LRP1 consists of 2 main chains – alpha and beta. Alpha chain contains the intracellular, transmembrane and extracellular regions. The Beta chain is only extracellular is consists of 4 ligand binding domains called CCR. The alpha and beta chain are held together by strong noncovalent interactions between the two chains. (Created with Chem Draw)

Low density lipoprotein (LDL) Receptor-Related protein 1 (LRP1) is about a 600kDa membrane protein found on all cells.[17] It consists of an alpha and beta chain that is linked together via strong non-covalent interactions that can be severed.[17–20] The alpha chain is 85kDa, and contains an intracellular with ligand binding domains, a transmembrane and an extracellular domain where it binds to the beta-chain of LRP1 (Figure 1.3).[18,19] The beta-chain is 515kDa and only has an extracellular domain.[18,19] The beta-chain contains 4

main ligand binding domains called clusters of compliment like repeats (CCR) that are linked together as a single chain with epidermal growth factor receptor-like cystine repeats (Figure 1.3).[17] The CCR domains are numbered 1 though 4, starting with the first domain furthest away from the alpha chain.[17] These CCR domains are known to bind to over 30 different ligands and have different interactions depending on the bound ligand.[18] Certain ligands can lead to endocytosis, while others can lead various signaling pathways that may include dimerization of LRP1; thus, LRP1 can act as a ligand scavenger and a signaling receptor.[17,18,20] Certain cell types were found to have different glycosylation patterns and varying amounts of intracellular binding domains on the alpha chain that affected the types of responses from LRP1.[21]

SCs upregulate LRP1 during nerve injury, which indicates LRP1 dependent cell signaling is important for promoting SC survival.[16] LRP1 also promotes migration which is important for mobilizing SCs after nerve injury.[15] Thus, knowing which ligands of LRP1 can activate the SCs can play a vital role in preventing or treating neuropathic pain. An important agonist of LRP1 ligand that was found to be important in activating SCs during injury was MMP9.[15]

1.4 Matrix metalloproteinase 9 and Low density lipoprotein Receptor-Related protein 1

Matrix metalloproteinases (MMP) are a family of calcium dependent enzymes that play an important role in cleaving extracellular matrix protein.[22,23]

Being an extracellular matrix protein, MMPs are highly regulated in cell systems. MMPs can contain a pro-domain which needs to be cleaved by another MMP in order to be enzymatically active.[22,23] MMP enzymes can also be regulated by their respective inhibitor known as tissue inhibitor of metalloproteinases (TIMP).[22,24] Being a ligand of LRP1, MMPs can be scavenged and removed from the extracellular space though LRP1.[22]

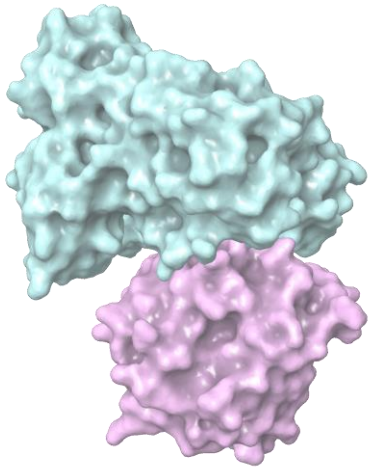

Figure 1.4 – Generalized structure of MMP. Top region of the structure (aqua) contains the pre, fibronectin, and catalytic domains of MMP. The bottom region (pink) contains the hemopexin domain. (Created with Maestro. PDB: 1CK7)[25]

In SCs, MMP, more specially MMP9, plays a role in activating SCs when bound to LRP1. MMP9 is a 92kDa Gelatinase-B protease that is secreted by SCs and plays an important role in LRP1-dependent cell signaling associated with SC migration during nerve injury and recovery.[15] MMP9 contains a signal, pro, enzymatic, fibronectin-like and hemopexin domain (Figure 2.1C).[22,24] When first secreted from the cell, MMP9 is inactive until the pro-domain is cleaved, reducing it to an 82kDa enzymatically active protein.[22]

MMP9 can be inhibited by its respective TIMP. The MMP9-TIMP complex can then bind to LRP1, but TIMP is not necessary to bind to MMP9 to be able to bind to LRP1. Binding of MMP9 to LRP1 activates ERK, AKT and cJUN pathway, which are important in activating SCs and pro-survival pathways.[15,16,24] Thus, finding a smaller, druggable peptide can lead to the development of a drug to activate SCs and treat neuropathic pain.

1.5 Goals of this dissertation

SCs play an important role in maintaining homoeostasis and in the nerve recovery process. Although genetics plays a role in the development of some neuropathies, many develop after neuropathic pain. Activating the SCs recovery phenotype and pro-survival signaling pathways via the interaction between LRP1 and MMP9, one can develop a drug to prevent or treat neuropathic pain. With this idea in mind, the main goal of this project was to:

1. Use rational designs to create peptides from MMP9 using known information about the structure of MMP9 (Chapter 2).
2. Use biological assays that would test the bioactivity and specificity of the peptides and compare them to the parent molecule of MMP9 (Chapter 3 and 4).
3. To develop delivery techniques to administer the drug or peptide to the peripheral nerve overtime (Chapter 5).

Chapter 2

Rational Design of MMP9 Hemopexin Domain Peptides

2.1 Introduction: Drug Design methods using crystal structures

Various biochemical and computational methods exist for exploring binding pockets of proteins and protein-protein interactions.[26] The use of these methods are important in exploring binding and bioactive properties of proteins. The type of method selected are limited by the information that is available on the structure and sequence of the protein.[26]

MMP-9 contains various domains, which include the signaling, pro, enzymatic, fibronectin-like, over glycosylated, and the hemopexin domain (Figure 2.1).[22] The signaling peptide shows that the MMP9 protein is secreted into the extracellular matrix, but is cleaved along with the pro domain when the enzyme is activated in the extracellular matrix.[22] Biochemical methods used mutations and deletions of domains of MMP9 to explore the binding of MMP9 to LRP1. Surface plasmon resonance was used to measure binding of LRP1 to mutations of MMP9 to find that the hemopexin domain of MMP9 was important in binding to LRP1.[24] Thus, the hemopexin domain of MMP9 will act as the key to find a peptide that can activate SCs to the recovery phenotype through LRP1 signaling.

Crystal structures of other MMPs exist, however, the crystal structure for the complete MMP9 is still absent. Even without the whole MMP9 structure, certain MMPs, such as MMP2, have similar conserved structural features. Thus using the crystal structure information from MMP2 (PDB: 1CK7), the

orientation of MMP9's hemopexin domain in relation to the other domains of MMP9 can be inferred (Figure 2.1).[25] The hemopexin domain of human MMP9 has been crystalized (PDB: 1ITV) and can be used to explore the structure and regions of the protein that may play an important role in binding to LRP1 (Figure 2.2).[27]

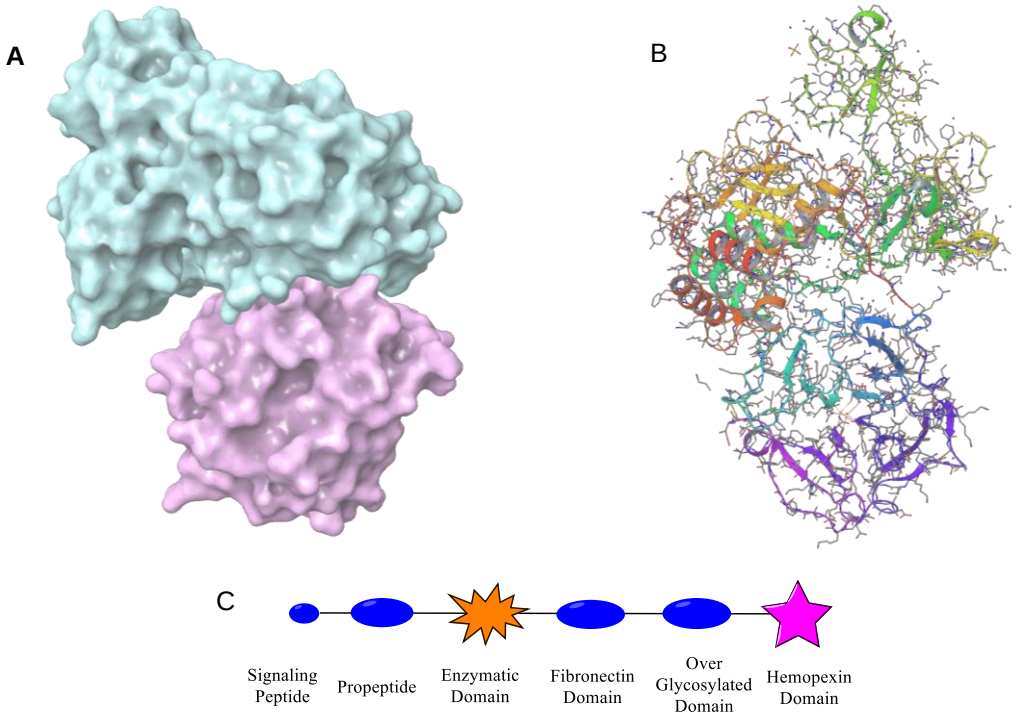

Figure 2.1 – MMP2 and MMP9 have very similar structures due to similar domains found in both proteins. The crystal structure representation of MMP2 (PDB: 1CK7) and is highlighting the surface of the protein (A) and secondary structure (B) using Maestro. The surface of the protein in (A) has been highlighted so that the teal is the main enzymatic body of the protein and the pink is the hemopexin domain. The domains found in MMP9 have been shown schematically (C) without the specific sequence.

Even though many crystal structures of MMPs exist, there are no complete crystal structure for LRP1. Current LRP1 crystal structures that exist are for short fragments of the CCR, or ligand binding domain.[28] However, no complete crystal structure exists for an entire CCR domain or most of LRP1

(Figure 1.3).[28] Without information on the structure of LRP1, using computational models to help predict the binding interaction is impossible. Even without the complete structure of LRP1, the crystal structure of MMP9 Hemopexin can be used to determine which short peptide fragments can bind to LRP1 based on location and composition of the secondary structure. These peptide fragments can then be synthesized and tested for bioactivity similar to the hemopexin domain.

2.2 MMP9 Peptides

MMP9 hemopexin domain is a 23 kDa protein that consists of 4 propeller or blade like structures that come together to form the overall windmill-like structure of the protein (Figure 2.2A).[27] Due to the 4 propeller like regions, the hemopexin domain contains a large percentage of secondary structure.[27] To determine the peptides that would be selected and tested for bioactivity, the regions that were hydrophilic, closest to the outer rim and open to the environment were selected (Figure 2.2).

Blade 1, closest to the N-terminus of the chain, was also the region closet to the rest of the protein (Figure 2.3). Being the least accessible, this region was disregarded when selecting peptides. The region closest to the C-terminus, blade 4, is the region where hemopexin domains can dimerize.[23,27] This region was not known if it can only dimerize with the hemopexin domain or could also bind to LRP1, thus was kept in the selection process. Using the aid of the crystal structure (PDB: 1ITV) to visualize the surface amino acids, 4

peptides were selected that would either contain little secondary structure, or would have some secondary structure to maintain the integrity of the peptide's structure (Figure 2.2B, 2.3).

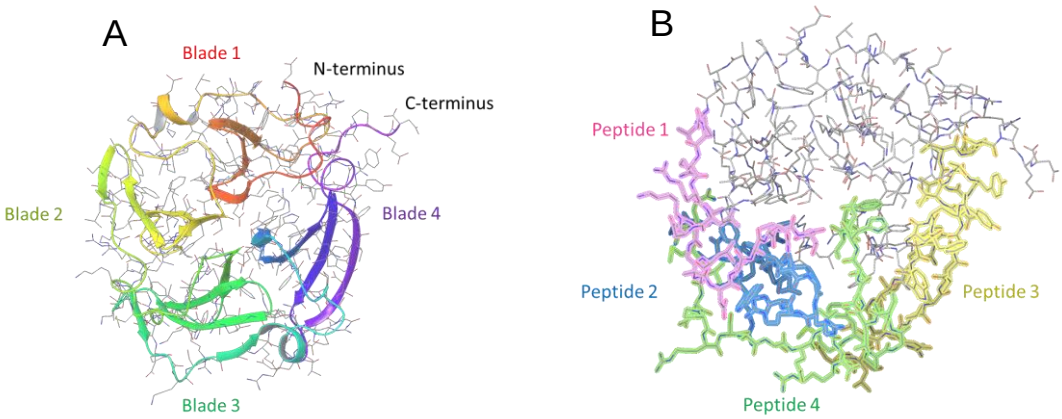

Figure 2.2 – Structural representation of MMP9 Hemopexin domain (PDB: 1ITV Chain A). Ribbons are used to show the secondary structure in the Hemopexin domain (A). The colors are arranged red to purple, with red being the start of the N-terminus and purple the end of the C-terminus. Secondary structures can be seen as helices or β-sheets with the bolded arrow showing directionality. The 4 blades or propellers are labeled in each section. The 4 selected peptides are highlighted using the structure of the hemopexin domain (B). Each color represents a different peptide. Molecular structural models made via Maestro.

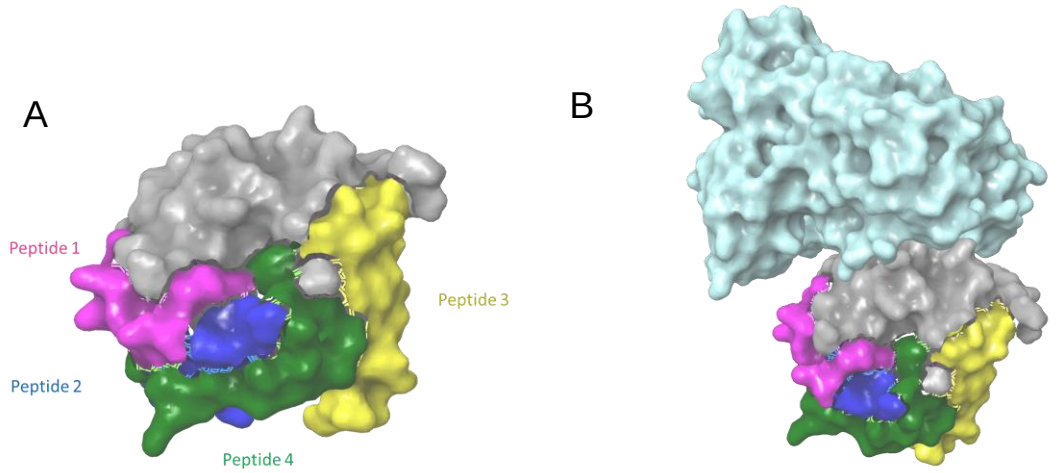

Figure 2.3 – Structural representation of MMP9 Hemopexin domain (A) and entire MMP2 (2) with the protein surface highlighted. (A) the hemopexin domain of MMP9 surface is highlighted along with the peptide sequences and its surface coverage highlighted in colors indicated. Hemopexin domain of MMP9 and highlighted proteins are superimposed with the structure of MMP2 to show the coverage of selected peptides. The teal color surface represents the rest of the domains of MMPs outside of the hemopexin domain.

2.3 Properties of the 4 Peptides

Table 2.1 – Summary of peptide sequences of MMP9 Hemopexin domain. Sequences along with the highlighted colors in corresponding figures (Figure 2.2, 2.3) are listed.

Peptide	Sequence	Residue number (PDB: 1ITV)	Total Residue count	Highlighted sequence
1	LGPRRLDKLGLGADVAQVTG	84 - 103	20	Pink
2	SGRGKMLLFSGRRLWRFDVKAQ	107 - 128	22	Blue
3	DRFYWRVSSRSELNQVDQVGYVTYDILQC	164 - 192	29	Yellow
4	AQMVDPRSASEVDRMFPGVPLDTHDVF	127 - 153	27	Green

Chosen peptides were synthesized at 95% or greater purity by PL Laboratories and verified for correct sequence and purity (Table 2.1). All peptides were tested for solubility in water, PBS and media. Circular Dichroism (CD) can be used to estimate the amount of secondary structure in short peptide sequences. Although it is better at estimating alpha helixes, it can be used to measure some beta sheets as well.[29,30] Since CD does not guarantee secondary structure, these were crude measurements to observe if any organization existed in the peptides. Online databases and computational programs were used to estimate the amount of secondary structure that can exist based on the sequence.[26,31]

2.3.1 Properties Peptide 1

Peptide 1 is composed of 20 amino acids and has the sequence “LGPRRLDKLGLGADVAQVTG.” It is found on blade 1 of MMP 9 hemopexin

domain and in the protein, and contains very little secondary structure. Peptide 1 was completely soluble in water up to a concentration of 50 μg/μL.

Using computational algorithms JPred[32] on peptide 1 for secondary structure (Figure 2.4), one of the algorithms predicted some beta strands, but at low confidence, with much of the structure showing no secondary structure. When the peptide was measured in CD at 1mg/mL, and the spectroscopy analyzed by capito,[33] the program estimated that there was 33% beta strand and 60% was unstructured, which matches the estimations given by the JPred algorithm.

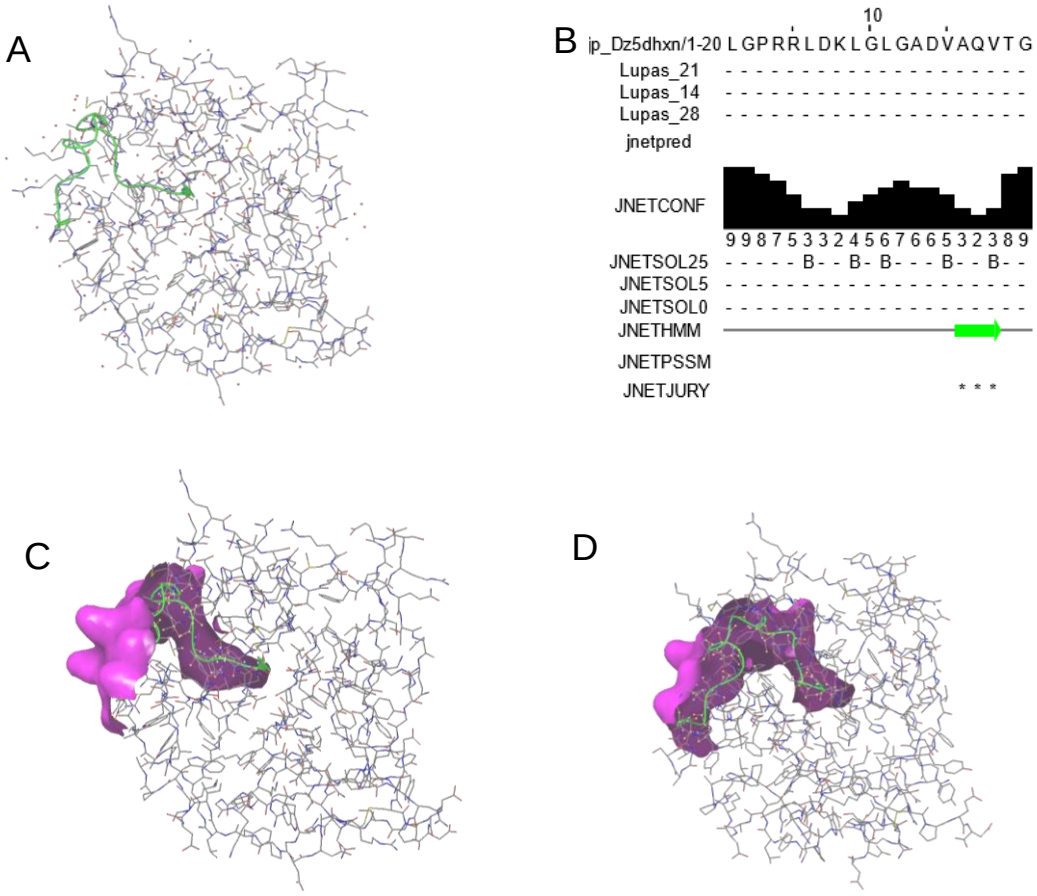

Figure 2.4 – Structural representation of peptide 1 in MMP9 hemopexin domain. (A) highlights the location and secondary structure of the peptide in the protein. All secondary structures are shown as directional arrows. (B) Secondary structure predictor algorithm JPred analysis on the peptide shows which amino acids are likely to be buried (JNETSOL25) in the sequence. Confidence levels on secondary structure predictions and predictions are shown with a solid green arrow representing β-strand like structure (Jnetpred). (C,D) Two different views are given of the peptide in protein along with the surface representation of the peptide.

Graph 2.1 – CD spectrogram of peptide 1 dissolved in pH 7.0 phosphate buffer at 1mg/ml. CD was analyzed using capito to evaluate the amount of secondary structure.

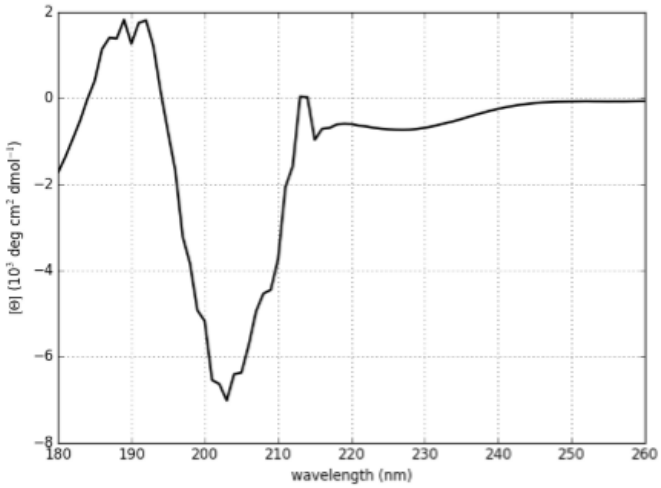

2.3.2 Properties Peptide 2

Peptide 2 is composed of 22 amino acids and has the sequence “SGRGKMLLFSGRRLWRFDVKAQ.” It is found on blade 3 of MMP 9 hemopexin domain and in the protein, contains a high amount of β sheets. Peptide 2 was completely soluble in water up to a concentration of 50 μg/μL.

Using computational algorithms JPred[32] on peptide 2 for secondary structure (Figure 2.5), JPred strongly predicted β strands in the sequence. When the peptide was measured in CD at 1mg/mL, and the spectroscopy analyzed by capito,[33] the program estimated that there was 51% beta strand and 51% was unstructured, which matches the estimations given by the JPred algorithm.

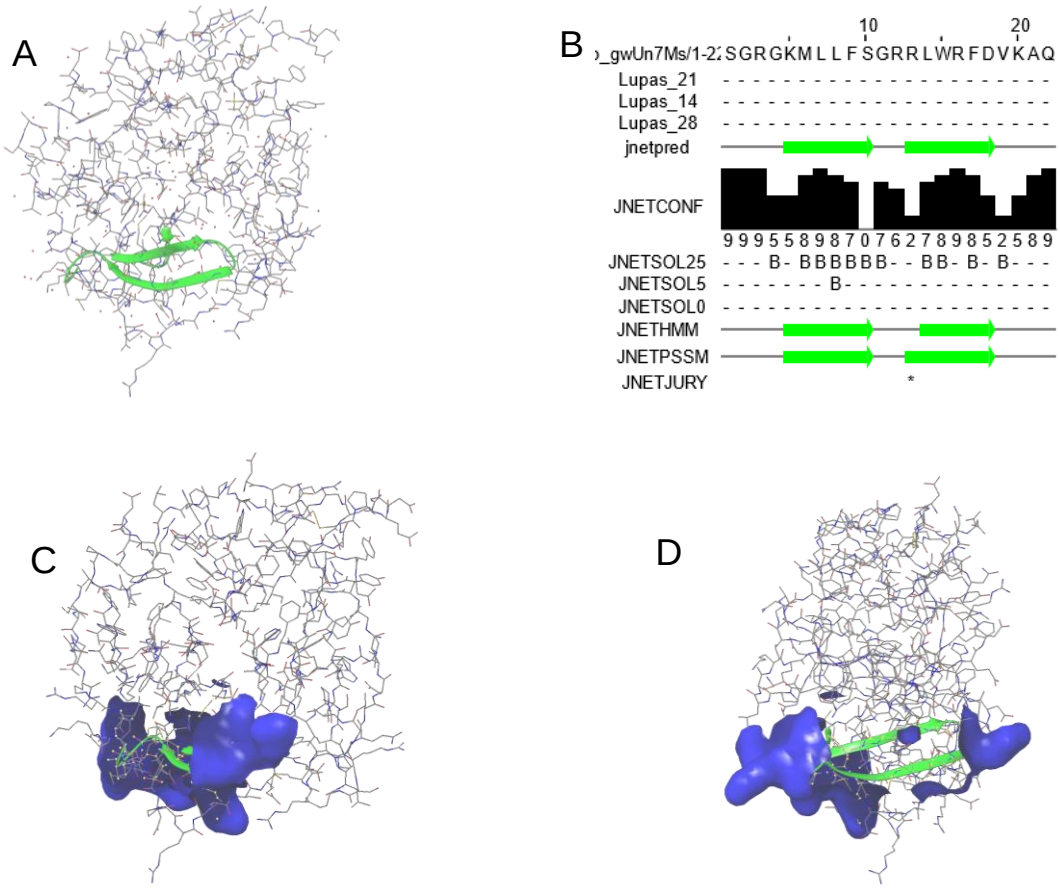

Figure 2.5 - Structural representation of peptide 2 in MMP9 hemopexin domain. (A) highlights the location and secondary structure of the peptide in the protein. All secondary structures are shown as directional arrows. (B) Secondary structure predictor algorithm JPred analysis on the peptide shows which amino acids are likely to be buried (JNETSOL25) in the sequence. Confidence levels on secondary structure predictions and predictions are shown with a solid green arrow representing β-strand like structure (Jnetpred). (C,D) Two different views are given of the peptide in protein along with the surface representation of the peptide.

Graph 2.2 - CD spectrogram of peptide 2 dissolved in pH 7.0 phosphate buffer at 1mg/ml. CD was analyzed using capito to evaluate the amount of secondary structure.

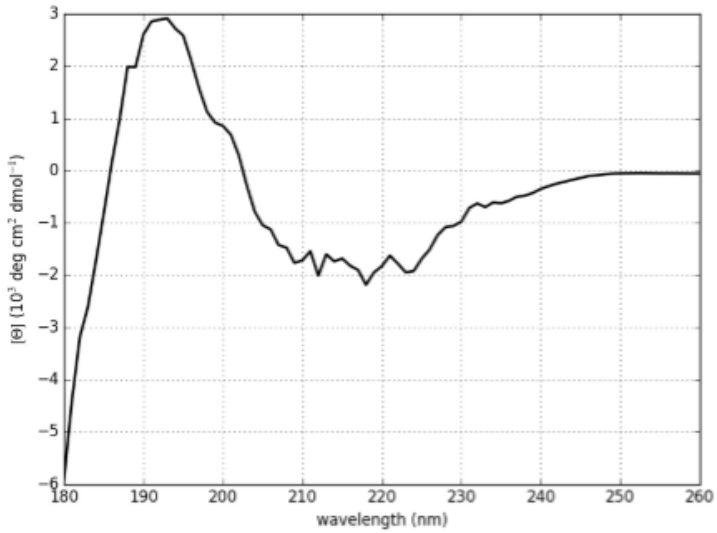

2.3.3 Properties Peptide 3

Peptide 3 is composed of 29 amino acids and has the sequence “DRFYWRVSSRSELNQVDQVGYVTYDILQC.” It is found on blade 4 of MMP 9 hemopexin domain and in the protein, it contains vast amounts of beta sheets and is the region that dimerizes MMP9 hemopexin domain. Peptide 3 was not soluble in water and was dissolved in dimethyl sulfoxide (DMSO).

Using computational algorithms JPred[32] on peptide 3 for secondary structure (Figure 2.6), different algorithms had conflicting interpretations of whether the peptide contained β or α strands, but it did agree that secondary structure existed. When the peptide was measured in CD at 1mg/mL, and the spectroscopy analyzed by capito,[33] the program estimated that there was 53% beta strand and 55% was unstructured, which does not conform the results

seen by JPred's estimation, but does not deny the presence of secondary structure. But, the measurements of this peptide were done in DMSO due to it being insoluble in water, thus these measurements are hard to interpret for the actual estimation of secondary structure in solution.

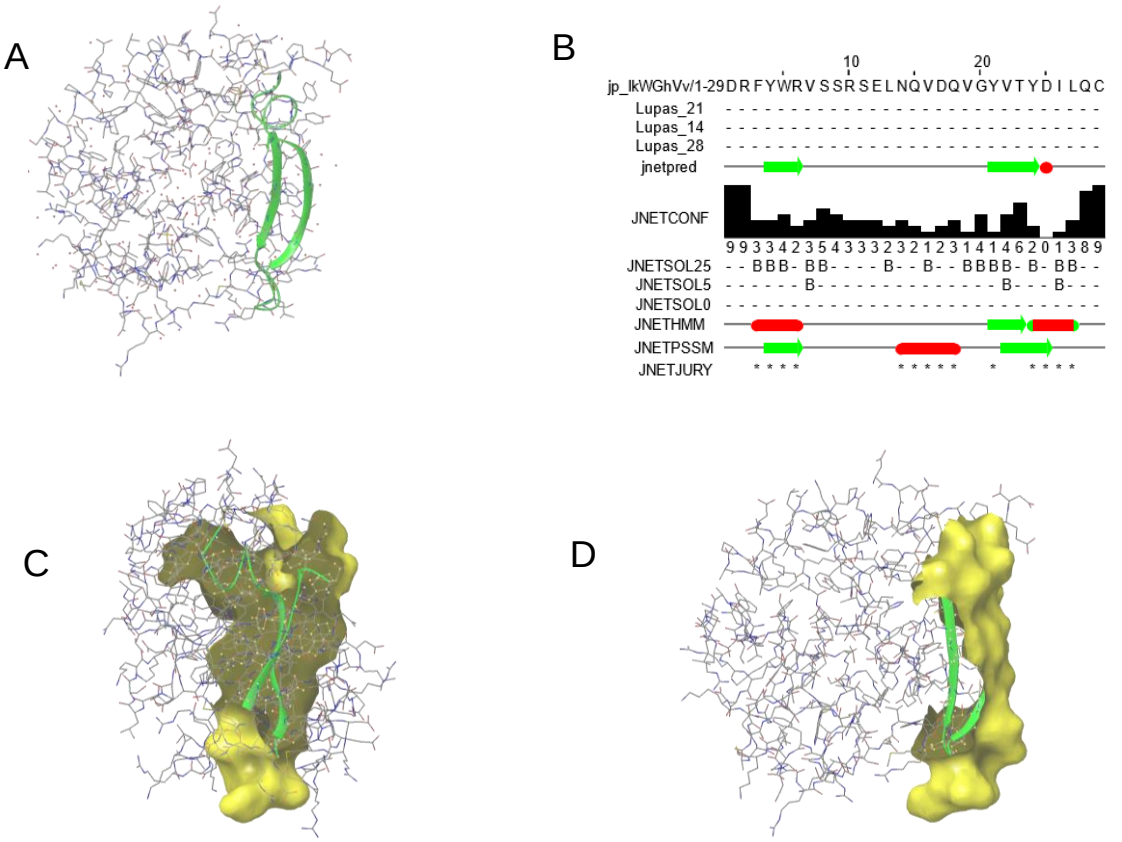

Figure 2.6 – Structural representation of peptide 3 in MMP9 hemopexin domain. (A) highlights the location and secondary structure of the peptide in the protein. All secondary structures are shown as directional arrows. (B) Secondary structure predictor algorithm JPred analysis on the peptide shows which amino acids are likely to be buried (JNETSOL25) in the sequence. Confidence levels on secondary structure predictions and predictions are shown with a solid green arrow representing β-strand like structure, and red barrels representing α helix like structures (Jnetpred). (C,D) Two different views are given of the peptide in protein along with the surface representation of the peptide.

Graph 2.3 - CD spectrogram of peptide 3 dissolved in 10% DMSO in pH 7.0 phosphate buffer at 1mg/ml. CD was analyzed using capito to evaluate the amount of secondary structure.

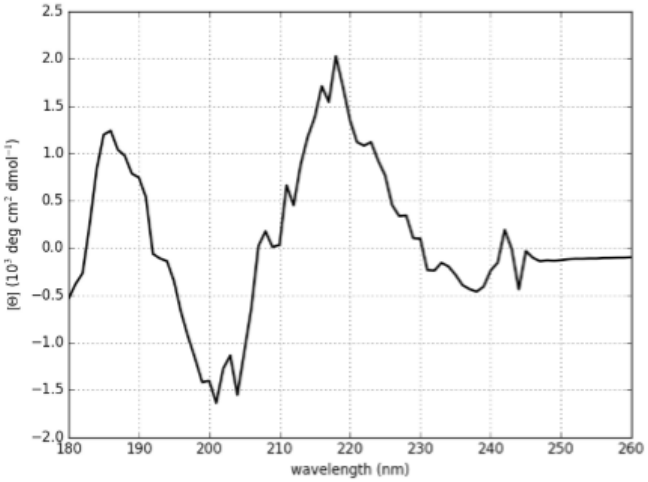

2.3.4 Properties peptide 4

Peptide 4 is composed of 27 amino acids and has the sequence “AQMVDPRSASEVDRMFPGVPLDTHDVF.” It is found on blade 3 of MMP 9 hemopexin domain and in the protein, contains both α and β sheets, but is mostly unstructured. Peptide 4 was completely soluble in water up to a concentration of 50 µg/µL.

Using computational algorithms JPred[32] on peptide 4 for secondary structure (Figure 2.7), JPred predicted no secondary structure. When the peptide was measured in CD at 1mg/mL, and the spectroscopy analyzed by capito,[33] the program estimated that there was 54% beta strand and 52% was unstructured, which provides evidence of secondary structure existing, and goes against jPred’s analysis.

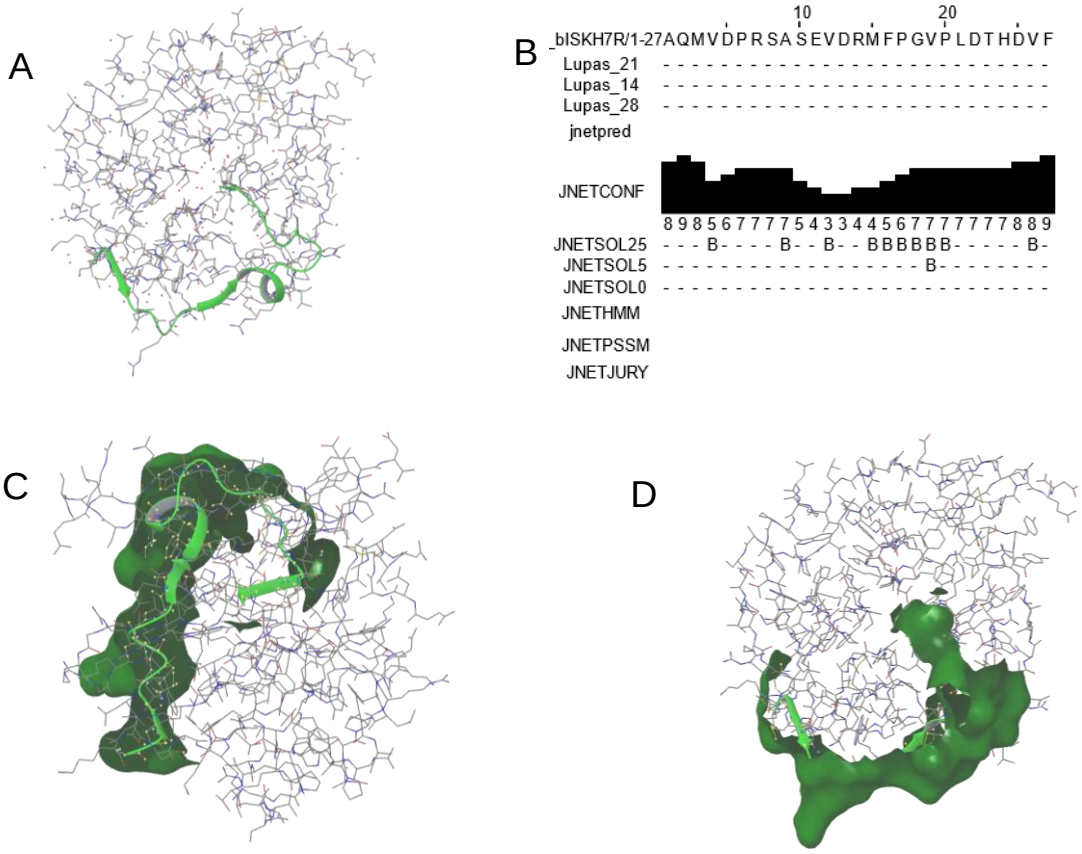

Figure 2.7 – Structural representation of peptide 2 in MMP9 hemopexin domain. (A) highlights the location and secondary structure of the peptide in the protein. All secondary structures are shown as directional arrows. (B) Secondary structure predictor algorithm JPred analysis on the peptide shows which amino acids are likely to be buried (JNETSOL25) in the sequence. Confidence levels on secondary structure predictions and predictions are shown with a solid green arrow representing β-strand like structure (Jnetpred). (C,D) Two different views are given of the peptide in protein along with the surface representation of the peptide.

Graph 2.4 - CD spectrogram of peptide 4 dissolved in pH 7.0 phosphate buffer at 1mg/ml. CD was analyzed using capito to evaluate the amount of secondary structure.

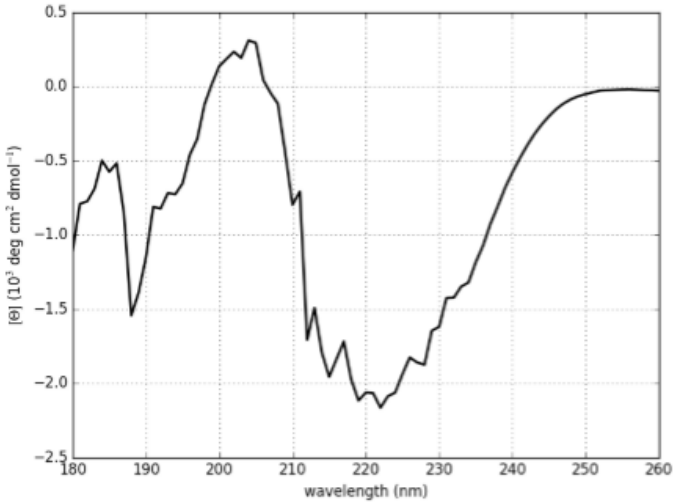

2.4 Experimental methods

Peptide synthesis and purity. Peptides 1 to 4 (Figure 1) were synthesized by PL Laboratories at >95% purity and verified by HPLC. Synthesized peptide sequences were verified by tandem mass spectroscopy. Peptides were all soluble in water up to 10 mg/mL, except for peptide 3, which was dissolved in 10% DMSO.

Circular Dichroism. Circular dichroism (CD) was measured on a JASCO J-810 with a PFD-425S temperature controller at 25°C in a 1 mm pathlength quartz cuvette. Measurements were made every 1 nm from 260 to 178 nm. Samples soluble in water were dissolved at a concentration of 1 mg/mL of pH 7.0 phosphate buffer. Insoluble samples were dissolved in 10% DMSO in pH 7.0 phosphate buffer.

2.5 Conclusion

Using computational and crystal structure data of MMP9's hemopexin domain (PDB: 1ITV), 4 peptides were selected based on hydrophilicity, proximity in the protein and secondary structure. Peptides were seen to maintain some source of secondary structure in the crude CD taken, and be soluble in water. These peptides can now be tested in biological assays to determine if biological activity is maintained like the parent protein. Once the bioactive peptides are determined, biochemical techniques can be applied to further sought out the specific chain or structure that maintains biological activity.

2.6 Acknowledgements

The initial peptide predictions were made by Professor Jerry Yang on MMP2 hemopexin domain before the project was given to me, which gave me a great platform to start the project. Andi Flütsch provided much feedback and help into using Maestro and interpreting surface interactions of MMP9 hemopexin domain.

I received so much help on CD measurements from various peers in the Chemistry & Biochemistry department at UCSD. Megan Stone helped on educating and troubleshooting CD measurements on the JASCO in the Molinsky lab. Lewis Churchfield and Robert Alberstein helped make more CD measurements on the Aviv 62DS spectrophotometer in the Tezcan lab.

Chapter 2 is currently being prepared for submission for publication as a communication in the development of peptides that can cause signaling in Schwann cell. John Kim, Jerry Yang, and Wendy Campana. This dissertation author is the primary researcher and author of this material.

Chapter 3

Bioactivity of MMP9 Hemopexin domain Peptides

3.1 In vitro Schwann Cell signaling assays

Erk1/2 and AKT signaling pathways in SCs though LRP1 has been shown to be important in SCs become activated to a repair phenotype.[9,19] Using recombinant MMP9 hemopexin domain fusion GST protein (now referred to as Pex), it was found that binding of Pex to LRP1 had the same in vitro signaling in rSCs that can lead to the activation SCs ERK1/2 and AKT pathways.[15] With this information at hand, the peptides were also tested in a similar fashion to explore which peptides would have the same bioactivity as Pex.

Graph 3.1 – Iodine radiolabeled Pex homologus competitive binding to LRP1 on human Schwann cells. Increasing concentrations of unlabeled Pex was used to compete radiolabeled Pex on hSCs at 4°C.Gamma counts and cell lysate protein concentrations were used to quantify bound and radiolabeled Pex.

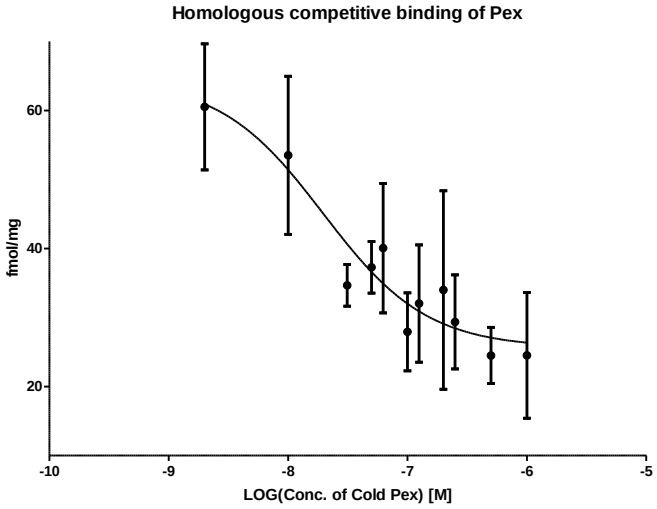

Past studies have been conducted in only rSCs and not in hSCs. Since Pex is a recombinant human protein, similar experiments were conducted on hSCs to check for bioactivity. Since hSCs came from an adult Schwannoma,

hSCs were checked for SC and LRP1 markers using immunofluorescence (Figure 3.2). Then the ability of hSCs to bind to Pex was established using radiolabeled Pex competitive binding assays. The IC_{50} of Pex to human SC LRP1 was found to be 19nM (Graph 3.1). This is comparable to other reported literature values of LRP1 to MMP9 binding to LRP1 which was reported to be 51nM.[24]

3.1.1 In vitro rat Schwann cell signaling assays

The 4 peptides were tested for their ability to activate ERK1/2 signaling in primary rSCs similar to protocols used for Pex signaling.[15] To ensure the peptides had or did not have biological activity, high doses of peptides, 10μM, were used in the assays. To reduce background ERK1/2 signaling in rSCs, the cells need to be placed in serum free media, also known as starvation media. Too long of a starvation activates ERK1/2 signaling, so a balance of starvation time and treatment time was key to achieving a measurable signal that was not masked by the background ERK1/2 signal (Figure S3.3).

From peptide treatments on rSCs, only peptide 1 showed consistent signaling of ERK1/2 similar to that of Pex (Figure 3.1A). Even with consistent signaling, the fold increase of ERK1/2 signaling with Pex and peptides were only 1.5 fold, and much lower compared to previously reported experiments.[15] The lower levels of signaling is most likely due to the lack of my experience with primary rSCs and the balance between starvation and treatment in these cells. Regardless, with the various repeats of the experiment only 1 peptide

signaled consistently. Peptide 2 and 4 also had varying levels of ERK1/2 signaling with rSC but was not significantly different from the no treatment group. Although it is hard to say if peptide 2 and 4 are true signaling or background, but from a statistical standpoint, the signaling was not significant.

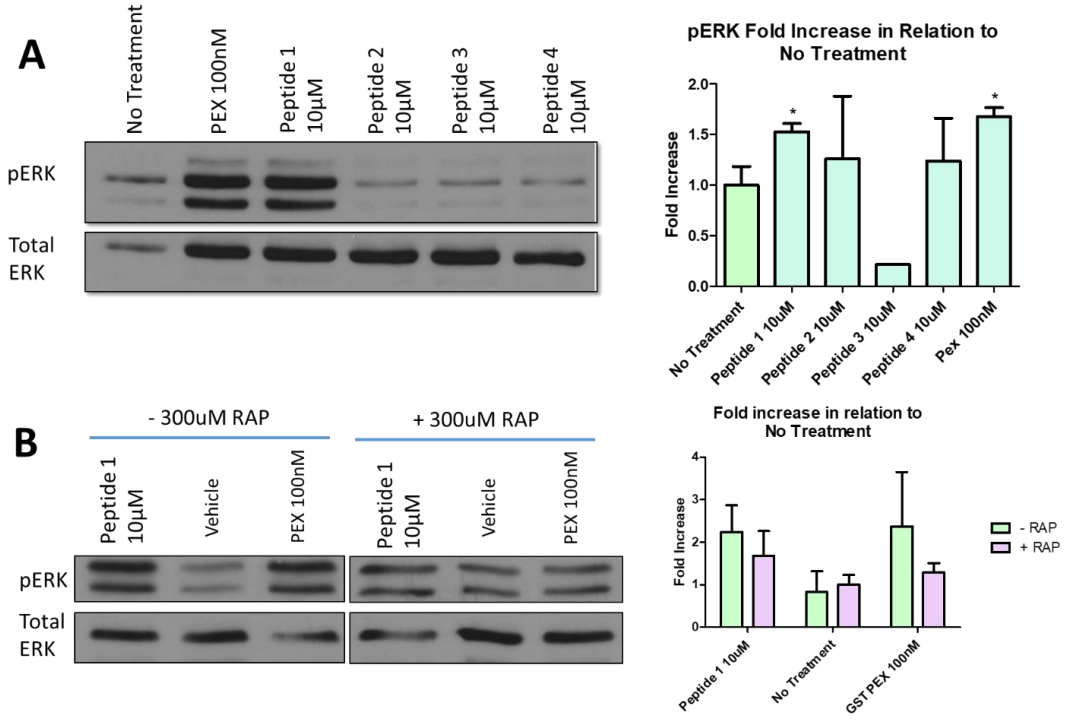

Figure 3.1 – Rat Schwann cell ERK1/2 signaling with the 4 peptides and Pex. rSCs were starved to bring down background ERK1/2 levels, and then treated with peptides and Pex for 10 minutes before lysing and using immunoblot to quantify the level of signaling (A). Recombinant fusion GST-RAP is used as a LRP1 ligand to block PEX signaling and to check if RAP can block peptide signaling as well (B).

Receptor associated protein (RAP) is a chaperone of LRP1 that binds to the clusters of complement like repeat (CCR) domains that are known as the ligand binding domains of LRP1 (Figure 1.3). RAP can be made as a recombinant protein, and in LRP1 type assays, it can act as a competitive ligand and signaling inhibitor of LRP1.[15,17,34] RAP has been previously shown

to block binding of Pex to LRP1 using the same signaling assay, but with a prior incubation time with RAP.[15,34] The RAP blocking experiment was conducted with only peptide 1 since it was the only peptide to show consistent ERK1/2 signaling. rSCs should not show variation in ERK1/2 level when RAP is added to the experiment, but due to varying background, it was difficult to determine if there was ERK1/2 signaling because of a low fold increase when activation was seen. These studies did show blocking of ERK1/2 signaling from Pex, but was not statistically significant enough (Figure 3.1B). Even without statistical significance, since previous studies showed RAP blocking Pex signaling, and so we were able to infer information about peptide 1. From the statistical standpoint, peptide 1 does not seem to be blocked by RAP binding to LRP1. Although there is a depression of signal, it is difficult to prove if RAP is blocking peptide 1 signaling or not. Different experimental method would be needed to determine binding of peptide 1.

3.1.2 *In vitro* human Schwann cell signaling assays.

Pex sequence and peptides are modeled after a human variant of the protein. Signaling of the peptides on hSCs would be important in determining if the peptide could have a medicinal or translational relevance. The hSC line are classified as a primary cell line, similar to rSCs, but was isolated from a patient with Schwannoma. Schwannomas are SCs that grew into tumor like structure in the nerve. Since the cells were from an adult and tumorous growth,

the viability of using the cell line in signaling assays needed to be assed. Using immunofluorescence, hSCs were seen to have LRP1 (Figure 3.2), and have been used by used by other research groups as a hSC model for studying neuropathies and ERK1/2 signaling.[35–37] Using radiolabeled Pex, it was determined that Pex can bind to LRP1 on hSC at a similar binding constant as reported in literature (Graph 3.1). With this in mind, the same signaling assays as rSCs can be used on the hSCs to determine if the peptides can signal ERK1/2 and AKT though LRP1.

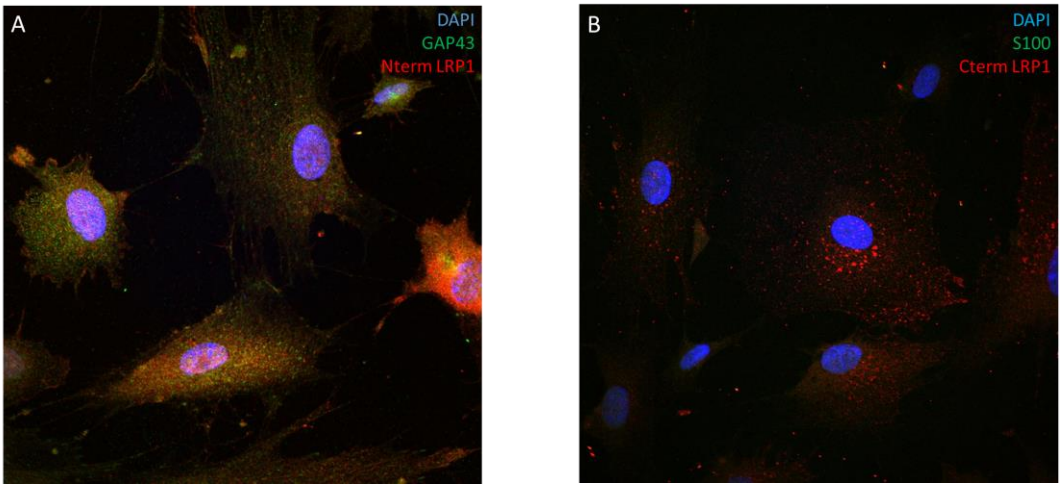

Figure 3.2 – Immunohistochemistry of human Schwann cells at 60x magnification. hSCs were stained for DAPI, GAP43 and the N-terminal of LRP1 (A). hSCs were also permeabilized and stained for S100 and the C-terminal of LRP1 (B).

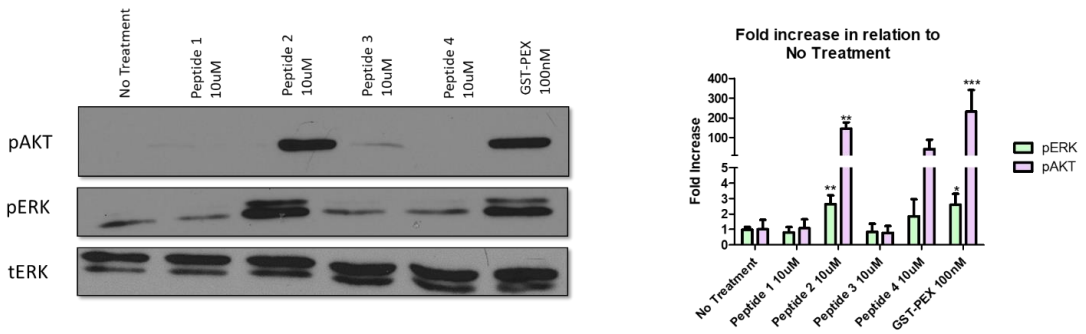

Figure 3.3 – Human Schwann cell ERK1/2 and AKT signaling with the 4 peptides and Pex. hSCs were starved to reduce background signaling levels, and then treated with peptides and Pex for 10 minutes before lysing and using immunoblot to quantify the level of signaling.

Compared to the signaling in rSCs, the hSCs had a stronger fold increase in Pex signaling with both ERK1/2 and AKT. With a higher fold increase, a signaling response was easier to discern from background noise. In rSCs (Figure 3.1A), peptide 1 was seen to have the most robust signaling. However, in hSCs, peptide 1 did not show signaling in either pathway, and instead, peptide 2 showed consistent signaling in both ERK1/2 and AKT pathways. Peptide 4 also showed some activity but was not statistically significant. With such varying data between rSC and hSC data, there needed to be an assay outside of cell signaling that can confirm the binding of peptide to LRP1. Using recombinant LRP1 binding domains, the peptides can be tested for binding to LRP1.

3.2 Pull down assays

LRP1 contains 4 ligand binding domains that are also known as CCR domains (Figure 1.3) that bind to over 30 ligands.[9,18] Although no crystal structure for these domains exist, recombinant proteins of these domains can

be produced in eukaryotic cells as fusion recombinant proteins.[17] Among the 4 CCR domains, domain 2 and 4 have shown the most diverse ligand binding properties.[17] CCR domain 1 is the shortest and has not shown *in vitro* ligand binding, and more recently CCR 3 has been shown to bind to select ligands.[38] In our experiments, only CCR 2 and 4 will be used due to their broad ability to bind to ligands and availability of the plasmids. These constructs are based on human LRP1 and will be expressed as fusion proteins with a rabbit Fc antibody fragment that can be used to detect for the CCR protein.

To show binding between the CCR domains and peptides, a pulldown assay can be used to probe for specific binding. Since the peptides are more difficult to detect for without a label, the peptides will be used as the bait and linked to the beads using NHS esters. To ensure the peptides were coupled to the NHS ester beads, a modified Sakaguchi's qualitative test for arginine was used to check for the presence of the amino acids on the beads (Figure S3.4).[39] Then the CCR domain proteins will be used as prey and checked for binding to the peptides via the fusion rabbit Fc domain in immunoblotting.

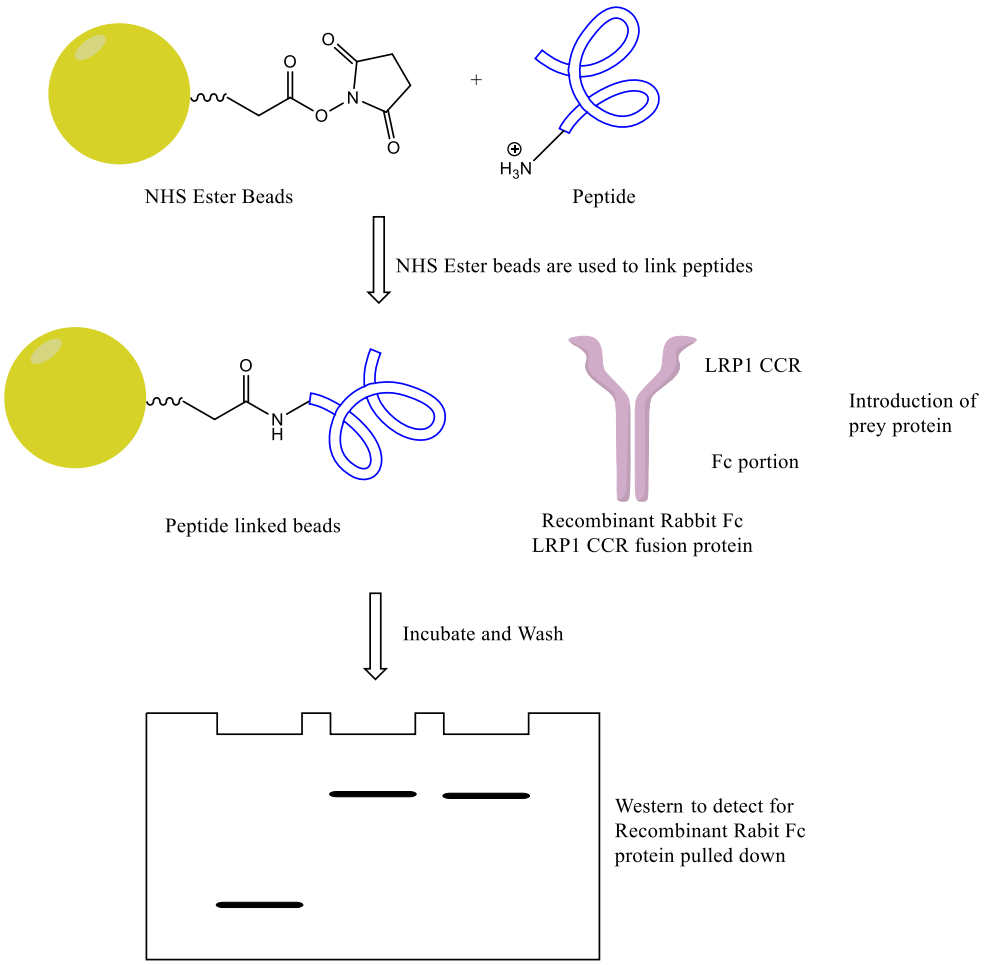

Figure 3.4 – Simplified scheme for the pulldown assay using peptides and recombinant LRP1 CCR fusion proteins. Peptides and proteins were immobilized on NHS-ester beads and checked for coupling using a modified Sakaguchi qualitative test for arginine.

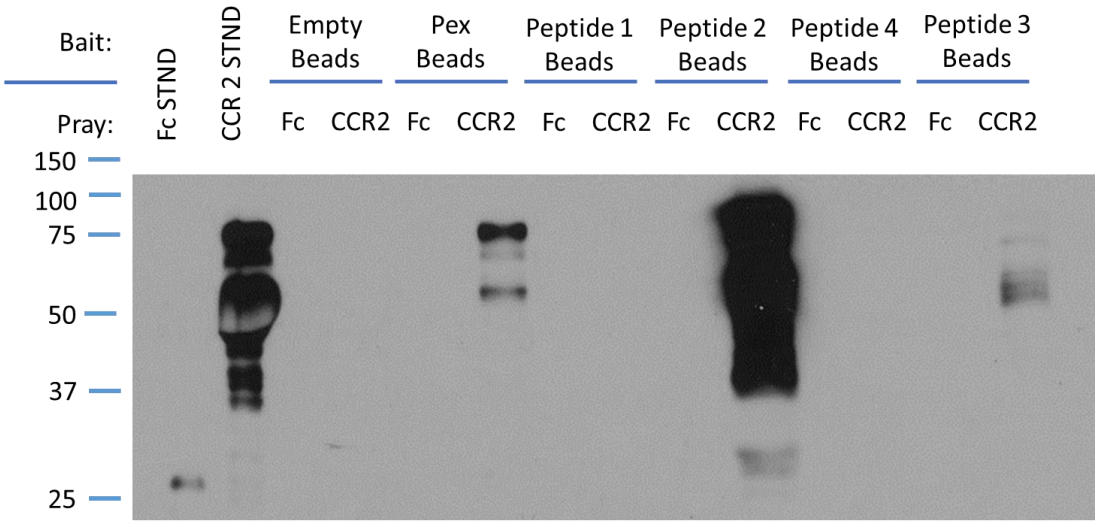

Figure 3.5 – Recombinant LRP1 CCR2 domain pulldown assays using peptide and protein coupled beads. Peptides and proteins were linked to NHS ester beads and incubated with recombinant LRP1 CCR2 with a rabbit antibody Fc domain. After strenuous washing, immunoblots were used to detect for presence of LRP1 CCR2 binding to peptides. Since the recombinant LRP1 CCR2 contained a hybrid rabbit Fc portion, a control with coupled beads and Fc only domains were used as controls to detect nonspecific binding. Fc only domain was about 25kDa, recombinant LRP1 CCR 2 fusion with Fc domain is 66.5 kDa as a monomer and 133 kDa as a dimer.

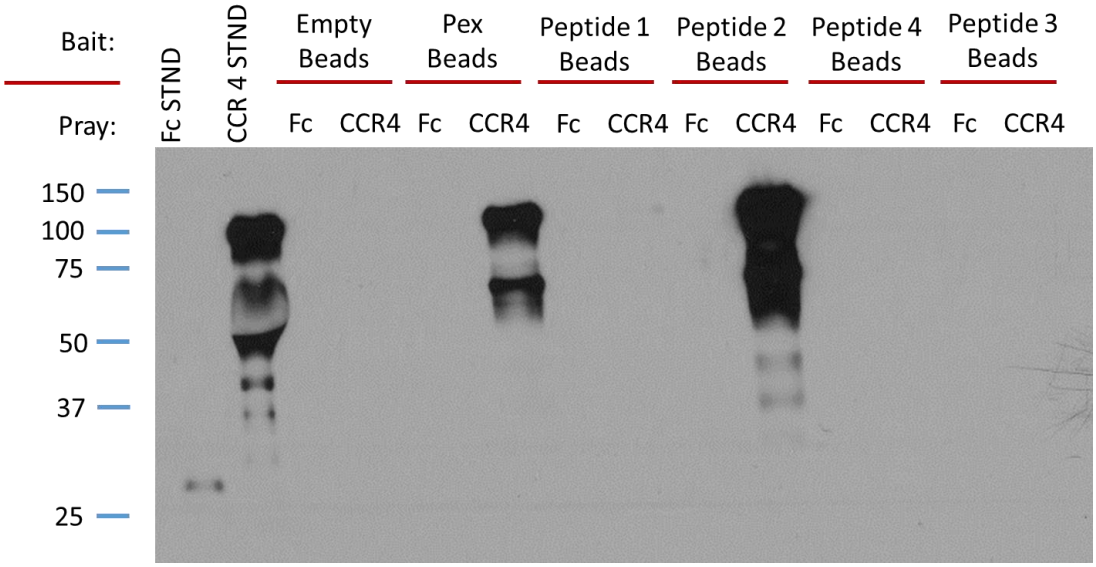

Figure 3.6 - Recombinant LRP1 CCR4 domain pulldown assays using peptide and protein coupled beads. Peptides and proteins were linked to NHS ester beads and incubated with recombinant LRP1 CCR4 with a rabbit antibody Fc domain. After strenuous washing, immunoblots were used to detect for presence of LRP1 CCR4 binding to peptides. Since the recombinant LRP1 CCR4 contained a hybrid rabbit Fc portion, a control with coupled beads and Fc only domains were used as controls to detect nonspecific binding. Fc only domain was about 25kDa, recombinant LRP1 CCR 4 fusion with Fc domain is 72.3 kDa as a monomer and 144 kDa as a dimer.

Using human LRP1 CCR constructs as well as a human Pex sequence, the peptide that should bind should be similar to the peptide that showed signaling with the hSCs (Figure 3.3). The results with the pulldown were consistent with the hSC signaling data in which Pex and peptide 2 both pulldown CCR2 and CCR4 of LRP1 (Figure 3.5 & 3.6). Peptide 3 seems to faintly bind to LRP1 CCR2 and showed some signaling, but the signaling was statistically not significant and the binding in the pulldown was not as strong. Since peptide 2 showed the most robust signaling in both signaling and its ability to pulldown and bind CCR domains, the peptide was tested for competitive binding against Pex, RAP and itself.

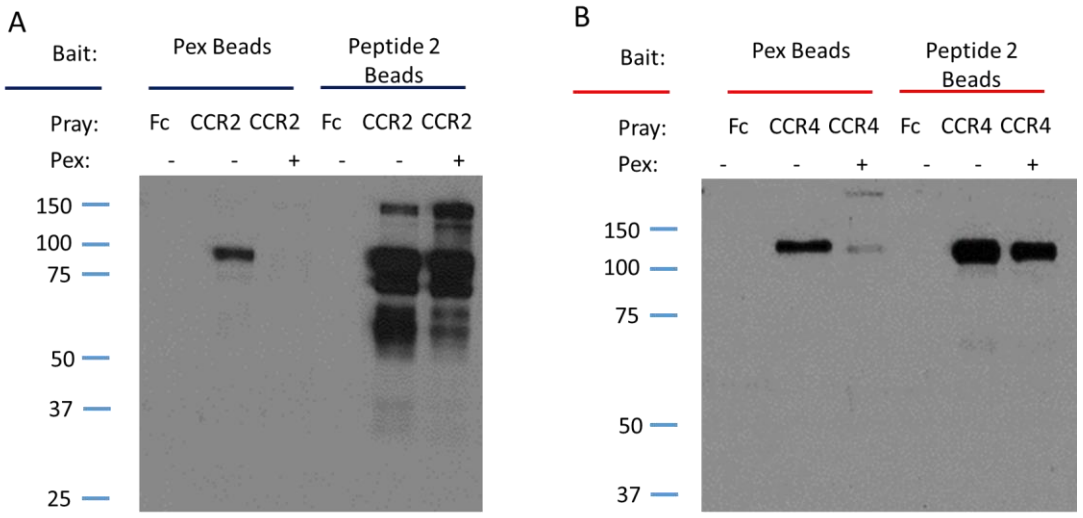

Figure 3.7 – Competitive pulldown assay with PEX using peptide or protein coupled beads and LRP1 CCR domains. Pulldown assays were conducted using the same procedure, but when LRP1 CCR2 (A) or CCR4 (B) were added, a 180 mole excess of unbound Pex was added as competition. Immunoblots of the pulldowns are shown using anti-rabbit Fc antibody.

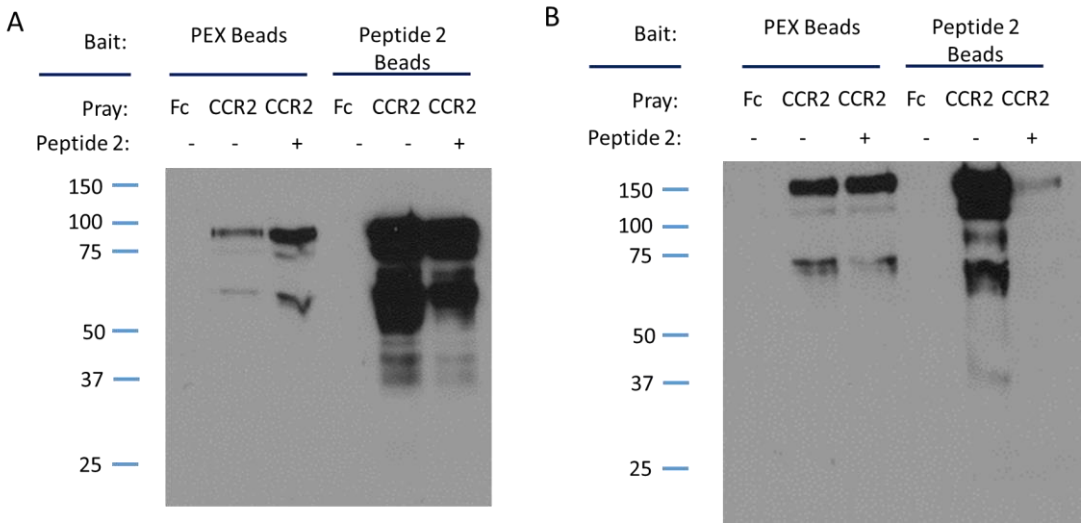

Figure 3.8 – Competitive pulldown assay with peptide 2 using peptide or protein coupled beads and LRP1 CCR domains. Pulldown assays were conducted using the same procedure, but when LRP1 CCR2 were added, a 50 fold excess (A) or 1000 mole excess (B) of unbound peptide 2 was added as competition. Immunoblots of the pulldowns are shown using anti-rabbit Fc antibody.

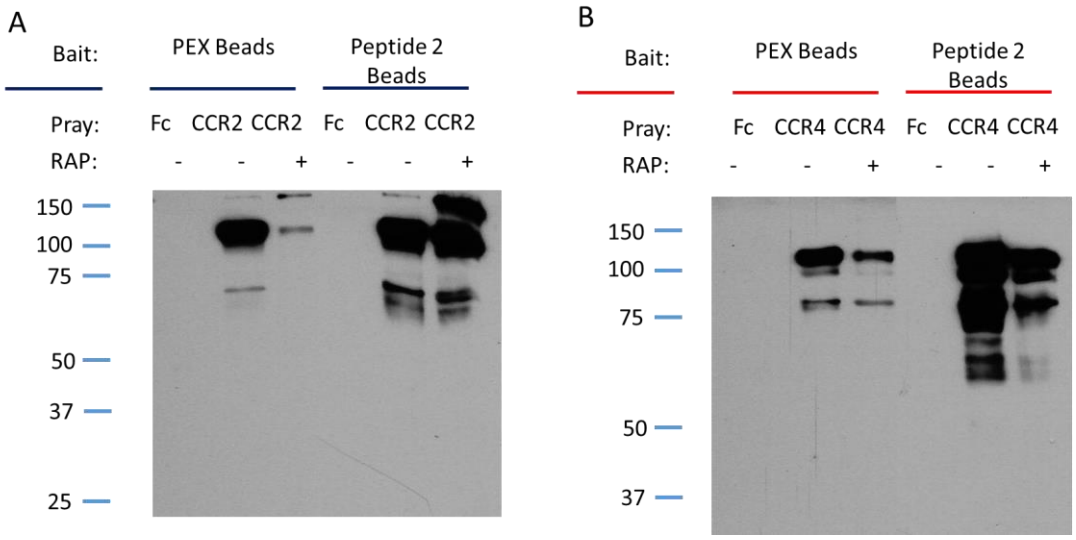

Figure 3.9 – Competitive pulldown assay with RAP using peptide or protein coupled beads and LRP1 CCR domains. Pulldown assays were conducted using the same procedure, but when LRP1 CCR2 (A) or CCR4 (B) were added, a 100 mole excess of RAP was added as competition. Immunoblots of the pulldowns are shown using anti-rabbit Fc antibody.

With the binding of peptide 2 onto LRP1 CCR 2 and 4 domains being seen though pulldowns, a question that still remained was whether or not the peptide bound to the same binding site as Pex on the CCR domains. Using competitive assays, an excess of unbound Pex was mixed with CCR 2 and 4 domains with the peptide coupled beads (Figure 3.7). Due to stock Pex being too dilute, only an 180 fold excess of Pex to CCR was added. At this excess, it was observed that Pex can compete itself off, but the peptide could not be competed off. Looking at band intensity in the CCR4 pulldown, it may look like a larger excess of Pex can complete off peptide 2, but is difficult to determine, since pulldowns are mostly qualitative instead of quantitative (Figure 3.7B). This could imply that a large fold increase was needed due to the peptides

stronger affinity for CCR 2 and 4, or that Pex and peptide 2 might bind to different sites.

Since peptide 2 could be delivered at much higher concentrations, peptide 2 was added in excess in an attempt to compete off Pex and peptide 2 from CCR 2 binding (Figure 3.8). At an 50 fold excess of peptide 2 to CCR 2, there seems to be no competition in binding from Pex or the peptide itself (Figure 3.8A). At a 1000 fold excess, the peptide is able to compete off itself, however it does not compete off Pex (Figure 3.8B). This provides stronger evidence that the peptide might bind at a different pocket or area of CCR2. Since CCR domains are much larger than Pex and peptide, it is hard to determine the number of binding regions that are available. This brings up the question of whether or not RAP can actually block binding of peptides to the CCR domains.

Biologically, RAP is the chaperone protein of LRP1 and does not associate with protein once it is on the extracellular space of the cell. Experimentally, RAP can be used to bind to the CCR domains of LRP1 to block ligand binding.[17,34] If RAP binds to the CCR domains in the pulldown, then both Pex and peptide 2 should be blocked from binding to the CCR domains and not be pulled down. From the pulldowns with RAP (Figure 3.9), there is evidence to show RAP blocks blinding of Pex to CCR 2 and 4, but not completely as shown though signaling data. Peptide 2 seems to not show any reduction in binding by RAP. The absence of complete blocking by RAP for

Pex binding can be due to the limited molar excess of RAP because of the multiple binding sites of the CCR domains. Peptide 2's ability to evade blocking by RAP can be attributed to it's smaller size. Since most ligands of LRP1 are much larger than a 22 amino acid peptide, sterics can play a role in RAPs inability to block peptide binding to LRP1 CCR domains. Another possibility is that the RAP's binding to CCR domains are different binding pockets to that of the peptide. These questions currently cannot be answered though the pulldown assays, but may be able to answered though other molecular assays to probe the binding of peptide 2 to LRP1.

3.3 *In vivo* rat sciatic nerve crush assay

Ultimately, all of the SC signaling and pulldown assays were used to determine if a peptide could be made from Pex to activate SCs and treat neuropathic pain. In vitro cell signaling methods showed that peptide 2 can signal like Pex and the pulldown showed that peptide 2 binds to LRP1. To determine if these peptides can have a biological effect, sciatic nerve crush models can be used to directly study the effect of peptides and proteins on the nerve.

After an injury in the peripheral nerve, SCs have been shown to upregulate the expression of LRP1 and MMP9, which play an important role in activating these cells towards the repair phenotype.[9,15] After injury, since SCs contain more LRP1, they would be more prone to activation if Pex or peptides are injected to the injury site. In previous studies, rat sciatic nerves

were surgically crushed and after 24 hours, injected with Pex, and found to have an increase in ERK1/2 and AKT signaling in the distal, or away from the spinal cord, portions of the sciatic nerve. Along with ERK1/2 and AKT signaling, pCJun has also been seen to be an important signaling pathway for activation of recovery SCs.[13] If peptide 2 was to act similar to Pex, then peptide 2 should also show strong activation of ERK1/2, AKT and pCJun signaling in injected into the nerve 24 hours after crush injury. The activation of these proteins can be verified from harvesting the nerve and immunoblotting the nerve lysates.

Although previous studies have shown robust ERK1/2 and AKT signaling though Pex injections, I was unable to reproduce that data due to high background from PBS injections in some repetitions of work, thus making the fold increase seem insignificant. The high background can be due to the amount of harvested nerve and the distance from the crush site, which affects the amount of signaling seen. From this data set, the activation does not look significant; however, if more repetitions of these experiments were carried out, peptide 2 could showed promise in the signaling though these pathways, like its parent Pex.

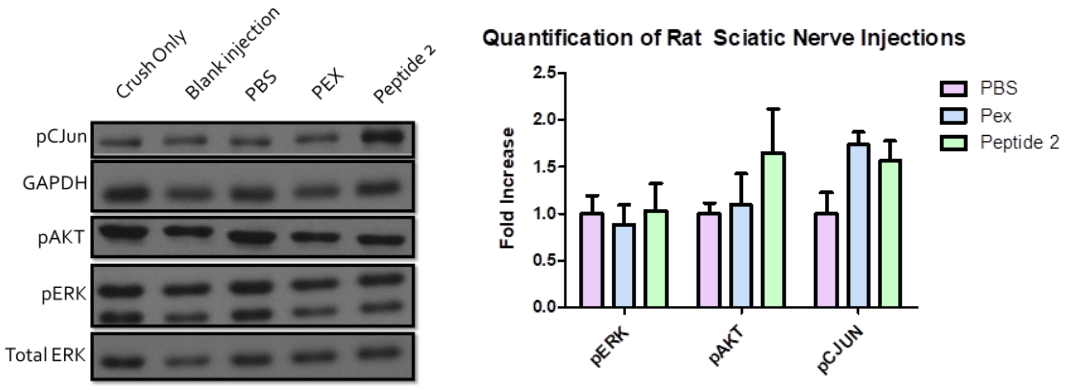

Figure 3.10 – Immunoblots and quantification of distal ends of rat sciatic nerve crush and injection. 24 hours after crush injury, injections were used to deliver compounds to the injury site. After 5 minutes, the nerves were harvested, and the distal, proximal and injury site were segregated before lysing. Immunoblots were used to analyze protein content.

3.4 Conclusions & Future Directions

From the 4 peptides that were made from Pex as a model, 2 peptides showed promise in terms of mimicking Pex's ability to bind and signal through LRP1. Peptide 1 showed signaling with rSCs, whereas peptide 2 showed signaling through hSCs. When using LRP1 pulldowns, peptide 2 showed binding to human LRP1 CCR2 and 4, but could not be competed off with Pex or RAP. The inability to compete off peptide 2 though RAP or Pex may indicate a different binding site or that the peptide is too small to be blocked by either of these ligands. In rSC signaling, peptide 1 showed signaling, but it did not show binding to recombinant human LRP1 CCR2 and 4, which may suggest that there are differences in LRP1 binding in rats and humans or peptide 1 can be signaling in rSCs though a different receptor than LRP1.

Unfortunately, there was not enough data to confirm the significance of peptide 2 showing signaling in vivo due to the low number of sample size and

the amount of background. However, this does not signify that peptide 2 has no activity in vivo. Peptide 2 can be delivered and other signaling outputs, such as mRNA, can be interpreted to analyze biological activity.

From this point onward, there are many directions that this project can progress. The biological activity of peptide 2 can be further explored using other biological assays, such as migration assay and LRP1 silencing experiments. The effect of peptide 1 on rSC and peptide 2 on hSCs can also be a point of interest in assessing how LRP1 models might differ. LRP1 silencing experiments can also be used to discern if peptide 1 is signaling though LRP1 or though a different signaling pathway in rSCs. More molecular analysis of peptide 2 can be studied as well. In chapter 4 I will focus on shortening peptide 2 in an attempt to scope out the binding region of peptide 2.

3.5 Experimental methods

Primary Rat and Human Schwann Cell (SC) cultures. Rat SCs (rSCs) were cultured from 1-day old Sprague-Dawley rat sciatic nerves and enriched for SCs using Cytarabine (Sigma C-1768), Anti-Thy1.1 antibody (Sigma M-7898) and rabbit complement (Sigma S-7764) as previously described in (Brockes, et al., 1979). SCs were grown in humidified incubators at 37°C and 5% CO_2 and verified by immunofluorescence using S-100 for at least 95% purity. SCs were grown on poly-d-lysine (PDL) coated plates in Low Glucose DMEM

containing 10% heat inactivated fetal bovine serum (FBS), 100 U/mL penicillin, 100µg/mL streptomycin, 21 µg/mL bovine pituitary extract, and 4 µM forskolin. Human SCs (hSCs) were purchased from ScienCell (Cat. 1700) and grown according to manufacturer's product description. Corresponding Schwann Cell Medium (Cat. 1701), which consisted of 5% FBS, Schwann Cell growth supplement and 100 U/mL penicillin, 100µg/mL streptomycin, was used to culture hSC in humidified incubators at 37°C and 5% CO_2.

Recombinant MMP-9 Hemopexin domain fusion protein (Pex). Recombinant Pex was produced as a GST-fusion protein using pGEX-5X-2 plasmid (GE Health Sciences 28954554). The gene sequence for human Pex was synthesized by Genscript with EcoRI and XhoI restriction sites, which was spliced into the pGEX plasmid and sequence verified by Eton Bioscience. Expression of recombinant fusion protein GST-PEX was expressed as previously described in (Mantuano, et al., 2008).

In short, plasmid was transformed into BL21 (DE3) pLysS Competent Cells (Promega L1195) following protocol provided by manufacturer. Bacterial colonies were expanded in 1L of LB media with 100 µg/mL Ampicillin and 34 µg/mL in a baffled flask shaken at 150 rpm in a 37°C incubator. At an OD600 of 0.60 and IPTG was added at a final concentration of 0.1 µM to induce protein production. The cells were harvested by centrifugation in 2000 xg for 10 minutes, then lysed with a pH 7.4 50mM tris buffer with 250mM sodium chloride, 1.0 mM PMSF, 1.0mM dithiothreitol and 1% Triton X-100, and snap

frozen. The lysate was sonicated and spun at 12K xg for 30 minutes and the pellet was collected. The pellet was re-suspended in a 7.0M Urea, 7.4 50mM tris buffer for 1 hour at 4°C with gentile shaking. The suspension was spun for 1 hour at 18.5K xg and the supernatant was collected. The supernatant was dialyzed overnight with 3 changes of pH 7.4 1x PBS buffer to remove urea and refold the protein. The supernatant was gently mixed at 4°C with glutathione beads overnight. The beads were then washed with pH 7.4 1x PBS buffer with 150mM sodium chloride. Protein was eluted using a pH 8.0 50mM Tris buffer with 20mM reduced glutathione, 0.2M sodium chloride and 0.2% SDS. Eluent was then concentrated and dialyzed at room temperature overnight with 3 changes of pH 7.4 1x PBS to remove excess glutathione and SDS. Protein concentration was calculated using bicinchoninic acid (BCA) assay (ThermoFisher 23225).

PEX plasmid sequence. Pex sequence was made with EcoRI and Xhol overhangs to be spliced into pGEX-5X-2 plasmid. Pex sequence was spliced into the pUC vector by GenScript with the following sequence: (EcoRI)GAATTCGATGCCTGCAACGTGAACATCTTCGACGCCATCGCGGA
GATTGGGAACCAGCTGTATTTGTTCAAGGATGGGAAGTACTGGCGATTC
TCTGAGGGCAGGGGGAGCCGGCCGCAGGGCCCCTTCCTTATCGCCGA
CAAGTGGCCCGCGCTGCCCCGCAAGCTGGACTCGGTCTTTGAGGAGC
GGCTCTCCAAGAAGCTTTTCTTCTTCTCTGGGCGCCAGGTGTGGGTGTA
CACAGGCGCGTCGGTGCTGGGCCCGAGGCGTCTGGACAAGCTGGGCC

TGGGAGCCGACGTGGCCCAGGTGACCGGGGCCCTCCGGAGTGGCAG

GGGGAAGATGCTGCTGTTCAGCGGGCGGCGCCTCTGGAGGTTCGACG

TGAAGGCGCAGATGGTGGATCCCCGGAGCGCCAGCGAGGTGGACCGG

ATGTTCCCCGGGGTGCCTTTGGACACGCACGACGTCTTCCAGTACCGA

GAGAAAGCCTATTTCTGCCAGGACCGCTTCTACTGGCGCGTGAGTTCC

CGGAGTGAGTTGAACCAGGTGGACCAAGTGGGCTACGTGACCTATGAC

ATCCTGCAGTGCCTCGAG(Xhol)

Radiolodine labeling of Pex. Pierce Iodination Beads (Cat. 28665) were used to radioactively label Pex using Sodium Iodide (^{125}I). Manufacturer's protocol was followed. In summary, beads were washed with 1x PBS and 1mCi of ^{125}I was added and incubated at room temperature for 5 minutes. About 25ug of Pex was added to the beads and allowed to react for 10 minutes. The solution was collected and removed from the beads. A PD-10 desalting column (GE 17085101) was used to remove excess Iodine and collect labeled Pex. Fractions were collected, and quantified using a gamma counter and Pex's 280nm extension coefficient.

Homologous competitive binding assay of Pex to hSCs. hSCs that were plated at 100k cells 24 hours prior were placed in starvation media which was complete media without FBS. Cells were placed in a 4°C cold room and allowed 15 minutes to equilibrate to the temperature. Starvation media was then removed and replaced with starvation media containing 2nM radiolabeled Pex (hot Pex) with varying concentrations of unlabeled Pex (cold Pex) ranging

from 500 mole excess of to 31.25 mole excess of cold pex cold to hot Pex in 2 fold serial dilutions. Cells were incubated with ligands for a total of 4 hours to allow equilibrium to occur. After 4 hours, the cells were washed thrice with cold pH 7.4 HBSS buffer with 10mM Hepes and 1mg/mL of BSA. After the last wash, the cells were lysed with 0.1M NaOH and 1%SDS. Cell lysates were quantified by a 1470 Wallac Wizard Automatic Gamma Counter and Lowry protein assay (Pierce 23240).

Recombinant receptor associated protein (RAP). Recombinant RAP was produced as a GST-fusion protein using a pGEX plasmid previously reported in (Mantuano, et al., 2008).

In short, plasmid was transformed into BL21 (DE3) pLysS Competent Cells (Promega L1195) following protocol provided by manufacturer. Bacterial colonies were expanded in 1L of LB media with 100 µg/mL Ampicillin and 34 µg/mL in a baffled flask shaken at 150 rpm in a 37°C incubator. At an OD600 of 0.60 and IPTG was added at a final concentration of 0.1 µM to induce protein production. The cells were harvested by centrifugation in 2000 xg for 10 minutes, then lysed with a pH 7.4 50mM tris buffer with 250mM sodium chloride, 1.0 mM PMSF, 1.0mM dithiothreitol and 1% Triton X-100, and snap frozen. The lysate was sonicated and spun at 12K xg for 30 minutes and the supernatant was collected. The supernatant was gently mixed at 4°C with glutathione beads overnight. The beads were then washed with pH 7.4 1x PBS buffer with 150mM sodium chloride. Protein was eluted using a pH 8.0 50mM

Tris buffer with 20mM reduced glutathione, and 0.2M sodium chloride. Eluent was then concentrated and dialyzed at room temperature overnight with 3 changes of pH 7.4 1x PBS to remove excess glutathione and SDS. Protein concentration was calculated using bicinchoninic acid (BCA) assay (ThermoFisher 23225).

Immunofluorescence of hSC for LRP1. PDL coated glass coverslips were plated with 50k hSCs and grown until 90% confluency in complete media. For fixing, the cells were washed with cold PBS and fixed with warm 4% paraformaldehyde in pH 7.4 PBS for 15 minutes. The fixed cells were washed again with PBS, and permeabilized for 10 minutes in PBS with 0.5% Triton X-100. Cells were then blocked for 30 minutes with 5% sera of secondary host antibodies in 22.52mg/mL glycine in pH 7.4 PBS with 0.1% Triton-X 100. Cells were then incubated with primary antibodies at manufacturer's recommended concentration in the same buffer as the blocking buffer over night at 4°C. After incubation, cells were washed in PBS with 0.1% Triton-X100 and then incubated with secondary antibody at manufacturer's recommended concentration in the same buffer as blocking buffer for 1 hour. Cells were then thoroughly washed and mounted in DAKO media containing DAPI. Images were taken at the UCSD neuroscience microscopy core using an Olympus FV1000 confocal microscope with SIM scanner.

Recombinant LRP1 ligand binding domains CCR2 and 4 fusion protein. Cryopreserved CHO cells containing LRP1 CCR2 and 4 domain sequences

spliced into a pFUSE vector containing rabbit Fc antibody domain were donated from the Gonias lab (See Stiles et al., 2013). Vector sequences were isolated and verified for containing sequences of respective fusion proteins. CHO cells were grown in DMEM low glucose with 1x non-essential amino acids, 2mM glutamine, 10% heat inactivated FBS, and 100 U/mL penicillin, 100µg/mL streptomycin. Cells were selected for vector using Zeocin at a final concentration of 300ug/mL. Once cells reached 70% confluency, cells were changed to expression media PowerCHO 2 (Lonza 12-771Q) containing 4mM glutamine, 100 U/mL penicillin, 100µg/mL streptomycin and 300ug/mL zeocin. Media was collected at 24 and 48 hours. Collected media was filtered using 0.22um vacuum filter and concentrated to 50mL using a spin column. Concentrated media was incubated with protein A beads overnight with gentle shaking at 4°C. Beads were then washed with 2 bed volumes of 1xPBS, and 1 bed volume of PBS with 5mM EDTA and PBS with 500mM sodium chloride. Protein was eluted with a pH 3.0 0.1M citric acid buffer. Eluted proteins were dialyzed overnight in pH 8.0 100mM Tris at 4°C with 3 changes of buffer and protein concentration was determined by BCA.

In vitro SC signaling assays. SCs (50,000 cells) were plated on poly-D-lysine (PDL) coated 6 well plates and grown in complete media until 80% confluent. The cells were then washed with serum free media (SFM) and incubated in SFM for an hour before treatments. Substrates were then added to each well and cells were treated for 10 minutes. Media was aspirated off and cells were

washed with cold PBS before adding cold RIPA buffer (1% Trion-X, 5% Deoxycholate, 1% SDS, 20mM Vanadate and EDTA free protease inhibitor) to lyse the cells. Cell lysates were centrifuged at 20K x g for 15 minutes at 4°C and the supernatant was collected. BCA was used to quantify the protein concentrations and proteins were analyzed by immunoblot.

Pull down assays. NHS-activated sepharose beads were used to immobilize peptides or PEX. Beads were washed and prepared according to GE manufacturer's protocols. PEX or peptides were introduced to the washed beads with a 0.02M pH 8.0 phosphate buffer and allowed to react for 2 hours at room temperature with top down agitation. Remaining NHS-beads were quenched with 0.1M ethanolamine at pH 8.5 for another hour. Beads were then blocked for non-specific binding using 0.5% BSA in pH 8.0 phosphate buffer for 30 minutes at room temperature. Prey protein (CCR2 or CCR4) were added and allowed to incubate for 1hour at room temperature with top down agitation. In competitive ligand binding assays with GST-RAP, 5 molar excess of RAP was mixed added with CCR2 or CCR4 prior to being introduced to the beads. Beads were stringently washed with pH 8.0 phosphate buffer in 0.1% Tween 20. Sample buffer was added to the beads, boiled and analyzed by immunoblot.

Sakaguchi's reaction for arginine. Micro-scale reactions of Sakaguchi's reactions were carried out in 1.5mL microcentrifuge tubes. Peptide and protein coupled beads were prepared according to procedure in the pull down assay.

After the beads were washed several times for un-coupled proteins, they were placed on ice. The supernatant of the beads were removed after centrifugation and replaced with 50 µL of a 10% sodium hydroxide solution with 25 µL of an 0.02% 1-naphthol solution in water. The mixture was mixed well and chilled on ice. Once chilled, 10 µL of a sodium hypobromite (2% bromine in a 5% sodium hydroxide in water) was added to the mixture and shaken. Immediately 50 µL of a 40% urea solution in water was added to the mixture. Microcentrifuge tubes were allowed to sit for 2 minutes before checking for color. Note that the color dissipates in 10 minutes if not checked.

In vivo rat crush assay. 250g Sprague Dawley rats (IUCUC protocol S12331) were placed under anesthesia using 2% isoflurane in oxygen and opened on the left side along the femur. The sciatic nerve was crushed with flat headed forceps for 15 seconds and the fascia was sown closed and skin stapled for 24 hours. After 24 hours, the nerve was re-opened and the crush injury site was found. Samples, up to 2 uL, were injected into the nerve at the crush site and allowed to incubate for 5 minutes before nerves were collected. Nerve samples of 5 mm were collected just distal and proximal from the crush site. Nerves were the placed in RIPA buffer (1% Trion-X, 5% Deoxycholate, 1% SDS, 20mM Vanadate and EDTA free protease inhibitor), agitated with motar and pestle, and then centrifuged to collected soluble nerve lysates. Lysates were quantified for protein amount using a BCA assay and analyzed for protein content using immunoblots.

3.6 Acknowledgement

Many of the biochemical skills I learned and developed were thanks to the many lab members in the Campana and Gonias Lab. Kenneth Henry, PhD. was the first to train me on Schwann cell prep, culturing and signaling assays. Thanks to Dr. Elisabetta Mantuano, PhD. and Pardis Azmoon for continually helping with trouble shooting and helping with signaling assays. Hyo Jun Kwon and Andi Flütsch, PhD. have also been very important in the development and progress in SC signaling assays.

Pex and RAP were plasmids made by Kenneth Henry, PhD. and the purification methods were optimized by him and Pardis Azmoon. LRP1 CCR domain recombinant protein plasmids were donated by the Gonias lab. These proteins were cultured and purified by Andi Flütsch, PhD.. He also was important in providing assistance in troubleshooting and developing the pulldown assays.

Radiolabeling of Pex and training in radioisotope safely was thanks to Emilia Laudati. Emilia was also a great help in the analysis and troubleshooting Pex competitive binding assays. All handling and safety of radioactive waste was thanks to Andrew Gilder and his trainings.

Immunostaining of hSCs and training came from many people in various labs. Immunostaining techniques and troubleshooting help came from Kevin Cao, PhD. and Patricia Gaffney, PhD.. Handling and fixing of hSCs on

glass coverslips procedures and troubleshooting help came from Kenneth Henry, PhD and Andi Flütsch, PhD..

All surgical methods and skills were taught to me by the various visiting Japanese scholars in the Campana lab. Masataka Shibayama, M.D. PhD. and Go Kubota, M.D. PhD. played a large role in training me in surgical techniques and methods of finding and producing sciatic nerve models in rats.

Chapter 3 is currently being prepared for submission for publication as a communication in the development of peptides that can cause signaling in Schwann cell. John Kim, Jerry Yang, and Wendy Campana. This dissertation author is the primary researcher and author of this material.

3.7 Supplemental Information

Purification of recombinant fusion GST-Pex protein

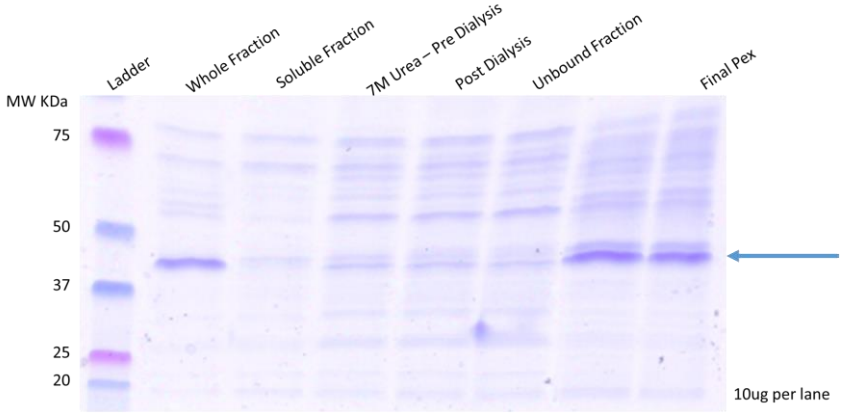

Figure S3.1 – Coomassie of the purification of recombinant fusion protein GST-Pex. Fractions representing the major steps in GST-Pex purification are shown on the 10% acrylamide gel using a Coomassie stain. GST-Pex is found in the insoluble fraction that requires a urea denaturation step to re-solubilize the protein. Dialysis is used to refold GST-Pex, which can then be purified though affinity chromato1y using a glutathione column. Final GST-Pex has a molecular weight of 46kDa.

Starvation time effect on ERK1/2 signaling in SCs

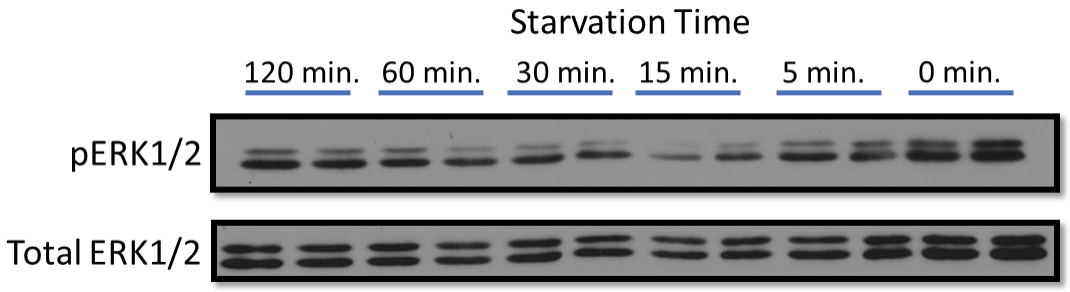

Figure S3.2 – Human Schwann cell starvation affecting ERK1/2 signaling. hSCs were starved for varying time points while in starvation media, which is absent in FBS. ERK1/2 background signaling is seen to reduce overtime, and then start to re-appear after a certain time point.

Recombinant fusion GST-RAP protein

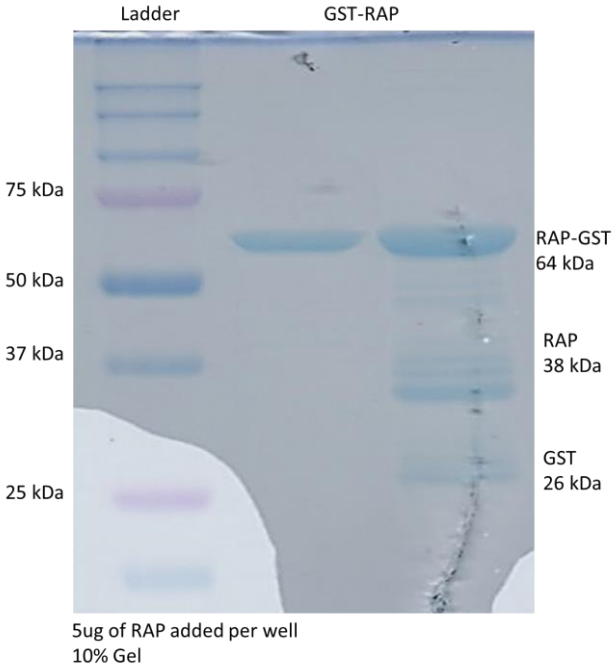

Figure S3.3 – Coomassie of recombinant fusion protein GST-RAP. In the purification of GST-RAP, this protein is found in the soluble fraction and can be isolated using BioRAD FPLC systems with affinity and size exclusion chromatography. The final fractions of GST-RAP are shown on this 10% acrylamide gel Coomassie stain.

Sakaguchi’s reaction for arginine on beads

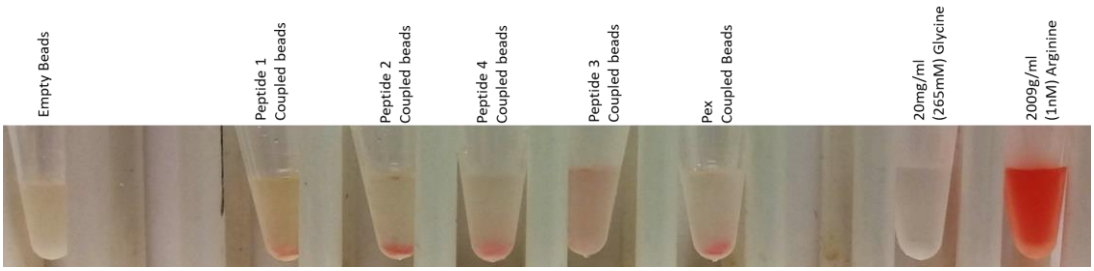

Figure S3.4 – Sakaguchi’s reaction for arginine qualitative assay on peptide or Pex coupled beads. Using NHS-ester beads, peptides or Pex was conjugated onto the beads. Sakaguchi’s reaction was used to verify if the beads were coupled to targets after the reaction. Sakaguchi’s reaction is a qualitative test that turns red in the presence of arginine. Each peptide contained at least one arginine residue. The presence of red at the bottom tips of the microcentrifuge tube verify that peptides are coupled to the beads, which are prone to settle.

Chapter 4

Verification and Modifications of Peptide 2

4.1 Molecular analysis of Peptide 2

With peptide 2 showing biological and binding activity to LRP1, there are many questions about how and what sequence amino acids of the peptide can be causing this activity. There are biochemical methods for analyzing and determining peptide binding. One of the methods is to use an alanine scan to check which residue or group of residues that affect the binding of the peptide.[26,40] Modifications, truncations and scrambled libraries of the peptide can also be made to study how the amino acid sequence affects secondary structure and binding to the ligand. For this chapter, I will be mainly focusing on the key amino acids that may play a role in the binding of peptide 2 to LRP1, and how we used a molecular approach to understanding of the key residues that may play a role in binding.

An important control to show specificity of the peptide to a ligand is using a scrabbled peptide, which contains the same amino acids as the parent, but in different order. This control is important in showing that the sequence of the amino acid residues are important for the binding of the peptide to the target. To form a scrambled peptide, a randomizer was used to generate a library of scrambled sequences of peptide 2 (Table 4.1). The library was then compared to an Eukaryotic linear motif (ELM) library that scans for short amino acid sequences that have been known to have biological activity.[41] Those with similar ELMs to peptide 2 were removed from the list until a more condensed list was produced (Table 4.1). Then the remaining sequences were analyzed

for secondary structure. Since peptide 2 has high amounts of secondary structure, finding a scrambled peptide that contained less secondary structure and was drastically different than the parent peptide was important in the selection process. Although multiple scrambled peptides could have been synthesized, one of the peptide sequences that fit the criteria was randomly selected from the list of randomized peptides sequences (Table 4.1). The selected scrambled peptide had the sequence, "FMSQVGGFRARDLRLGRWLSKK." This peptide will be tested and used along side peptide 2 to ensure that peptide 2's specific sequence is what caused binding and signaling activity.

Table 4.1 – Peptide 2 Eukaryotic Linear Motif (ELM) analysis and scramble peptide sequences. Scrambled peptide sequences of peptide 2 were randomly generated using a scramble generator. The scrambles were then compared for shared peptide sequences with the original, ELM generators to evaluate potential activity of scramble peptides. Peptide highlighted in peach was the scrambled peptide chosen.

	Sequence	Matching ELM motifs	Largest peptide shared with original sequence	Length of longest peptide shared with original sequence
Original sequence	SGRGKMLLFSGRRLWRFDVKAQ	CLV_PCSK_KEX2_1, LIG_CYCLIN_1, LIG_BIR_II_1, MOD_Cter_Amidation, MOD_GlcNHglycan, CLV_NDR_NDR_1, TRG_LysEnd_APsAcLL_1, CLV_PCSK_SKI1_1		22
Randomly scrambled	GKMKARLSDWQVGFRLGLRFRS	MOD_PKA_2, TRG_PEX	GKM	3
	GLRWRSVGGFDRFASMLQKLKR	MOD_PK_1	WR	2
	LRVKMRFRDQKGGWSARLFLGS	MOD_GlcNHglycan, CLV_PCSK_SKI1_1	VK	2
	DGKKLRSRSWALRQFGLGFMRV	LIG_14-3-3_3, MOD_Cter_Amidation	GK	2
	RVSKAWRMSRLGDRLKLQGGFF	MOD_PKA_2, LIG_MAPK_1, LIG_PDZ_3	KA	2
	FMSQVGGFRARDLRLGRWLSKK	LIG_CYCLIN_1	RL	2
	DSAWMKFSRFLRGVQRLKGRGL	MOD_GlcNHglycan	GRG	3

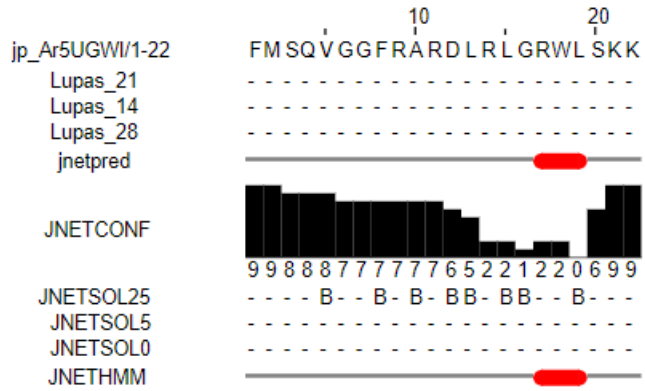

Figure 4.1 – JPred analysis of the chosen scrambled peptide 2. The red barrels shown represent the likelihood of alpha helixes to form with the selected peptides. The confidence for these predictions is shown under JNETCONF.

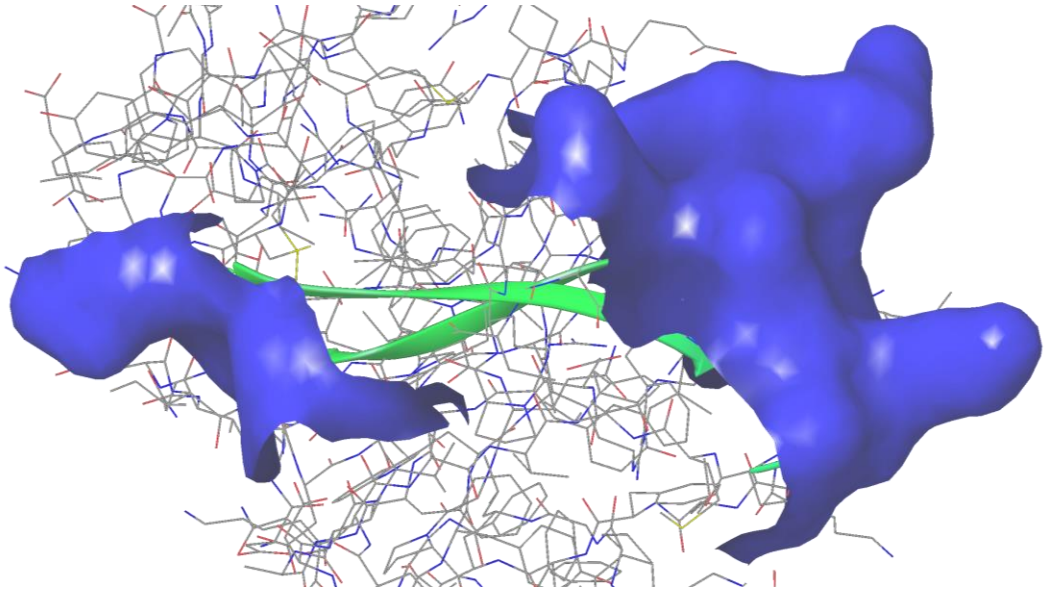

Figure 4.2 – In-depth look at peptide 2 inside MMP9 hemopexin domain. The green ribbon represents the peptide sequence inside the protein. The thicker lines with a directionality arrows represents β-sheets formed from the peptide sequence. The blue represents the peptide sequence that are on the surface of the MMP9 hemopexin domain.

Using the crystal structure of MMP9 Hemopexin domain (PDB: 1ITV), it can be seen that the β-sheet structure of the peptide is buried inside of the protein, and only the loop and tail ends of the secondary structure are on the surface (Figure 4.2).[27] As a free peptide outside of the protein, the peptide

seems to maintain the β-sheets like structure with similar amino acids (Figure 2.5). If the peptide is interacting with LRP1, similar to how it is organized in Pex, it can be hypothesized that the β-sheets would play an important role in maintaining the structural integrity of the peptide, but not in binding. Whereas, the loop and tail ends of the peptide can play a larger role in binding to LRP1. Previous studies with ligands of LRP1 found that positively charged amino acids of the ligand played a key role in binding to the CCR domains of LRP1.[42] With this in mind, select changes in residues can be made to test for the importance of the each amino acid in binding of peptide 2 to LRP1.

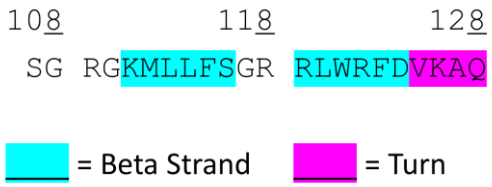

Figure 4.3 – Peptide 2 sequence with secondary structure and 1ITV residue numbers. Peptide 2's sequence is shown with highlighted secondary structure from JPred predictions. Residue number written on top are based on the residue sequence of MMP9 Hemopexin domain (PDB 1ITV).

Peptide 2 contains 22 amino acids with the sequence SGRGKMLLFSGRRLWRFDVKAQ. About 12 residues are involved in the β-sheets structure of the peptide (Figure 2.5, 4.3). Outside of the β-sheets structure, there are 4 positively charged amino acids – Arg 109, Arg 118, Arg 119, and Lys 126 (Figure 4.3). Including the β-sheet residues, there are a total of 6 positively charged amino acids that include Arg 122 and Lys 111. Each of these residues play a role in the shape of the hydrophilic surface and any secondary structure of peptide 2. In the parent protein of PEX, only the

residues outside of the β-sheets should play a role in binding since the β-sheets itself is buried inside of the protein. Thus, only the residues found outside of the β-sheets will be highlighted.

Arg 109 (Figure 4.4) and Lys 126 (Figure 4.6) are located on the N-terminal and C-terminal sides respectively of the β-sheet structure, or the tail ends, of the peptide. Both of these ends make up a significant part of the surface interacting residues in peptide 2. Since there are no secondary structures on either end, these structures have the most degree of freedom in this peptide sequence. On the other end of the β-sheet structure, there are 2 neighboring arginine residues 118 and 119 (Figure 4.5). These arginine residues are located on the turn part of the peptide connecting the two parts of the β-sheet structure. Since the turn is bound by the β-sheet, this region and the two arginine residues are more structured compared to the tail ends of the peptide. A method of studying if these amino acids and determining which play a large role in binding, would be to replace these residues with another residue, such as alanine; or make a deletion of peptides or portions of the sequence itself.[40]

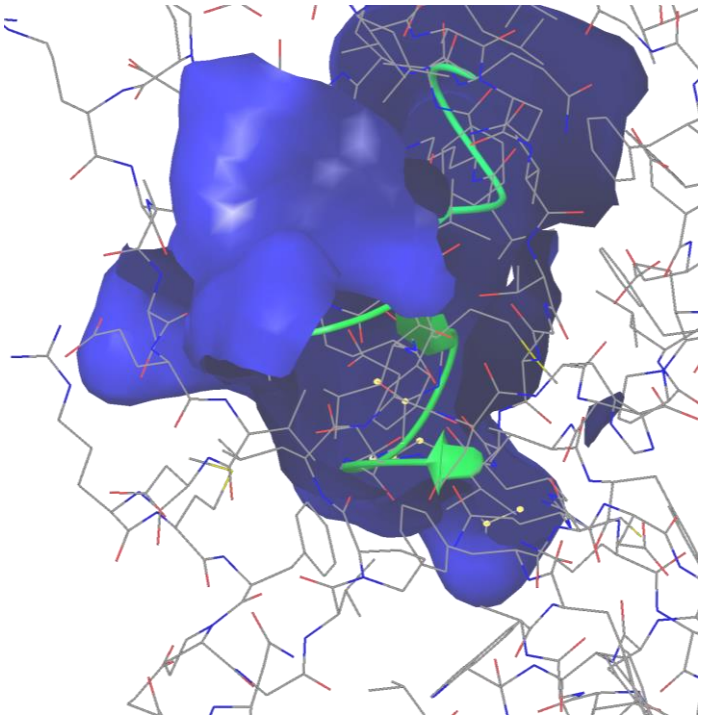

Figure 4.4 – Highlighted view of Arg 109. Residue Arg 109 is highlighted in yellow dots alone the peptide, highlighted in green, and the surface interaction shown in blue. This residue is located at the N-terminal tail end of the β-sheets.

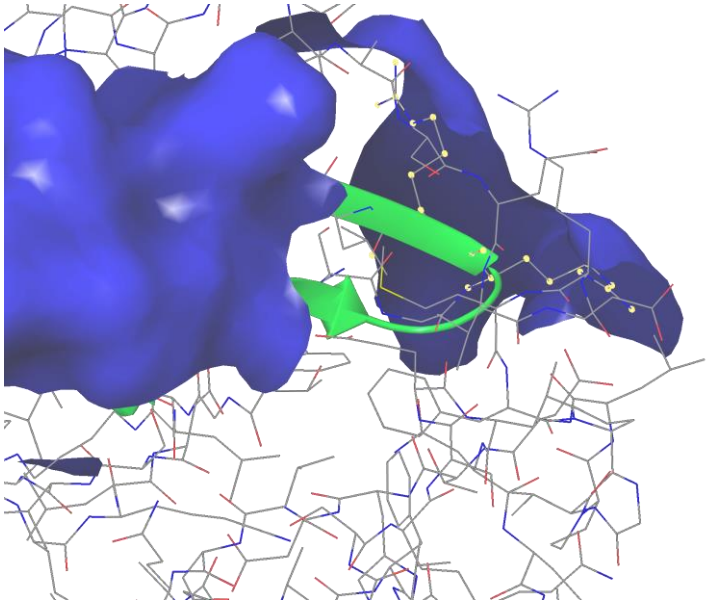

Figure 4.5 – Highlighted view of Arg 118 and 119. Residues Arg 118 and 119 are highlighted in yellow dots alone the peptide, highlighted in green, and the surface interaction shown in blue. This residue is located at the loop between the β-sheets. The two arms of the arginine residue make up a large portion of the surface residues on the loop end of the peptide.

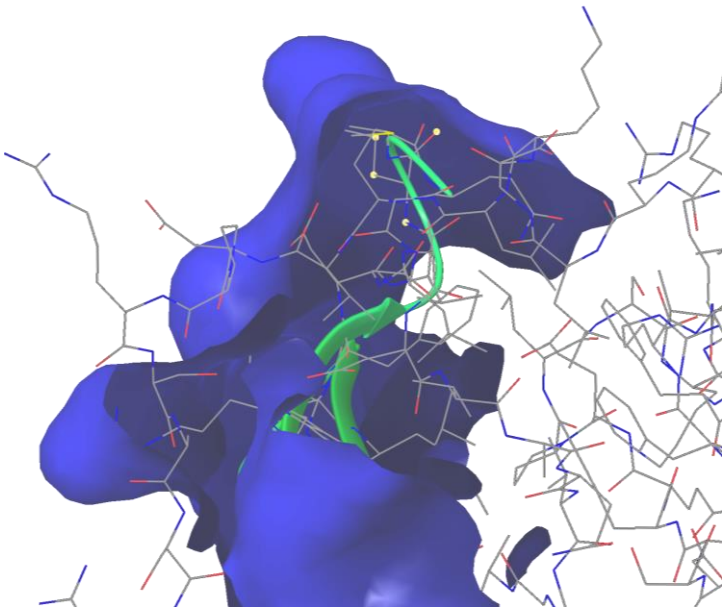

Figure 4.6 – Highlighted view of Lys 126. Residue Lys 126 is highlighted in yellow dots alone the peptide, highlighted in green, and the surface interaction shown in blue. This residue is located at the C-terminal tail end of the β-sheets.

Table 4.2 – Summary of Sequences derivatives of peptide 2. Names of the peptides will be name referred to in this dissertation.

	Named	Sequence	# of residues
Original Peptide 2	Peptide 2	SGRGKMLLFSGRRLWRFDVKAQ	22
Srambled Peptide 2	Peptide 2SCR	FMSQVGGFRARDLRLGRWLSKK	22
Shortened Peptide 2	Peptide 2Red	GKMLLFSGRRLWRFDV	16

With the secondary structure of peptide 2 and with 4 possible important amino acid residues, one possibility was to reduce the peptide by removing a segment. One hypothesis was that the β-sheet structure and loop containing Arg 118 and 119 was playing a role in binding to CCR domains because these portions of the peptide would contain the more rigid structure than the tail ends. The tail ends on both sides of the β-sheet were hypothesized to have the least amount of structure since the residues were not tied down or organized by any

secondary structure. With this in mind, and to study how this peptide might be binding, the peptide was reduced to a modified 16 amino acid sequence that only contained the β-sheet and the turn residues. This peptide will be called “peptide 2RED” and contains the amino acid sequence of “KMLLFSGRRLWRFD.” Compared to peptide 2, peptide 2RED had drastically different properties. This peptide was not soluble in water, and was partly soluble in 10% DMSO in water. Since the peptide was so insoluble in water, it was difficult to study the secondary structure of the peptide through CD like the other peptides. Also, since the peptide was under 20 residues long, JPred could not be used to make any predictions about the secondary structure that might be in the sequence. Without any of these analytical tools to study secondary structure, the peptide was used in functional assays to test for activity. Of the assays, the pulldowns were used to avoid using cell signaling assays that could show false positives if the peptide signaled using other receptors on the SCs.

With knowledge on other LRP1 ligands, the significant peptides could be teased out as well and point mutations can be used to determines the residues involved in binding to LRP1. Using the sequence and the locations of the residues, Alanine point mutations were made of each of the positively charged amino acids and tryptophan – leading to a total of 7 point mutations. As previously stated, positively charged amino acids, lysine and arginine, were found to be important in other LRP ligands in binding.[42,43] Tryptophan was

investigated since this residue is usually found in low abundance in proteins. The 7 mutants had similar solubility properties as peptide 2 since the only difference was an alanine. These peptides were used in pulldown assays, similar to previously used ones, to avoid cell signaling assays that can lead to false positives if the mutants signaled though other receptors on SCs.

4.2 Pulldown assay with modified peptides

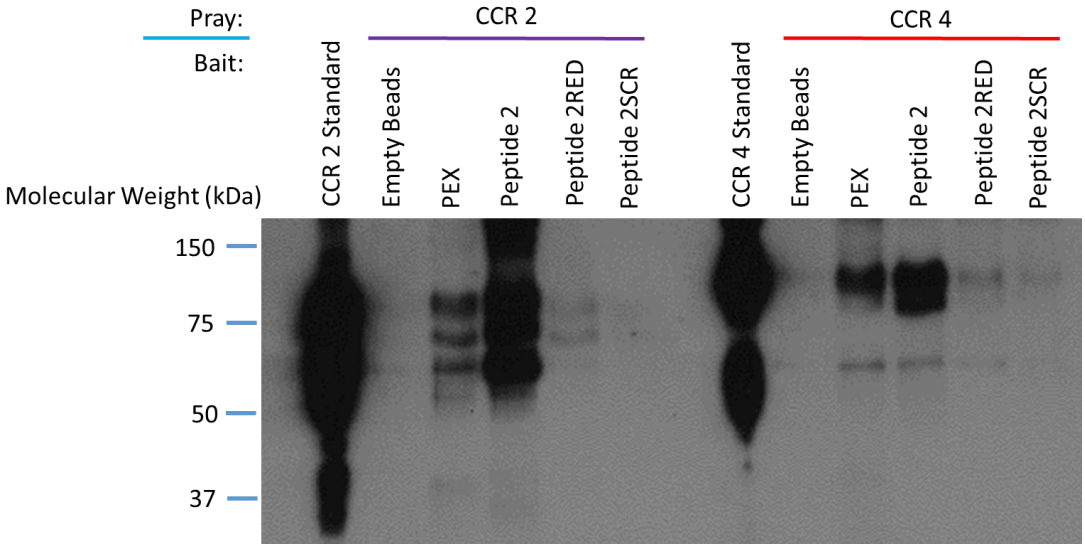

Figure 4.7 – Pulldown studies with LRP1 CCR ligand binding domains with peptide 2 derivatives. Peptides were linked to NHS ester beads and incubated with recombinant LRP1 CCR domains with a rabbit antibody Fc domain. After strenuous washing, immunoblots were used to detect for presence of LRP1 CCR binding to peptides. Recombinant LRP1 CCR 2 fusion with Fc domain is 66.5 kDa as a monomer and 133 kDa as a dimer. Recombinant LRP1 CCR 4 fusion with Fc domain is 72.3 kDa as a monomer and 144 kDa as a dimer.

Pulldowns with recombinant LRP1 CCR fusion proteins showed reproducible results in which both Pex and peptide 2 were able to pulldown these proteins (Figure 4.7, 3.5, 3.6). Peptide 2SCR did not show binding to LRP1 CCR domains, which provides evidence the that sequence of peptide 2

played an important role in the binding of the peptide to LRP1. Peptide 2RED did not show any binding to any LRP1 CCR domain, which provides information that the tail ends of the peptide can play a large role in the binding of the peptide to LRP1. Without secondary structure information, it is difficult to determine if this reduced peptide contains β-sheet and if the two arginine residues in the turn of this peptide actually maintained the correct fold and do not take part in binding; or if the peptide did not maintain a similar structure as the parent peptide, and the arginine residues were not in the correct confirmation.

4.3 Alanine point mutations of Peptide 2

Other than truncations and scrambles, point mutations are another method of studying protein-peptide interactions. On a 22 amino acid peptide, doing every possible point mutation can be very costly, especially if a mutation is made on each amino acid.[26,40] Also, determining the type of mutation to use on each position can make the interpretation of the results difficult. For example, a positively charged residue such as arginine, can be mutated to a neural residue, such as alanine, or a negatively charged amino acid such as aspartic acid. Thus the combinations of mutations can be numerous, but one of the most common starting points is using an alanine residue or alanine scanning.[26]

From previous studies on other ligands of LRP1, it was found that positively charged residues play a large role in the binding of the ligand to LRP1.[42] There are a total of 6 positively charged residues in peptide 2, 4 of which are arginine residues. Of the 4 arginines, two exist on the tail ends of the β-sheet structure (Figure 4.4(R109) and (R122)), and the other side of the β-sheet that is more structured in the intact, full length PEX (Figure 4.5 (R108 and R109)). The two lysines, residue 111 and 126, are in positions that are estimated to be part of the β-sheet (K111) or on the terminal end (K126). Another amino acid of interest was the tryptophan (W121) residue. Tryptophan is an uncommon amino acid in proteins and have been found to have specific roles in stabilizing membrane proteins and β-sheet structures.[44,45] With these amino acids in mind, a common mutation method to investigate whether or not these residues play a significant role in binding is to use alanine point mutations. Using an alanine would eliminate the positive charge in the lysine and arginine residues and remove the aromaticity of the tryptophan residue.

Table 4.3 - Summary of Alanine point mutations of peptide 2. Names of the peptides will be name referred to in this dissertation in the column "Mutation."

Question:	Type of modification	Mutation	Sequence
	Original peptide		SGRGK MLLFS GRRLW RFDVK AQ
Do the Arg play a role in binding?	Single mutation	109R --> A	SGAGK MLLFS GRRLW RFDVK AQ
	Single mutation	118R --> A	SGRGK MLLFS GARLW RFDVK AQ
	Single mutation	119R --> A	SGRGK MLLFS GRALW RFDVK AQ
	Single mutation	122R --> A	SGRGK MLLFS GRRLW AFDVK AQ
Do the Lys play a role in binding?	Single mutation	111K --> A	SGRGA MLLFS GRRLW RFDVK AQ
	Single mutation	126K --> A	SGRGK MLLFS GRRLW RFDVA AQ
Other Mutations	Single mutation	121W --> A	SGRGK MLLFS GRRLA RFDVK AQ

With the mutations, CCR pulldowns similar to those used in the previous methods can be used to identify if the peptides lose or retain binding ability. If the peptide loses binding ability, the peptide mutation signifies that the residue is important in the peptide's ability to bind to the CCR domain. If the peptide retains its ability to bind, then the mutated peptide does not play a significant role in binding of the peptide to the CCR domain of LRP1. From the results seen in Figure 4.8, all bands can be compared to the positive control (peptide 2). In comparison, the negative control can be seen as the 22AA SCR peptide and the amount or lack of binding can be compared to this sample (Graph 4.1).

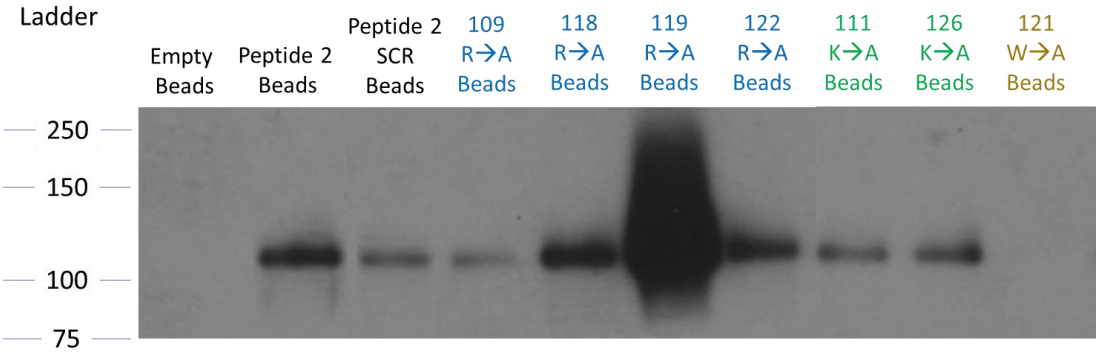

Figure 4.8 – Pulldown studies with LRP1 CCR ligand binding domains with peptide 2 Alanine point mutations. Peptides were linked to NHS ester beads and incubated with recombinant LRP1 CCR2 with a rabbit antibody Fc domain. After strenuous washing, immunoblots were used to detect for presence of LRP1 CCR binding to peptides. Recombinant LRP1 CCR 2 fusion with Fc domain is 66.5 kDa as a monomer and 133 kDa as a dimer. The band for CCR2 can be seen much higher than the predicted value because of the glycosylation that can occur on the protein when expressed in eukaryotic CHO cells.

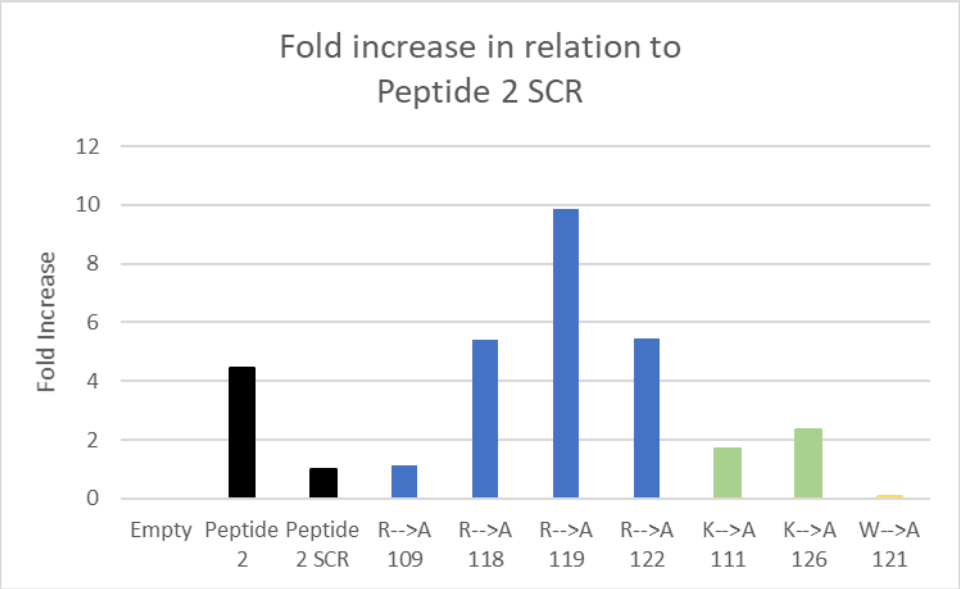

Figure 4.9 – Quantification of the pulldown studies with LRP1 CCR ligand binding domains with peptide 2 Alanine point mutations. Band intensity of the CCR2 domain was measured using imageJ and the intensity of each lane was calculated in relation to the negative control - peptide 2 SCR.

From the alanine point mutation pulldown study (Figure 4.8), arginine 118, 119, and 122 mutations appear to have binding greater than that of the peptide 2 SCR and similar or greater than the peptide 2. Of the arginine mutations the 119R→A mutation seems to have the greatest binding, showing that this residue did not affect binding and, if anything, removing it greatly increased the binding ability of the peptide. On the other hand, the 109R→A mutation seems to be at the same level of binding as the peptide 2 SCR peptide, which means this residue plays an important role in binding to LRP1. From the lysine mutations, both mutations seem to bind similarly in intensity as the peptide 2 SCR peptide. This can imply that the lysine residues are important in binding of peptide 2 to the CCR domain. Of all the mutations, the tryptophan mutation had the most significant reduction in binding that was

below the binding of the peptide 2 SCR. This was the most surprising result since tryptophan was not expected to take part in binding as previously studies found that positive charges were important for binding to CCR domain of LRP1.

4.4 Conclusions and future directions

Using peptide 2 and the crystal structure of MMP9 hemopexin domain, a more in-depth analysis of how this peptide might be binding to the LRP1 CCR domain was explored. With the guidance from ELM scanners, a scrambled peptide was synthesized and shown to not bind to LRP1 CCR domains in invitro pulldowns. This provides evidence that the sequence and organization of peptide 2 is essential for the of the peptide to LRP1. The peptide 2SCR can now play a role of a peptide control in future experiments to ensure that any random peptide is not causing a response, and that responses to peptide 2 are sequence specific.

When the peptide was truncated to peptide 2RED, and the tail ends of the peptide were removed, the peptide became insoluble in water and did not bind to LRP1 CCR domains. Since analytical techniques have a more difficult time estimating β-sheet structure, it is difficult to explain if this loss of binding is due to the two arginine residues not playing a role in binding, or if the peptide still maintains the correct conformation of the two arginines as on the parent peptide 2.

Alanine point mutations provided more insight into the properties and important residues of peptide 2. The residue that had the most significant role in binding was surprisingly found to be the tryptophan residue (Figure 4.8). tryptophan amino acids are seen to play an important role in maintaining β-sheets structures in proteins and found more commonly in antibiotics and membrane anchoring proteins.[44–46] The role that tryptophan plays in the binding of the peptide to LRP1 cannot be completely understood with the experiments presented so far in this thesis. In the crystal structure of Pex, this specific tryptophan residue should be buried within the Pex itself. So it is not understood if there is a conformational change that can expose this residue and help it bind, or if in the peptide it is playing a large role in stabilizing the peptide binding to the LRP CCR domain.

On the other hand, the residues that did not play a major role in binding of the peptide to the CCR domain seems to be R118, R119 and R122 (Figure 4.8). This seems to be supported by the peptide 2 RED data as well. The shortened peptide was made with the hypothesis that R118 and R119 play a large role in binding. But seeing the reduced peptide not bind, and the Alanine mutations of these residues not affect binding shows that these residues were not the key players in binding to LRP1.

The positively residues that mostly affected binding were R109 and the two lysine (K111 and K126) mutations. Using the same logic as the tryptophan residue, K111 is part of the β-sheets that should be buried within Pex and

might not play a role in the actual binding, unless there is a conformational change in Pex itself; thus K111 might play an important role in stabilizing the structure of the peptide to bind to the CCR domain of LRP1. R109 and K111 are both on the tail ends of peptide 2 that are exposed to the hydrophilic environment. With peptide 2RED, these 2 residues were cleaved away. But seeing that these two Alanine mutations affected binding, shows that these residues may be vital in binding to LRP1. Although just a single point mutation didn't knock out the binding completely, these residues are seen to affect the binding showing they may play an important role in binding.

A future approach to better understanding the properties of peptide 2 would be to a double knockout of these two residues or do a truncation to remove the loop portion of R118 and R119. With the already mutated Alanine point mutations, CD can be used to see if the secondary structure is preserved, or if has deviated from the secondary structure of peptide 2. Another hypothesis lies in whether or not the β-sheet structure is needed for organization and binding of peptide 2 to LRP1. Selective amino acids can be changed in the β-sheet structure to disrupt the secondary structure and to observe if this organization is necessary for binding. With this information, peptide 2 can be reduced to a shorter peptide and a more likely a druggable compound.

Ultimately, if the essential amino acids are found from doing further mutations, these changes can be made in the recombinant Pex itself to test if

those amino acids alone played a significant role in the binding of Pex to LRP1. These changes in amino acid residues can be used to scope out the binding pocket of Pex to better understand how to target LRP1 in SCs.

4.5 Experimental methods

Peptide synthesis and purity. Peptides 2 derivatives (Table 4.2) were synthesized by GenScript at >95% purity and verified by HPLC. Synthesized peptide sequences were verified by tandem mass spectroscopy. Peptide 2SCR was soluble in water up to 10 mg/mL. Peptide 2RED stock solution was dissolved in DMSO, and in working concentrations, the peptide was dissolved in 10% DMSO.

Pull down assays. NHS-activated sepharose beads were used to immobilize peptides or PEX. Beads were washed and prepared according to GE manufacturer's protocols. PEX or peptides were introduced to the washed beads with a 0.02M pH 8.0 phosphate buffer and allowed to react for 2 hours at room temperature with top down agitation. Remaining NHS-beads were quenched with 0.1M ethanolamine at pH 8.5 for another hour. Beads were then blocked for non-specific binding using 0.5% BSA in pH 8.0 phosphate buffer for 30 minutes at room temperature. Prey protein (CCR2 or CCR4) were added and allowed to incubate for 1hour at room temperature with top down agitation. In competitive ligand binding assays with GST-RAP, 5 molar excess of RAP was mixed added with CCR2 or CCR4 prior to being introduced to the beads. Beads were stringently washed with pH 8.0 phosphate buffer in 0.1%

Tween 20. Sample buffer was added to the beads, boiled and analyzed by immunoblot.

4.6 Acknowledgements

A large part of the analysis and thought process behind identifying the key amino acids that may play a role in binding was from professor Steven Gonias. In the actual design of producing the reduced peptide was from the guidance and help from Andi Flütsch, PhD..

Chapter 4 contains unpublished material co-authored with Jerry Yang and Wendy Campana. This dissertation author is the primary researcher and author of this material.

Chapter 5

Drug Delivery to the Sciatic Nerve and Pain Behavioral Assay

5.1 Introduction to pain studies and drug delivery to the nerve

Signaling assays can be used to observe cell specific activated signaling pathways and pulldowns can be used to show binding to specific proteins. Both of these types of experiments can be used to infer if SC specific pathways can occur with the biding of peptides or Pex to LRP1; however, these experiments do not show if these pathways can treat neuropathic pain. Thus, using animal models, and delivery of the peptide and Pex to the sciatic nerve, we can observe if these compounds can help alleviate neuropathic pain.

Studying pain in animals is not an easy task. In humans, pain is measured by a verbal response and can be subjectively placed on a numerical scale to determine the severity of the pain.[47] Since animals cannot verbally express if they are in pain, behavior models of the animals must be used to infer pain. In animal models, behaviors such as paw lifting, licking, or grooming is used to determine if an animal is showing behavioral signs of pain.[48,49] Unfortunately, in order to study pain in animals, a pain system must be developed in the animal itself. There are several models that develop pain models in animals, but to be chronic neuropathic pain, a controlled injury can be made to the nerve to form a pain system similar to neuropathic pain.[50] There are various surgical methods that have been used as models of neuropathic pain in animals. These models can vary in injury in the peripheral or central nervous system. In our animal models, we will be using a partial sciatic nerve

ligation (PNL) to establish a pain, also known as the Seltzer model (Figure 5.1).[50,51] Of the neuropathic animal pain models, PNLs are known to be the one of the mildest pain models that show the greatest effect on mechanical allodynia, a pain modality that can be used as a behavioral readout.[52]

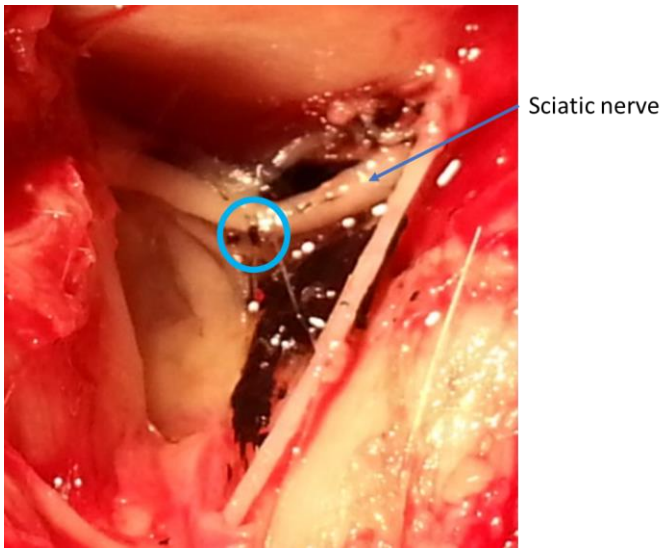

Figure 5.1 – Partial Sciatic Nerve Ligation model in a rat. The sciatic nerve can is 1 to 2 mm thick and is found along the hind leg of the rat. In a PNL model, a 4-0 silk suture is used to tie off half to a third of the nerve, and tied tightly enough to cause pain (circled).

Mechanical allodynia is a painful stimuli that was caused by a light physical interaction – like touch.[53] To test for mechanical allodynia, vonFrey hairs are used to test for sensitivity to touch. These hairs are non-noxious filaments that apply a specific amount of pressure when applied correctly to the test area.[54] Prior to a PNL surgery, rats are baselined to these vonFrey hairs, to assess the baseline of pressure that will cause a reaction in the rats. A reaction counts as a rat withdrawing their foot away or grooming of their foot after the pressure is applied for 5 seconds. Using the Chaplain method, all measurements start with the same filament and move upwards in weight until

a reaction occurs, or downwards in weight until there is no reaction. Then 5 subsequent measurements are made around that reactionary filament to calculate the 50% withdrawal threshold of the animal (Figure 5.2).[54] Around baseline, all animals should have similar baselines, and after surgery, the sensitivity should fall significantly, which represents that the animal is in more pain due to a lower weighted filament causing a reaction. The severity of the pain can be assessed based on the reaction to the filaments as well as the drugs that are given to the animal to treat the on-going pain. Animals can be monitored and assessed for pain over several days, similar to how a patient with neuropathic pain would have chronic constant pain.[48,49] Now that pain can be assessed, a method of delivering the peptides to the sciatic nerve needs to be addressed.

Delivery of peptides or drugs that targets SCs LRP1 can be difficult to accomplish. If a drug or peptide that targets LRP1 enters the circulatory system, it will most likely be filtered out by the liver since all cells express LRP1 and liver cells are known to have high expression of LRP1.[55] Thus to directly deliver the drug to the area, a system would need to be established that can allow for the diffusion or delivery to the nerve. For the CNS, systems such as the Alzet® osmotic minipump have been previously used to continually drip a drug into a local area.[56,57] Unlike the CNS, the PNS, more specially the sciatic nerve, is a very dynamic area which makes it very difficult to implement one of these

pumps. Instead of using a physical pump, the use of a hydrogel could allow for the local delivery of peptides to the nerve.

50% Withdrawl Threshold:	11.42						8.87						7.96						7.66					
VonFrey Filament ↓	Rat 1						Rat 2						Rat 3						Rat 4					
6.65																								
6.45																								
6.1																								
5.88																								
5.46																								
5.18						o												x						
5.07					o							o					o			x				x
4.93		x		o							o			x		o			o		x		o	
4.74	o		o					x		o			o		o				o			o		
Starting Filament 4.56	o						o		o				o						o					
4.31																								
4.17																								
4.08																								
3.84																								
3.61																								
3.22																								
2.83																								
2.44																								
2.36																								
1.65																								

Figure 5.2 – Sample vonFrey assay for mechanical allodynia. A non-response is recorded as an “o” and is seen as the animal not responding to the filament after 5 seconds of applied pressure. A response is recorded as an “x” and is seen as the animal withdrawing or grooming their foot after the filament is applied. All animals start at the same filament that is below the baseline of the sensitivity of the animal. If the animal does not respond to the starting filament, then the next filament is applied until the animal responds to a vonFrey hair. From this point, 5 more filaments are tested based on the previous response and the total of all 6 responses are used to calculate the 50% withdrawal threshold.

The use of hydrogels in the PNL were focused upon the use of hydrogel conduits to observe nerve regeneration or develop mediums for nerve grafts.[58–60] Hydrogels have not been previously used as a drug delivery medium for a PNL type model to directly deliver drugs to the injury site. In this

chapter, the main focus will be devoted to developing hydrogels that can deliver the peptides or Pex directly to the nerve to observe if any of these compounds may be able to treat neuropathic pain.

5.2 Alginate Hydrogels

Alginate hydrogels have been used in various applications for drug delivery to different parts of the body in many different forms.[61] Its versatility can allow it to be molded as thin as skin to act as a wound healing bandage, or can be made into microspheres to allow for slow diffusion of drugs into the gut.[60–62] Alginate is also a natural product from brown algae that has low toxicity to the body and, compared to synthetic hydrogels, has low immunoreactivity with the body.[61] We wanted to take advantage of the versatility, moldability and biocompatibility of the alginate hydrogel to place it into the muscle cavity of the PNL injury, and allow the peptide to slowly diffuse out into the nerve though the PNL suture site.

Since alginates are known as tunable hydrogels, it was important to ensure that there was a slow release of proteins from alginate instead of a burst release at the start. It was not vital to measure the release kinetics of the protein itself, because finding a release model for the gel in an environment like the muscle cavity of a rat is difficult. Most release kinetics that were studied of alginate were done in large diffusion assays within a solution in dialysis membranes.[63] The muscle cavity itself is not flooded with fluids, but it is still a moist environment. Instead of fully trying to mimic a muscle cavity, the dynamic

environment of the muscle was mimicked using a stir bar in the same well of the alginate gel. Using this simple assay, it was confirmed that Pex could slowly diffuse out of the hydrogel. In Graph 5.1, a 1.5% alginate gel was used to show the diffusion of Pex. Other test concentrations of alginate gels were used without loaded protein and gels lower than 1.5% alginate were seen to degrade much faster than the 1.5% alginate gel. With an alginate hydrogel that can allow Pex to diffuse out of the hydrogel, the hydrogel itself needed to placed into a PNL model to ensure that the gel itself would not cause any adverse pain behavior or effects within the animal while delivering the protein.

Graph 5.1 – Gel diffusion assay of Pex from alginate hydrogels. Amount of Pex released from hydrogels was measured using a GST ELISA at the time points. The total amount of Pex was measured by breaking the remaining hydrogel at the end timepoint and adding up all of the Pex released overtime.

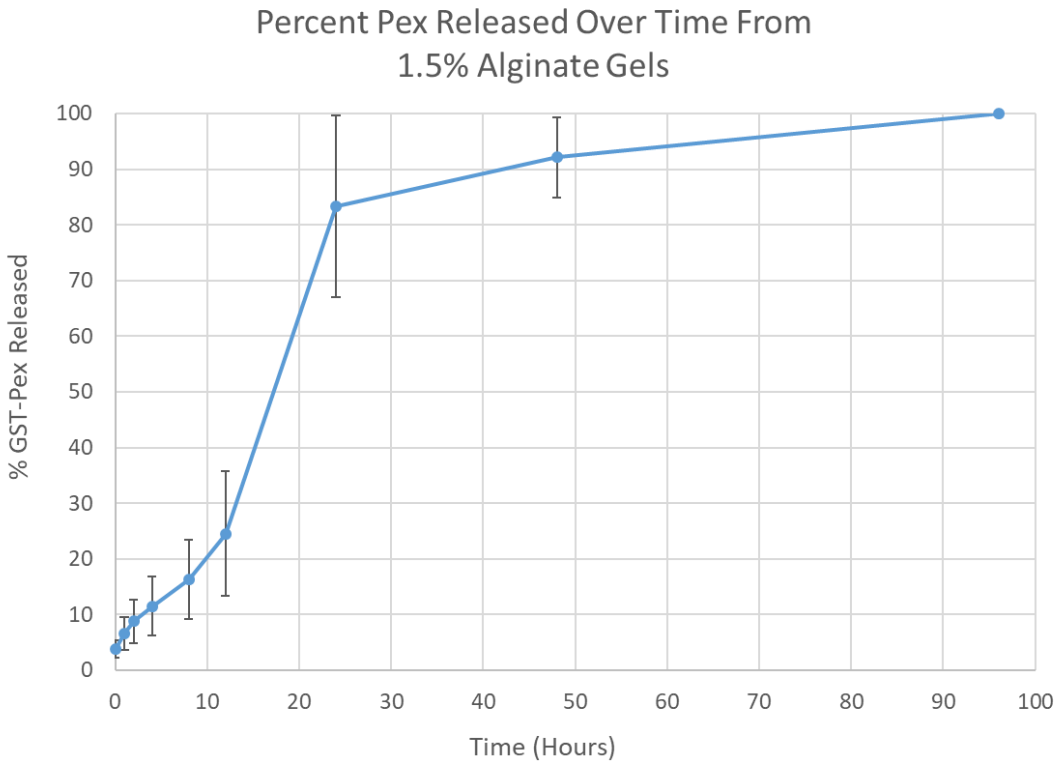

Graph 5.2 – 50% withdrawal threshold measured from rats with a PNL injury and alginate hydrogel. Surgical date is marked as day 0, and all days prior to surgery are baseline days. All measurements taken after surgical date and below the green doted line represent the onset of allodynia in which the rats are more sensitive to vonFrey hairs with lower pressures.

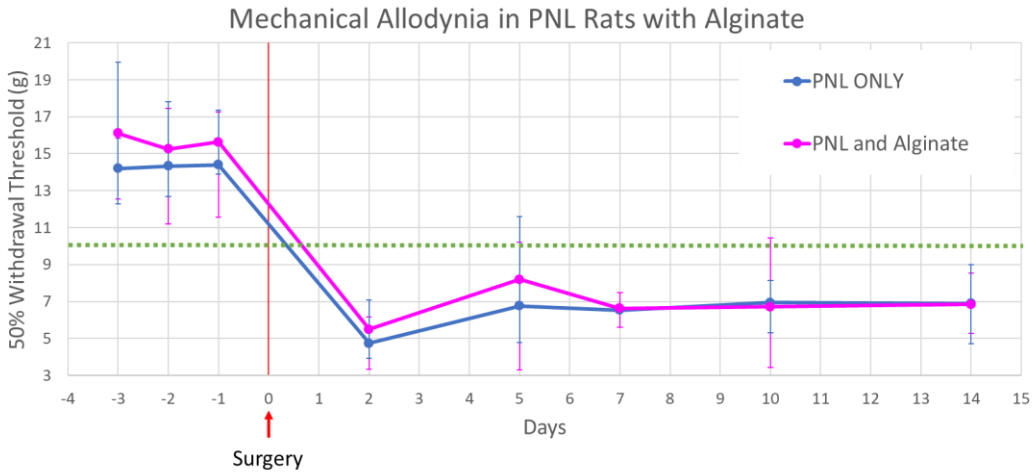

To observe if the alginate hydrogels would affect the pain behavior in the PNL models, alginate hydrogels were formed inside the sciatic nerve cavity after performing a PNL on the animal. These animals were then tested for mechanical allodynia using vonFrey hairs for various time point after surgery. From the pain response (Graph 5.2), the rats with alginate hydrogel did not look different than the control PNL group when tested for mechanical allodynia. To ensure that biologically the alginate was not causing a response, the sciatic nerves were collected after the behavior assays and checked by immunoblot for key inflammatory markers. ATF3 and p38 MAPK are inflammation markers that play an important role in the nerve recovery pathway.[8] These pathways are upregulated during times of nerve injury and play an important role in axon survival, but as the nerve continues to recover and return to homeostasis, these pathways start to become more regulated.[8,64,65] When comparing the

expression of these markers in the alginate group to the control PNL group, the alginate group had significantly higher levels of ATF3 and phosphorylated p38 MAPK (Figure 5.4). A key cell that plays a role in prolonged inflammation are macrophages, which express CD11B. Although macrophages play an important role in clearing out old nerve debris and allowing for nerve recovery, macrophages also start to change phenotypes into a non-inflammatory macrophage that should aid in nerve recovery and not inflammation.[66] Thus, the number of macrophages should start to diminish as the nerve starts to recover with the growing axon and the SC interaction. When the nerves were stained with CD11B, the amount of staining in the alginate gel were much higher than that of just the PNL (Figure 5.3). With the number of CD11B positive cells in the alginate group, and the immunoblot of the nerve, the alginate gels are seen to have a much higher level of inflammation.

Although the alginate hydrogels showed much promise in the behavioral aspect of the study, the immunoblot and histology analysis of the nerves show that there are high levels of inflammation occurring in the nerve, which may cause long term effects to pain we were not able to see because of the limited time period of the behavioral study. If the behavioral study with the alginate gels were extended, the alginate group might be seen to develop more sensitivity than the PNL due to the prolonged inflammation. Although the cause of inflammation is difficult to pinpoint from the studies conducted, there is evidence to show that the cause of continued inflammation may be due to

the high levels of calcium used to form the alginate hydrogels.[67] Other groups using alginates in the peripheral nerve have used chitosan or other chelating factors that may allow for lower concentrations of calcium use.[68–70] To be able to deliver hydrogels to the sciatic nerve, a different hydrogel delivery system would need to be employed.

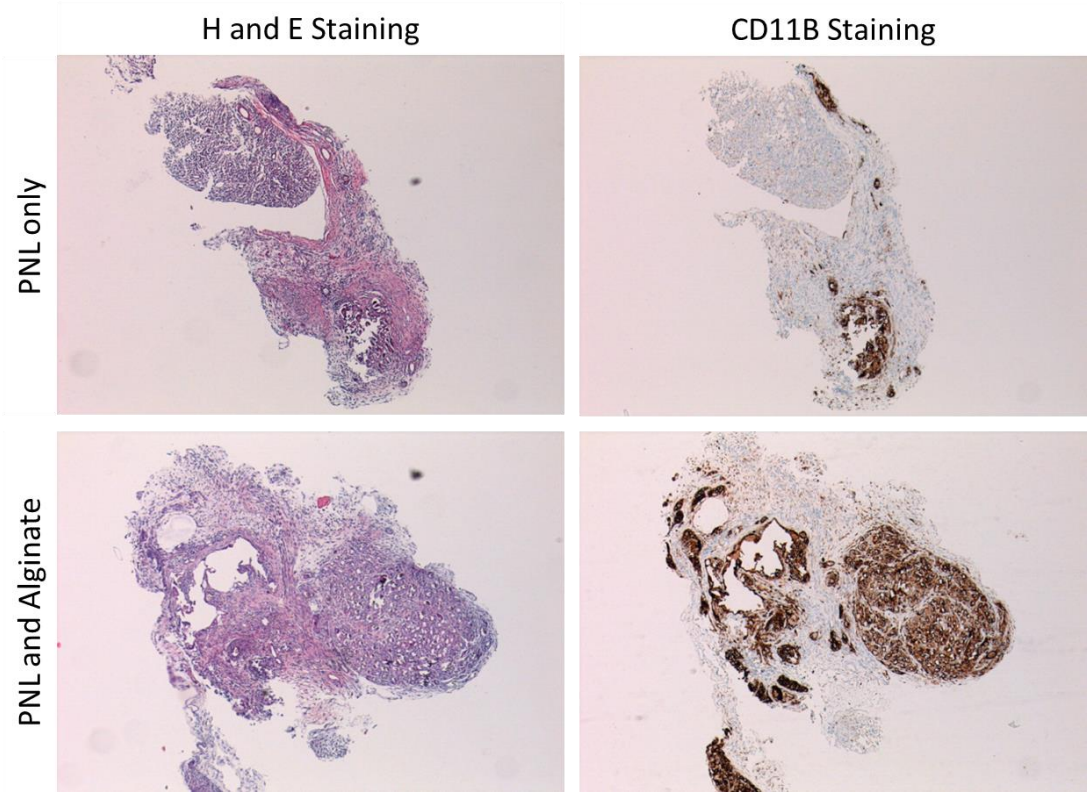

Figure 5.3 – Immunohistochemistry of the sciatic nerve distal to the PNL injury. Sciatic nerves were collected after the behavior studies, fixed in paraffin and embedded in paraffin. H and E and CD11B staining of the nerves were taken about 0.5mm distal from the injury site. H and E is a standard stain used to show structure and organization of the tissue and can highlight different cell types based on the coloration. The DAB stain with CD11B stains all cells that express CD11B in a brown color against the counterstain.

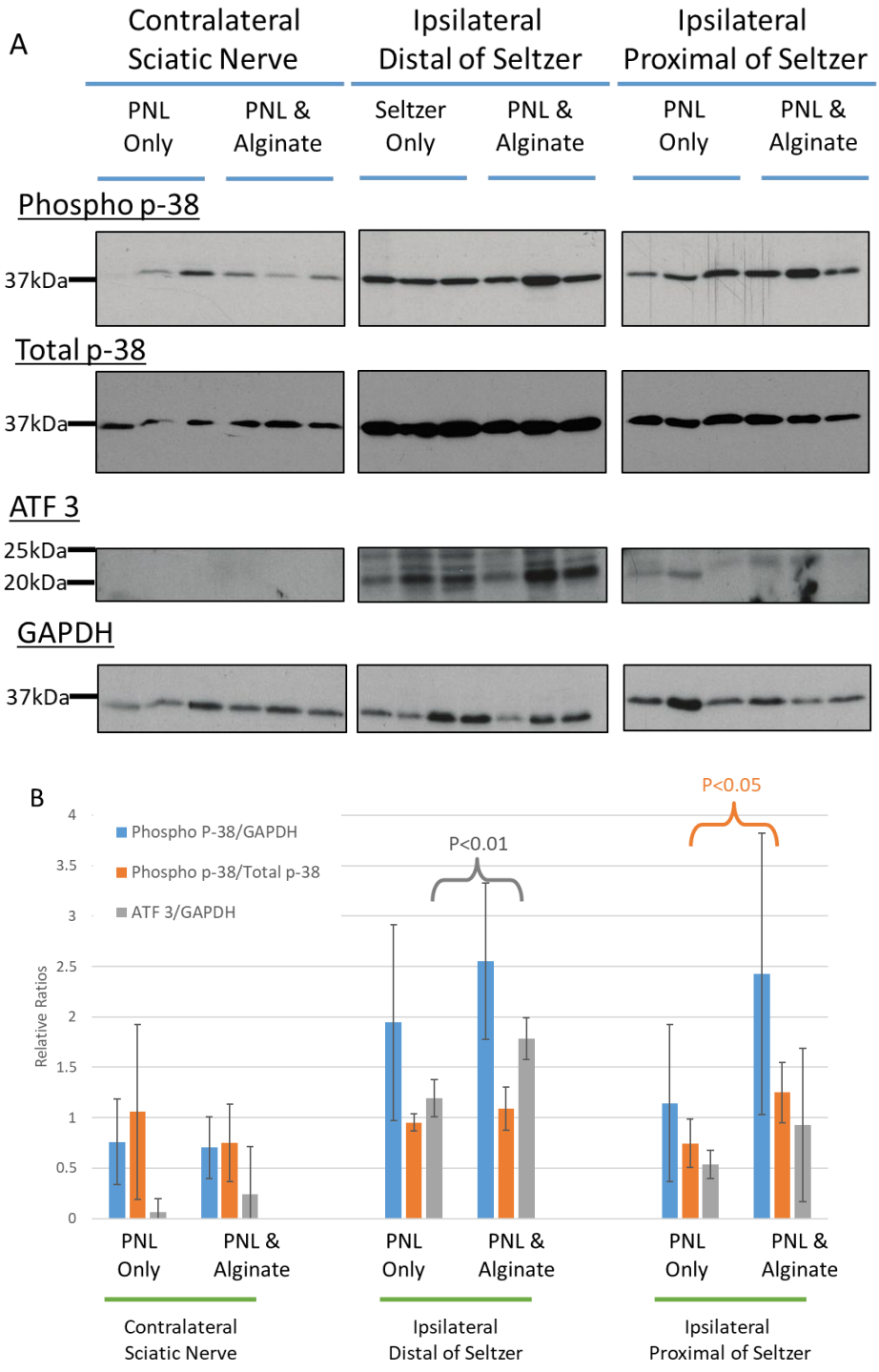

Figure 5.4 – Immunoblots of the sciatic nerves from PNL models with alginate gels. The blots are shown in A, with just the bands highlighted for each protein and experimental groups. All quantifications were carried out by ImageJ and compared to their respective loading controls.

5.3 Poly(ethylene glycol) derived Hydrogels

Poly(ethylene glycol), or PEG, is a commonly used polymerizable hydrogel that is also used in many drug delivery systems. There are many derivatives of PEG that can accommodate various sizes of proteins, thermogenic properties and slow release of drugs.[71–73] A collaborator, Timothy O'Shea, from UCLA works extensively with PEG derived hydrogels, and fine tunes many of these hydrogels for use in the CNS.[74–76] O'Shea donated his PEG derived hydrogels that were capable of being formed in the nerve cavity and delivering peptides to the sciatic nerve. With this in hand, we were able to test if peptides were capable of treating neuropathic pain in PNL rat models.

Graph 5.3 – Mechanical allodynia in PNL rats with loaded PEG hydrogels. Due to variances in baselines between experiments, rat response were normalized using percent response to baseline for each rat and averaged per group.

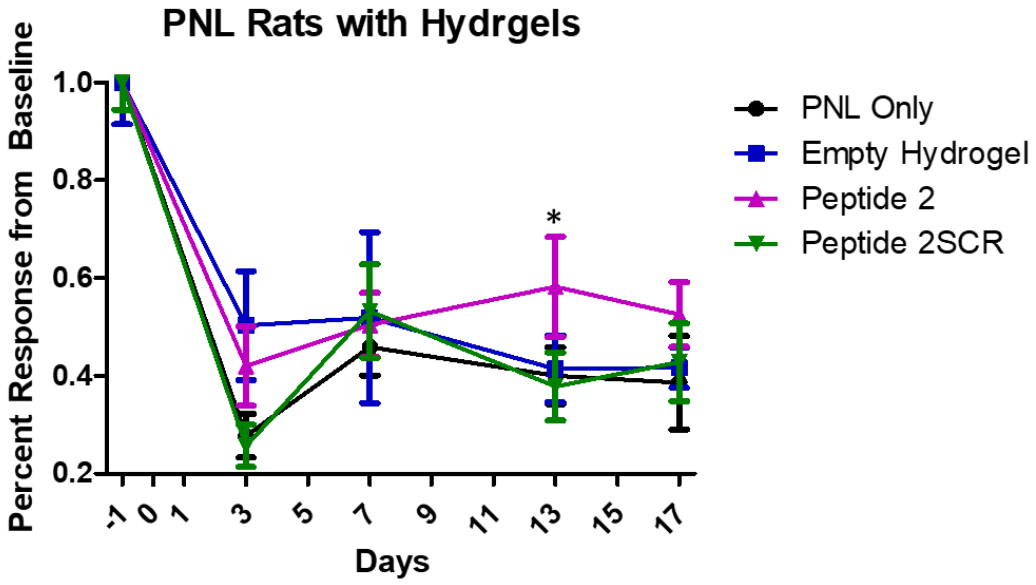

PEG hydrogels seem to be comparable to the alginate hydrogels, in that it does not seem to alter the pain behavior in animals and an allodynic response is still seen. The biggest difference in pain with just the hydrogel seems to be on day 3 post surgery, where the hydrogel seems to be protective and does not create as severe of a pain response as the PNL alone. Although no biological assays were used to check for molecular or signaling differences, behaviorally, the PEG hydrogel does not seem to alter the pain response at later time points. When the PEG hydrogels are loaded with peptides, a difference in these responses can be observed. Peptide 2 was previously seen to bind to LRP1 and cause signaling in SCs that were important in allowing SCs to differentiate into an activated recovery phenotype. Peptide 2SCR was the scrambled peptide of peptide 2 that was not able to bind to LRP1. From the response in the rats, a difference in the pain response is seen on day 10 of the rats, in which the rats with peptide 2 had a significant increase compared to other conditions (Graph 5.3). This shows promise that peptide 2 might be affecting pain responses at this timepoint and alleviating pain in a neuropathic pain model. By day 17, the effects of peptide 2 seems to have diminished, which can be due to the loss of peptide or biological activity. With the same peptide showing activity in binding, *in vitro* and *in vivo*, it brings up many possibilities of how this project can continue.

5.4 Conclusions & Future Directions

Drug delivery to target SC LRP1 in the sciatic nerve is a difficult process due to how ubiquitous LRP1 is in the body and the dynamic nature of the sciatic nerve. With the use of hydrogels, peptides and drugs can be placed in the muscle cavity of the sciatic nerve with a PNL injury. The hydrogel will allow for slow diffusion of the drug into the cavity, which then can enter the sciatic nerve and injury site though the PNL suture. Although alginate hydrogels showed much promise with the pain modality, the amount of inflammation that was seen would have changed the nature of the behavioral studies due to the high amounts of CD11B positive cells the gel recruited into the site. Using alginate hydrogels that contain much less calcium and other gelation factors can definitely improve the use of this hydrogel to deliver drugs into this model system. Currently another graduate student, Richard Niederecker, is developing alginate hydrogels that are almost absent of calcium and are a co-mixture of alginate and agarose that gel at body temperature. With a temperature dependent gelation, the use of calcium can be removed and the positive natures of alginate can still be obtained.

With the use of the PEG hydrogels, the delivery of the peptide to the sciatic nerve was able to be achieved. Although we did not carry out any validation studies to check if the peptide was actually seen in the nerve itself, it would be an important study to validate that the peptide was diffusing out of the hydrogel and into the nerve, and causing the effect we have seen. Since

peptide 2 was now seen to cause a protective pain response in the behavioral assay, there are many other biological and molecular studies that can be assessed from this point forward to further study how the peptide might be affecting pain behavior. An important time point to observe would be day 10 after surgery and gel injection. If there is a protective mechanism, it is important to verify the signaling pathways though immunoblotting and cellular organization though immunohistochemistry. Then determining the availability of peptide 2 after 10 days to verify if the effect of the peptide has worn off or if the gels were depleted would be important in continuing the pain studies to observe if the peptide can continue to protect or treat the pain would be important in further exploring the mechanism of this peptide.

From the start of the project to this point, there are many branch points in which this project can continue to expand. From the peptide standpoint, more molecular studies can be made on the peptide to sort out which residues are key to binding and activity. With the key structures identified, the peptide can be further developed into a drug-like peptide or small molecule mimetic. On the drug delivery aspect, hydrogels can continue to be explored to develop a compatible and tunable hydrogel that can be used to delivery drugs directly to the injury site of the nerve to aid in nerve recovery and prevent neuropathic pain. Finally, the two projects together can be further studied to further explore how a peptide or small molecule can be delivered to specifically to the nerve and activate SCs to prevent neuropathic pain. In these pain models, only

mechanical allodynia was studied, but thermal and tactile allodynia can be studied as well.

There are still many questions that remain to be answered revolving around this peptide, but hopefully this dissertation was the start to exploring more of this peptide and its interaction with SC LRP1 to treat neuropathic pain.

5.5 Experimental Methods

Partial Sciatic Nerve Injury rat model. IUCUC S12331 protocol at UCSD under Wendy Campana approved the use of this protocol. All tools and surgical area was sterilized and aseptic technique was practiced throughout the procedure. Sprague Dawley rats weighing from 175 to 200g were anesthetized using 2-4% isoflurane in 1.5 L/min of oxygen flow. The animal was placed with the left side up and limbs secured to the surgical table with the right leg to the back with the tail and the left perpendicular to the right leg. The skin was opened with a surgical scalpel blade size 15 along the femur with an incision size of no larger than 1 inch. The skin was gently loosened from the fascia. The gluteus superficiallis and bicep femoralis was located and the two muscles were gently separated closer to the spine using small scissors. The sciatic nerve was located and muscle separates were used to hold the incision open. A 4-0 silk suture was used to tie off a third to half of the sciatic nerve and a box knot was tightened until the leg was seen twitching. The fascia was sutured closed with 4-0 silk suture and the skin stapled closed. Animal's respiration was monitored throughout the entire procedure, and for 15 minutes

after the procedure was completed. The animals were monitored for 5 days post-operation to check for any surgical abnormalities or excessive pain behavior. Rats found to be in excessive pain were euthanized via deep anesthesia and decapitation. Rats were sacrificed at set timepoints after behavior or time and tissue harvested for immunoblotting.

Partial Sciatic Nerve Injury rat model with hydrogels. IUCUC S12331 protocol at UCSD under Wendy Campana approved the use of this protocol. Protocols for the partial sciatic nerve injury was followed for this protocol. After the 4-0 silk suture was tied to the nerve, 100 uL of hydrogel containing 10 ug of peptides were added directly into the injury site. Each hydrogel was hardened inside the muscle cavity following the protocol for each hydrogel. The animal was sutured and closed following the same protocol as the partial sciatic nerve injury.

vonFrey behavioral assay for mechanical allodynia. The behavior assay contained several phrases that started with acclimation, then baseline and then mechanical allodynia assessment following surgery. During acclimation, animals were brought to the behavior room outside of the vivarium and allowed to rest in their cages for up to 3 days. Then in the second part of acclimation, the animals were placed upon wired platforms in a clear enclosure, which would be the same location as where all pain measurements would take place. Total acclimation time would be up to 5 days spaced out between consistent days and times. After acclimation, the animal’s background allodynia is

recorded using vonFrey hairs on the back Left paw and recorded as baseline. The Chaplain method was used to calculate the withdrawal threshold from the last 6 withdrawal weight reactions around the threshold weight. A baseline was established after all animals showed a similar withdrawal threshold. Once baseline was established, surgical methods were performed on the animals. Then changes in mechanical allodynia were recorded in the animals using vonFrey for up to 3 weeks or until the animal was sacrificed for tissue collection.

Alginate gel formation. Stock solutions of 3% alginate were made from slowly dissolving 0.3g of Alginate agarose in 10mL of water with stirring at 37°C overnight. Note that this solution is very vicious, but can be syringe filtered to sterilize for animal use. Once sterilized, the stock solution can stay be stored in 4°C up to a month. Stock calcium solution was a 20% weight to volume solution made from 20g of calcium chloride di-hydride, in 100 mL of water. This solution was also syringe filtered to sterilize. To form alginate gels, the 3% stock solution was alginate was diluted to a final concentration of 1.5% with the drug or peptide of choice. This solution was then placed in the cavity or mold of desired alginate location, and then the stock 20% calcium solution was poured on top of the alginate for 5 minutes to develop the gel. After 5 minutes, the calcium solution was pipetted away and the gel was washed in a non-phosphate buffer to wash away excess calcium.

Alginate gel diffusion assay. Alginate gels were formed in the bottom of 16 well cell culture plates by angling the plate so that the gel formed against one

side of the side of the well wall. The alginate gels were made according to the alginate gel formation protocol seen above and the gels were stocked with 1uM of Pex. Wells with formed gels were flooded with 1 mL of phosphate buffer, placed with small stir rod, and then placed in a 37°C incubator with a stir plate to allow for slow agitation of the solution and hydrogel. Buffer collected and changed with fresh 1mL phosphate buffer at 1, 2, 4, 8, 24, and 48 hours or until the gel was completely dissolved away. If there was alginate hydrogels still left over after 48 hours, the gel collected in a separate tube and lysed open using a sonicator. Each time point was frozen as soon as it was collected to prevent more protein from being degraded. Once all time points or gels were collected, the samples were thawed, and spun at max speed to pellet any insoluble salts or left-over hydrogels. The supernatant was assayed using a GST ELISA (GenScript Cat. L00411) to quantify the amount of protein at each time point.

Histology staining of sciatic nerves. Harvested nerves from animals were placed on a small piece of filter paper, denoting the orientation of the proximal and distal ends of the nerve. The filter paper with the nerve attached to it was placed into a small dram vial containing 4% PFA and placed in the 4°C refrigerator overnight. The processed nerve was then sent to the histology core in the pathology department were the tissue was embedded in paraffin, sliced and stained with the desired dyes. Dyed and mounted tissue were observed using a light microscope.

Peg Derivative Hydrogel formation. PEG hydrogel derivatives were synthesized, purified and developed by Tim O'shea at UCLA and donate to use in this project. Of the hydrogels that were sent, "hydrogel 2" that contained oligomers "E" and "P" were used for the delivery of peptides. 20 uL of "E" was pipetted out and placed into a microcentrifuge tube. In another tube, 12.4 uL of "P" were combined with 100 uL of the drug solution diluted in PBS, mixed and placed on ice. All tubes with were kept on ice until they were ready to be formed into gels. When ready, all of the contents in "P" were moved into a tube of "E" and mixed until a homogenous mixture was formed. After waiting for 2 minutes, the hydrogel was placed in its final container and the hydrogel formed within 5 minutes.

5.6 Acknowledgements

All surgical methods and skills were taught to me by the various visiting Japanese scholars in the Campana lab. Masataka Shibayama, M.D. PhD. and Go Kubota, M.D. PhD. played a large role in training me in surgical techniques and methods of finding and producing sciatic nerve models in rats.

All behavioral assays and techniques were thanks to the training and guidance from Kenneth Henry, PhD. and Corinne Lee-Kubli, PhD. Ken helped train me with the methods in the behavioral assays, and Corinne provided the calculator for assessing mechanical allodynia.

All of the immunohistochemistry and paraffin embedding was carried out by Don Pizzo at the histology core in the Department of Pathology.

Timothy O'Shea played an integral role by providing the group with hydrogels that would be compatible in the nerve as well as delivering peptides to the sciatic nerve. Richard Niederecker is still playing a vital role in the development and continuation of the alginate hydrogel delivery project.

Chapter 5 contains unpublished material co-authored with Jerry Yang and Wendy Campana. This dissertation author is the primary researcher and author of this material.

REFERENCES

(1) Kerstman, E.; Ahn, S.; Battu, S.; Tariq, S.; Grabois, M. *Neuropathic Pain.*, 1st ed.; Elsevier B.V., 2013; Vol. 110. https://doi.org/10.1016/B978-0-444-52901-5.00015-0.

(2) Toth, C.; Lander, J.; Wiebe, S. The Prevalence and Impact of Chronic Pain with Neuropathic Pain Symptoms in the General Population. *Pain Med.* **2009**, *10* (5), 918–929. https://doi.org/10.1111/j.1526-4637.2009.00655.x.

(3) Doth, A. H.; Hansson, P. T.; Jensen, M. P.; Taylor, R. S. The Burden of Neuropathic Pain: A Systematic Review and Meta-Analysis of Health Utilities. *Pain* **2010**, *149* (2), 338–344. https://doi.org/10.1016/j.pain.2010.02.034.

(4) von Hehn, C. A.; Baron, R.; Woolf, C. J. Deconstructing the Neuropathic Pain Phenotype to Reveal Neural Mechanisms. *Neuron* **2012**, *73* (4), 638–652. https://doi.org/10.1016/j.neuron.2012.02.008.

(5) Finnerup, N. B.; Sindrup, S. H.; Jensen, T. S. Chronic Neuropathic Pain: Mechanisms, Drug Targets and Measurement. *Fundam. Clin. Pharmacol.* **2007**, *21* (2), 129–136. https://doi.org/10.1111/j.1472-8206.2007.00474.x.

(6) MacFarlane, B. V.; Wright, A.; O'Callaghan, J.; Benson, H. A. E. Chronic Neuropathic Pain and Its Control by Drugs. *Pharmacol. Ther.* **1997**, *75* (1), 1–19. https://doi.org/10.1016/S0163-7258(97)00019-3.

(7) *Glia*; Barres, B. A., Freeman, M. R., Stevens, B., Eds.; Cold Springs Harbor Laboratory Press: Cold Springs Harbor, 2015.

(8) Armati, P. J. *The Biology of Schwann Cells: Development, Differentiation and Immunomodulation*; Armati, P. J., Ed.; Cambridge University Press, 2007.

(9) Orita, S.; Henry, K.; Mantuano, E.; Yamauchi, K.; De Corato, A.; Ishikawa, T.; Feltri, M. L.; Wrabetz, L.; Gaultier, A.; Pollack, M.; Ellisman, M,; Takahashi, K.; Gonias S. L.; Campana, W. M. Schwann Cell LRP1 Regulates Remak Bundle Ultrastructure and Axonal Interactions to Prevent Neuropathic Pain. *J. Neurosci.* **2013**, *33* (13), 5590–5602. https://doi.org/10.1523/JNEUROSCI.3342-12.2013.

(10) Saida, T.; Saida, K.; Lisak, R. P.; Brown, M. J.; Silberberg, D. H.; Asbury, A. K. In Vivo Demyelinating Activity of Sera from Patients with Guillain-Barré Syndrome. *Ann. Neurol.* **1982**, *11* (1), 69–75. https://doi.org/10.1002/ana.410110112.

(11) Harrison, J. F.; Rinne, M. L.; Kelley, M. R.; Druzhyna, N. M.; Wilson, G. L.; Ledoux, S. P. Notch Signaling Modulates the Activation of Microglial Cells. *Glia* **2007**, *55* (14), 1416–1425. https://doi.org/10.1002/glia.

(12) Susuki, K. *Schwann Cell-Dependent Regulation of Peripheral Nerve Injury and Repair*; 2014; Vol. 9784431547. https://doi.org/10.1007/978-4-431-54764-8_5.

(13) Arthur-Farraj, P. J.; Latouche, M.; Wilton, D. K.; Quintes, S.; Chabrol, E.; Banerjee, A.; Woodhoo, A.; Jenkins, B.; Rahman, M.; Turmaine, M.; Wicher, G. K.; Mitter, R.; Greenshmith, L.; Behrens, A.; Raivich, G.; Mirsky, R.; Jessen, K. R. C-Jun Reprograms Schwann Cells of Injured Nerves to Generate a Repair Cell Essential for Regeneration. *Neuron* **2012**, *75* (4), 633–647. https://doi.org/10.1016/j.neuron.2012.06.021.

(14) Parrinello, S.; Napoli, I.; Ribeiro, S.; Digby, P. W.; Fedorova, M.; Parkinson, D. B.; Doddrell, R. D. S.; Nakayama, M.; Adams, R. H.; Lloyd, A. C. EphB Signaling Directs Peripheral Nerve Regeneration through Sox2-Dependent Schwann Cell Sorting. *Cell* **2010**, *143* (1), 145–155. https://doi.org/10.1016/j.cell.2010.08.039.

(15) Mantuano, E.; Inoue, G.; Li, X.; Takahashi, K.; Gaultier, A.; Gonias, S. L.; Campana, W. M. The Hemopexin Domain of Matrix Metalloproteinase-9 Activates Cell Signaling and Promotes Migration of Schwann Cells by Binding to Low-Density Lipoprotein Receptor-Related Protein. *J. Neurosci.* **2008**, *28* (45), 11571–11582. https://doi.org/10.1523/JNEUROSCI.3053-08.2008.

(16) Campana, W. M.; Li, X.; Dragojlovic, N.; Janes, J.; Gaultier, A.; Gonias, S. L. The Low-Density Lipoprotein Receptor-Related Protein Is a pro-Survival Receptor in Schwann Cells: Possible Implications in Peripheral Nerve Injury. *J. Neurosci.* **2006**, *26* (43), 11197–11207. https://doi.org/10.1523/JNEUROSCI.2709-06.2006.

(17) Neels, J. G.; Van Den Berg, B. M. M.; Lookene, A.; Olivecrona, G.; Pannekoekt, H.; Van Zonneveld, A. J. The Second and Fourth Cluster of Class A Cysteine-Rich Repeats of the Low Density Lipoprotein Receptor-Related Protein Share Ligand-Binding Properties. *J. Biol. Chem.* **1999**, *274* (44), 31305–31311. https://doi.org/10.1074/jbc.274.44.31305.

(18) Herz, J.; Strickland, D. K. Fundacja PlasticsEurope Polska. **2001**, *108* (6), 779–784. https://doi.org/10.1172/JCI200113992.Introduction.

(19) Gonias, S. L.; Campana, W. M. LDL Receptor-Related Protein-1: A Regulator of Inflammation in Atherosclerosis, Cancer, and Injury to the Nervous System. *Am. J. Pathol.* **2014**, *184* (1), 18–27. https://doi.org/10.1016/j.ajpath.2013.08.029.

(20) Makarova, A.; Bercury, K. K.; Adams, K. W.; Joyner, D.; Deng, M.; Spoelgen, R.; Koker, M.; Strickland, D. K.; Hyman, B. T. The LDL Receptor-Related Protein Can Form Homo-Dimers in Neuronal Cells. *Neurosci. Lett.* **2008**, *442* (2), 91–95. https://doi.org/10.1016/j.neulet.2008.06.070.

(21) May, P.; Bock, H. H.; Nimpf, J.; Herz, J. Differential Glycosylation Regulates Processing of Lipoprotein Receptors by γ-Secretase. *J. Biol. Chem.* **2003**, *278* (39), 37386–37392. https://doi.org/10.1074/jbc.M305858200.

(22) Vandooren, J.; Van Den Steen, P. E.; Opdenakker, G. Biochemistry and Molecular Biology of Gelatinase B or Matrix Metalloproteinase-9 (MMP-9): The next Decade. *Crit. Rev. Biochem. Mol. Biol.* **2013**, *48* (3), 222–272. https://doi.org/10.3109/10409238.2013.770819.

(23) Dufour, A.; Zucker, S.; Sampson, N. S.; Kuscu, C.; Cao, J. Role of Matrix Metalloproteinase-9 Dimers in Cell Migration: Design of Inhibitory Peptides. *J. Biol. Chem.* **2010**, *285* (46), 35944–35956. https://doi.org/10.1074/jbc.M109.091769.

(24) Van Den Steen, P. E.; Van Aelst, I.; Hvidberg, V.; Piccard, H.; Fiten, P.; Jacobsen, C.; Moestrup, S. K.; Fry, S.; Royle, L.; Wormald, M. R.; Wallis, R.; Rudd, P. M.; Dwek, R. A.; Opdenakker, G. The Hemopexin and O-Glycosylated Domains Tune Gelatinase B/MMP-9 Bioavailability via Inhibition and Binding to Cargo Receptors. *J. Biol. Chem.* **2006**, *281* (27), 18626–18637. https://doi.org/10.1074/jbc.M512308200.

(25) Morgunova, E.; Tuuttila, A.; Bergmann, U.; Isupov, M.; Lindqvist, Y.; Schneider, G.; Tryggvason, K. Structure of Human Pro-Matrix Metalloproteinase-2: Activation Mechanism Revealed. *Science (80-.).* **1999**, *284* (5420), 1667–1670. https://doi.org/10.1126/science.284.5420.1667.

(26) Otvos, L. *Peptide-Based Drug Design: Preface*; 2008; Vol. 494.

(27) Cha, H.; Kopetzki, E.; Huber, R.; Lanzendörfer, M.; Brandstetter, H. Structural Basis of the Adaptive Molecular Recognition by MMP9. *J. Mol. Biol.* **2002**, *320* (5), 1065–1079. https://doi.org/10.1016/S0022-2836(02)00558-2.

(28) Huang, W.; Dolmer, K.; Gettins, P. G. W. NMR Solution Structure of Complement-like Repeat CR8 from the Low Density Lipoprotein Receptor-Related Protein. *J. Biol. Chem.* **1999**, *274* (20), 14130–14136. https://doi.org/10.1074/jbc.274.20.14130.

(29) Greenfield, N. J. Using Circular Dichroism Spectra to Estimate Protein Secondary Structure. *Nat. Protoc.* **2007**, *1* (6), 2876–2890. https://doi.org/10.1038/nprot.2006.202.

(30) Kelly, S. M.; Jess, T. J.; Price, N. C. How to Study Proteins by Circular Dichroism. *Biochim. Biophys. Acta - Proteins Proteomics* **2005**, *1751* (2), 119–139. https://doi.org/10.1016/j.bbapap.2005.06.005.

(31) Dyson, H. J.; Wright, P. E. Defining Solution Conformations of Small Linear Peptides. *Annu. Rev. Biophys. Biophys. Chem.* **1991**, *20*, 519–538. https://doi.org/10.1146/annurev.bb.20.060191.002511.

(32) Cole, C.; Barber, J. D.; Barton, G. J. The Jpred 3 Secondary Structure Prediction Server. *Nucleic Acids Res.* **2008**, *36* (Web Server issue), 197–201. https://doi.org/10.1093/nar/gkn238.

(33) Wiedemann, C.; Bellstedt, P.; Görlach, M. CAPITO - A Web Server-Based Analysis and Plotting Tool for Circular Dichroism Data. *Bioinformatics* **2013**, *29* (14), 1750–1757. https://doi.org/10.1093/bioinformatics/btt278.

(34) Herz, J.; Goldstein, J. L.; Strickland, D. K.; Ho, Y. K.; Brown, M. S. 39-KDa Protein Modulates Binding of Ligands to Low Density Lipoprotein Receptor-Related Protein/A2-Macroglobulin Receptor. *J. Biol. Chem.* **1991**, *266* (31), 21232–21238.

(35) Joshi, A. R.; Holtmann, L.; Bobylev, I.; Schneider, C.; Ritter, C.; Weis, J.; Lehmann, H. C. Loss of Schwann Cell Plasticity in Chronic Inflammatory Demyelinating Polyneuropathy (CIDP). *J. Neuroinflammation* **2016**, *13* (1), 1–9. https://doi.org/10.1186/s12974-016-0711-7.

(36) Das, A.; Shergill, U.; Thakur, L.; Sinha, S.; Urrutia, R.; Mukhopadhyay, D.; Shah, V. H. Ephrin B2/EphB4 Pathway in Hepatic Stellate Cells Stimulates Erk-Dependent VEGF Production and Sinusoidal Endothelial Cell Recruitment. *Am. J. Physiol. - Gastrointest. Liver Physiol.* **2010**, *298* (6), 908–915. https://doi.org/10.1152/ajpgi.00510.2009.

(37) Cho, Y. R.; Lim, J. H.; Kim, M. Y.; Kim, T. W.; Hong, B. Y.; Kim, Y. S.; Chang, Y. S.; Kim, H. W.; Park, C. W. Therapeutic Effects of Fenofibrate on Diabetic Peripheral Neuropathy by Improving Endothelial and Neural Survival in Db/Db Mice. *PLoS One* **2014**, *9* (1). https://doi.org/10.1371/journal.pone.0083204.

(38) Croy, J. E.; Shin, W. D.; Knauer, M. F.; Knauer, D. J.; Komives, E. A. All Three LDL Receptor Homology Regions of the LDL Receptor-Related Protein Bind Multiple Ligands. *Biochemistry* **2003**, *42* (44), 13049–13057. https://doi.org/10.1021/bi034752s.

(39) Weber, C. J. A Modificiation of Sakaguchi's Reaction for the Quantitative Determination of Arginine. *J. Biol. Chem.* **1930**, *86*, 217–222.

(40) Jamieson, A. G.; Boutard, N.; Sabatino, D.; Lubell, W. D. Peptide Scanning for Studying Structure-Activity Relationships in Drug Discovery. *Chem. Biol. Drug Des.* **2013**, *81* (1), 148–165. https://doi.org/10.1111/cbdd.12042.

(41) Gouw, M.; Michael, S.; Sámano-Sánchez, H.; Kumar, M.; Zeke, A.; Lang, B.; Bely, B.; Chemes, L. B.; Davey, N. E.; Deng, Z.; Diella, F.; Gurth, C.; Huber, A.; Kleinsorg, S.; Schlegel, L. S.; Palopoli, N.; Roey, K. V.; Altenberg, B.; Remenyi, A.; Dinkel, H.; Gibson, T. J. The Eukaryotic Linear Motif Resource - 2018 Update. *Nucleic Acids Res.* **2018**, *46* (D1), D428–D434. https://doi.org/10.1093/nar/gkx1077.

(42) Gettins, P. G. W.; Dolmer, K. A Proximal Pair of Positive Charges Provides the Dominant Ligand-Binding Contribution to Complement-like Domains from the LRP (Low-Density Lipoprotein Receptor-Related Protein). *Biochem. J.* **2012**, *443* (1), 65–73. https://doi.org/10.1042/BJ20111867.

(43) Arandjelovic, S.; Hall, B. D.; Gonias, S. L. Mutation of Lysine 1370 in Full-Length Human 2 -Macroglobulin Blocks Binding to the Low Density Lipoprotein Receptor-Related Protein-1. **2005**, *438*, 29–35. https://doi.org/10.1016/j.abb.2005.03.019.

(44) Santiveri, C. M.; Jiménez, M. A. Tryptophan Residues: Scarce in Proteins but Strong Stabilizers of β-Hairpin Peptides. *Biopolymers* **2010**, *94* (6), 779–790. https://doi.org/10.1002/bip.21436.

(45) Jesus, A. J. De; Allen, T. W. Biochimica et Biophysica Acta The Role of Tryptophan Side Chains in Membrane Protein Anchoring and Hydrophobic Mismatch. *BBA - Biomembr.* **2013**, *1828* (2), 864–876. https://doi.org/10.1016/j.bbamem.2012.09.009.

(46) Chan, D. I.; Prenner, E. J.; Vogel, H. J. Tryptophan- and Arginine-Rich Antimicrobial Peptides : Structures and Mechanisms of Action. **2006**, *1758*, 1184–1202. https://doi.org/10.1016/j.bbamem.2006.04.006.

(47) Merskey, H.; Bogduk, N. *Part III: Pain Terms, A Current List with De?Nitions and Notes on Usage*; IASP Press: Seattle, 1994.

(48) Mogil, J. S.; Davis, K. D.; Derbyshire, S. W. The Necessity of Animal Models in Pain Research. *Pain* **2010**, *151* (1), 12–17. https://doi.org/10.1016/j.pain.2010.07.015.

(49) Blackburn-munro, G. Pain-like Behaviours in Animals – How Human Are They ? **2004**, *25* (6). https://doi.org/10.1016/j.tips.2004.04.008.

(50) Jaggi, A. S.; Jain, V.; Singh, N. Fundamental & Clinical Pharmacology. **2011**, *25*, 1–28. https://doi.org/10.1111/j.1472-8206.2009.00801.x.

(51) Seltzer, Ze'ev; Dubner, Ronald; Shir, Y. A Novel Behavioral Model of Neuropathic Pain Disorders Produced in Rats by Partial Sciatic Nerve Injury. *Pain* **1990**, *43*, 205–218.

(52) Kim, Kwang Jin; Yoon, Young Wook; Chung, J. M. Comparison of Three Rodent Neuropathic Pain Models. *Exp Brain Res* **1997**, *113* (August 1996), 200–206.

(53) Lolignier, S.; Eijkelkamp, N.; Wood, J. N. Mechanical Allodynia. **2015**, 133–139. https://doi.org/10.1007/s00424-014-1532-0.

(54) Chaplan, S. R.; Bach, F. W.; Pogrel, J. W.; Chung, J. M.; Yaksh, T. L. Quantitative Assessment of Tactile Allodynia in the Rat Paw. **1994**, *53*, 55–63.

(55) Moestrup, S. K.; Gliemann, J.; Pallesen, G. Cell Tissue Distribution of the 2-Macroglobulin Receptor / Low Density Lipoprotein Receptor-Related Protein in Human Tissues. **1992**, 375–382.

(56) Alvarez-Fischer, D; Guerreiro, S; Hunot, S; Saurini, F; Marien, M; Sokoloff, P; Hirsch, EC; Hartmann, A. M.; PP. Modelling Parkinson-like Neurodegeneration via Osmotic Minipump Delivery of MPTP and Probenecid. *J. Neurochem.* **2008**, *107*, 701–711. https://doi.org/10.1111/j.1471-4159.2008.05651.x.

(57) Lundin, K. E. *Oligonucleotide- Based Therapies*.

(58) Lin, Y.; Marra, K. G. Injectable Systems and Implantable Conduits for Peripheral Nerve Repair. *024102*. https://doi.org/10.1088/1748-6041/7/2/024102.

(59) Hashimoto, T.; Suzuki, Y.; Kitada, M.; Kataoka, K.; Wu, S.; Suzuki, K.; Endo, K.; Nishimura, Y., Ide, C. Peripheral Nerve Regeneration through Alginate Gel : Analysis of Early Outgrowth and Late Increase in Diameter of Regenerating Axons. *Exp Brain Res* **2002**, *146*, 356–368. https://doi.org/10.1007/s00221-002-1173-y.

(60) Mosahebi, A.; Simon, M.; Wiberg, M.; Terenghi, G. A Novel Use of Alginate Hydrogel as Schwann. **2001**, *7* (5), 525–534.

(61) Augst, A. D.; Kong, H. J.; Mooney, D. J. Alginate Hydrogels as Biomaterials. *Macromol. Biosci.* **2006**, *6* (8), 623–633. https://doi.org/10.1002/mabi.200600069.

(62) Bhopatkar, D.; Anal, A. K.; Stevens, W. F. Ionotropic Alginate Beads for Controlled Intestinal Protein Delivery: Effect of Chitosan and Barium Counter-Ions on Entrapment and Release. *J. Microencapsul.* **2005**, *22* (1), 91–100. https://doi.org/10.1080/02652040400026434.

(63) Gombotz, W. R.; Wee, S. F. Protein Release from Alginate Matrices. *Adv. Drug Deliv. Rev.* **2012**, *64* (SUPPL.), 194–205. https://doi.org/10.1016/j.addr.2012.09.007.

(64) Kato, N.; Matsumoto, M.; Kogawa, M.; Atkins, G. J.; Findlay, D. M.; Fujikawa, T.; Oda, H.; Ogata, M. Critical Role of P38 MAPK for Regeneration of the Sciatic Nerve Following Crush Injury in Vivo. *J. Neuroinflammation* **2013**, *10*, 1–13. https://doi.org/10.1186/1742-2094-10-1.

(65) Saito, H.; Dahlin, L. B. Expression of ATF3 and Axonal Outgrowth Are Impaired after Delayed Nerve Repair. *BMC Neurosci.* **2008**, *9*, 1–10. https://doi.org/10.1186/1471-2202-9-88.

(66) Chen, P.; Piao, X.; Bonaldo, P. Role of Macrophages in Wallerian Degeneration and Axonal Regeneration after Peripheral Nerve Injury. *Acta Neuropathol.* **2015**, *130* (5), 605–618. https://doi.org/10.1007/s00401-015-1482-4.

(67) Chan, G.; Mooney, D. J. Ca2+ Released from Calcium Alginate Gels Can Promote Inflammatory Responses in Vitro and in Vivo. *Acta Biomater.* **2013**, *9* (12), 9281–9291. https://doi.org/10.1016/j.actbio.2013.08.002.

(68) Gong, C.; Qi, T.; Wei, X.; Qu, Y.; Wu, Q.; Luo, F.; Qian, Z. Thermosensitive Polymeric Hydrogels As Drug Delivery Systems. *Curr. Med. Chem.* **2013**, *20* (1), 79–94. https://doi.org/10.2174/0929867311302010079.

(69) George, M.; Abraham, T. E. Polyionic Hydrocolloids for the Intestinal Delivery of Protein Drugs: Alginate and Chitosan - a Review. *J. Control. Release* **2006**, *114* (1), 1–14. https://doi.org/10.1016/j.jconrel.2006.04.017.

(70) Reis, C. P.; Neufeld, R. J.; Vilela, S.; Ribeiro, A. J.; Veiga, F. Review and Current Status of Emulsion/Dispersion Technology Using an Internal Gelation Process for the Design of Alginate Particles. *J. Microencapsul.* **2006**, *23* (3), 245–257. https://doi.org/10.1080/02652040500286086.

(71) Qiao, M.; Chen, D.; Ma, X.; Liu, Y. Injectable Biodegradable Temperature-Responsive PLGA-PEG-PLGA Copolymers: Synthesis and Effect of Copolymer Composition on the Drug Release from the Copolymer-Based Hydrogels. *Int. J. Pharm.* **2005**, *294* (1–2), 103–112. https://doi.org/10.1016/j.ijpharm.2005.01.017.

(72) Bhattarai, N.; Ramay, H. R.; Gunn, J.; Matsen, F. A.; Zhang, M. PEG-Grafted Chitosan as an Injectable Thermosensitive Hydrogel for Sustained Protein Release. *J. Control. Release* **2005**, *103* (3), 609–624. https://doi.org/10.1016/j.jconrel.2004.12.019.

(73) Hoare, T. R.; Kohane, D. S. Hydrogels in Drug Delivery: Progress and Challenges. *Polymer (Guildf).* **2008**, *49* (8), 1993–2007. https://doi.org/10.1016/j.polymer.2008.01.027.

(74) Anderson, M. A.; Burda, J. E.; Ren, Y.; Ao, Y.; O'Shea, T. M.; Kawaguchi, R.; Coppola, G.; Khakh, B. S.; Deming, T. J.; Sofroniew, M. V. Astrocyte Scar Formation AIDS Central Nervous System Axon Regeneration. *Nature* **2016**, *532* (7598), 195–200. https://doi.org/10.1038/nature17623.

(75) Wollenberg, A. L.; O'Shea, T. M.; Kim, J. H.; Czechanski, A.; Reinholdt, L. G.; Sofroniew, M. V.; Deming, T. J. Injectable Polypeptide Hydrogels via Methionine Modification for Neural Stem Cell Delivery. *Biomaterials* **2018**, *178*, 527–545. https://doi.org/10.1016/j.biomaterials.2018.03.057.

(76) O'Shea, T. M.; Aimetti, A. A.; Kim, E.; Yesilyurt, V.; Langer, R. Synthesis and Characterization of a Library of In-Situ Curing, Nonswelling Ethoxylated Polyol Thiol-Ene Hydrogels for Tailorable Macromolecule Delivery. *Adv. Mater.* **2014**, *27* (1), 65–72. https://doi.org/10.1002/adma.201403724.